Membrane Based Heat Exchanger

Sofie Marie Aarnes

NTNU

Norges teknisk-
naturvitenskapelige universitet

Institutt for energi- og prosessteknikk

EPT-M-2012-99

MASTEROPPGAVE

for

Stud.techn. Sofie Aarnes

Våren 2012

Membranbasert varmegjenvinner

Membrane based heat exchanger

Bakgrunn og målsetting

Målet med Zero Emission Buildings (ZEB) er å lage bygninger som gjennom levetiden har netto CO_2/miljøutslipp som er null eller lavere. For å få til dette må bygningen levere fornybar energi til nettet. Jo mindre energi som brukes til oppvarming, kjøling, ventilasjon etc., jo lettere er det å få til et netto energioverskudd.

For å kunne realisere ZEB er det derfor nødvendig å benytte komponenter og systemløsninger som har høye virkningsgrader og lave tap.

I bygninger med flere leiligheter benyttes ofte ett sentralt ventilasjonsaggregat. Ut fra kravet om høy virkningsgrad ville det være ønskelig å bruke roterende gjenvinnere i slike anlegg, men de har den ulempen at lukt (matlukt/tobakksrøyk) lekker over fra avtrekk til friskluft.

I kandidatens prosjektoppgave ble ulike varmegjenvinnerkonsepter vurdert og designmodeller for gjenvinnere utviklet. I masteroppgaven skal det legges vekt på utvikling av prototyper for membranbasert varemegjenvinnere.

Mål

Hovedmålet med masteroppgaven er å designe en testrigg for membraner og prøve ut en eller flere membraner i laboratorium for å undersøke egenskapene med hensyn til egnethet.

Oppgaven kan bearbeides ut fra følgende punkter

1. Videreutvikle designverktøyet

2. Velge materialer for vekslerflate

3. Designe testrigg for prøving av membran(er)

4. Bygge testrigg

5. Prøve membran(er) i testrigg

6. Vurdere måleresultatene med hensyn til virkningsgrader, fuktoverføring, trykktap, luktoverføring og evt annet i forhold til teoretiske beregninger og eksisterende løsninger

7. Rapportering.

" - "

Senest 14 dager etter utlevering av oppgaven skal kandidaten levere/sende instituttet en detaljert fremdrift- og eventuelt forsøksplan for oppgaven til evaluering og eventuelt diskusjon med faglig ansvarlig/veiledere. Detaljer ved eventuell utførelse av dataprogrammer skal avtales nærmere i samråd med faglig ansvarlig.

Besvarelsen redigeres mest mulig som en forskningsrapport med et sammendrag både på norsk og engelsk, konklusjon, litteraturliste, innholdsfortegnelse etc. Ved utarbeidelsen av teksten skal kandidaten legge vekt på å gjøre teksten oversiktlig og velskrevet. Med henblikk på lesning av besvarelsen er det viktig at de nødvendige henvisninger for korresponderende steder i tekst, tabeller og figurer anføres på begge steder. Ved bedømmelsen legges det stor vekt på at resultatene er grundig bearbeidet, at de oppstilles tabellarisk og/eller grafisk på en oversiktlig måte, og at de er diskutert utførlig.

Alle benyttede kilder, også muntlige opplysninger, skal oppgis på fullstendig måte. For tidsskrifter og bøker oppgis forfatter, tittel, årgang, sidetall og eventuelt figurnummer.

Det forutsettes at kandidaten tar initiativ til og holder nødvendig kontakt med faglærer og veileder(e). Kandidaten skal rette seg etter de reglementer og retningslinjer som gjelder ved alle (andre) fagmiljøer som kandidaten har kontakt med gjennom sin utførelse av oppgaven, samt etter eventuelle pålegg fra Institutt for energi- og prosessteknikk.

Risikovurdering av kandidatens arbeid skal gjennomføres i henhold til instituttets prosedyrer. Risikovurderingen skal dokumenteres og inngå som del av besvarelsen. Hendelser relatert til kandidatens arbeid med uheldig innvirkning på helse, miljø eller sikkerhet, skal dokumenteres og inngå som en del av besvarelsen.

I henhold til "Utfyllende regler til studieforskriften for teknologistudiet/sivilingeniørstudiet" ved NTNU § 20, forbeholder instituttet seg retten til å benytte alle resultater og data til undervisnings- og forskningsformål, samt til fremtidige publikasjoner.

Besvarelsen leveres digitalt i DAIM. Et faglig sammendrag med oppgavens tittel, kandidatens navn, veileders navn, årstall, instituttnavn, og NTNUs logo og navn, leveres til instituttet som en separat pdf-fil. Etter avtale leveres besvarelse og evt. annet materiale til veileder i digitalt format.

NTNU, Institutt for energi- og prosessteknikk, 16. januar 2012

Olav Bolland
Instituttleder

Hans Martin Mathisen
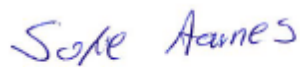*Faglig ansvarlig/veileder*

Medveileder(e): Maria Justo Alonso, SINTEF Energi

Preface

This master thesis was written at the Department of Energy and Process Engineering at the Norwegian University of Science and Technology in Trondheim, Norway through the spring semester 2012. The project was done as a part of the Zero Emission Building Research Center and in collaboration with SINTEF Energy. My supervisor was Professor Hans Martin Mathisen at EPT and co-supervisor was Engineer Maria Justo Alonso at SINTEF Energy. I want to thank both my supervisors for letting me be a part of this interesting project and for support and help through the process.

I would like to thank Håvard, Lars, Magnus, Reidar and Stein at the EPT-laboratory for help in building the test rig and set up of the measurement instruments, Erik Langøren for help in writing the HSE-report as well. Carol Pionneau was working with me for two months in the beginning of the project and came up with a lot of good ideas regarding the test rig and instrumentation. I would also thank Bjarne Malvik at SINTEF for help in measuring temperature and humidity in the preface testing of the test rig. Finally I would like to thank my fellow students for good discussions, support and a lot of social coffee breaks.

Sofie Marie Aarnes

Trondheim, June 2012

Sammendrag

Energibruken knyttet til ventilasjonsanlegg i boliger er et stort og viktig tema når utbredelsen av lufttette lavenergihus og passivhus øker i omfang. I boligkompleks med flere boligenheter og sentraliserte luftkondisjoneringsanlegg er det viktig å unngå lekkasjer av lukt og andre forurensinger fra avkastlufta til inntakslufta. Dette gjør at platevarmegjenvinnere er den vanlige varmegjenvinnertypen i slike anlegg. I denne oppgaven ble det sett på om en membranbasert platevarmegjenvinner som i tillegg til varme kan utveksle fukt, vil ha mindre problemer med kondensering og igjenfrysing enn en platevarmegjenvinner av plastmateriale. I tillegg ble det utviklet en matematisk metode og et enkelt regneverktøy for å simulere varme- og fuktoverføringsvirkningsgraden for en slik membranbasert varmegjenvinner.

For å sammenlikne de ulike typene av varmegjenvinnermateriale ble det bygd et testoppsett i laboratoriet hos institutt for energi- og prosessteknikk ved NTNU. Eksperimentene viste at det oppsto kondens og frost i noen områder inne i de plastbaserte varmegjenvinnerne, mens i den membranbaserte gjenvinneren var det ingen tegn til verken kondenserings- eller fryseproblemer for temperaturer ned mot -10 ^{o}C i de samme områdene. Membranen hadde derimot en tendens til å utvide seg mye ved høy luftfuktighet og dette førte til at membranene klistret seg sammen. Både kondensering og tilfrysing ble observert i et at forsøkene der dette skjedde. Den testede membranen var på grunn av dette dermed ikke optimal med tanke på videre bruk i en membranbasert varmegjenvinner.

Den utviklede metoden for å beregne virkningsgraden for fuktoverføring korrelerte meget godt med de eksperimentelle forsøkene. Det utviklede programmet kan dermed brukes for å forhåndspredikere andre membraners egnethet for bruk i en membranbasert varmegjenvinner.

Abstract

Reduction of the energy used to acclimatise buildings is a huge challenge simultaneously with the implementation of air tight low energy buildings. In residential buildings with several living units centralised air handling units are the most energy efficient system. However, in a centralised system there is important to avoid leakages of pollutions between the exhaust air and the supply air. This leads to that flat plate heat exchangers are used instead of the more energy efficient rotary heat exchanger in these types of buildings. Flat plate heat exchangers will have problems concerning water condensation and frost formation in the exhaust air channels at low supply inlet temperatures. In this thesis a membrane based heat exchanger, which also was able to transfer moisture, was compared to a plastic based heat exchanger to see if the membrane based exchanger had less problems concerning condensation and freezing. In addition a mathematical method was derived to predict the heat and moisture transfer effectiveness in a membrane based heat exchanger.

To compare the different heat exchanger plate materials a test rig was built in the laboratory at the Department of Energy and Process Engineering at NTNU. The experiments showed that the plastic based heat exchangers had problems with condensation and freezing in the tested conditions. The membrane based exchanger did not experience the same problems. However, additional problems with expansion of the membrane in high humidity showed that the tested membrane had drawbacks and was not really suitable.

The derived mathematical method to predict the moisture transfer effectiveness was shown to correlate very well with the experimental results. The derived method and the developed *Microsoft Excel* tool called *HXcalc* may then be used to investigate other membranes moisture transfer effectiveness.

Contents

List of Figures

List of Tables

Nomenclature

A	Area	m^2
n	Coefficient in the mass-heat transfer analogy	
C	Concentration	kg/kg or mol
K	Constant in resistance-humidity relation	
C	Constant in Zhang and Niu's sorption equation	
D	Diffusivity	s/m
$\dot{V}$	Flow rate	m^3/s
h	Heat transfer coefficient	$W/m^2 K$
d	Height of air layer in permeability test.	m
k_H	Henrys constant	Pa/mol
D_h	Hydraulic diameter	m
x	Length scale	m
Le	Lewis number	
$\tilde{x}$	Linear trend line value	
m	Mass	kg
$\bar{x}$	Mean value	
F	Moisture flow rate/flux	kg_w/s
h_M	Moisture transfer coefficient	m/s
R	Moisture transfer Resistance	s/m
n	Mol	mol
M	Molar weight	$kg/kmol$
n	Number of measurements	
NTU	Number of transfer units	
Nu	Nusselt number	
U	Overall heat transfer coefficient	$W/m^2 K$
U_M	Overall moisture transfer coefficient	m/s
P	Permeability	s/m
p	Pressure	Pa
R	Ratio between the min and max air flow	
S	Solubility	kg/kg
s	Standard deviation	
T	Temperature	K or ^oC
t	Thickness	m
t	Time	s
U	Uncertainty	
Δu	Uncertainty	
$\bar{R}$	Universal gas constant	$J/Kmol$
V	Volume	m^3
$\dot{V}$	Volumetric flow rate	m^3/s

Greek letters

ω	Absolute humidity	kg_w/kg_A
α	Aspect ratio (height/width)	
ρ	Density	kg/m^3
ε	Effectiveness	
η	Efficiency	
θ	Moisture content in membrane	kg_w/kg_{memb}
ε	Porosity	
ϕ	Relative humidity	%
τ	Tortuosity	
φ	Volume fraction	m_w^3/m_{memb}^3

Subscripts

A	Air
$conv$	Convection
E	Exhaust air side
f	Film
in	Inlet side
max	Maximum
$memb$	Membrane
min	Minimum
M	Moisture
out	Outlet side
r	Random
ref	Reference
S	Supply air side
s	Systematic
T	Total
w	Water

Keywords

Absolute humidity	The amount of water vapour in air. Given as the ratio between the kilograms of water to the kilograms of air mixture.
Air handling unit	Usually the mechanical components in the air condition system for a building is connected in a single box called an "air handling unit". Typical components are fans, filters, sound attenuators, heating and cooling elements and a heat recovery system.
Effectiveness	The same as the efficiency, but corrected for the difference in flow rates. This gives the same effectiveness for both streams and is a single number for the heat exchanger.
Efficiency	The amount of heat an air stream takes up or gives away from or to the other stream divided on the total heat difference in those two streams. The efficiency for both streams will coincide if the flow rates are equal.
Energy recovery ventilator (ERV)	Heat and moisture exchanger.
Heat recovery	Utilizing the heat in the exhaust air or waste heat from for example the discharged water in a heat exchanger to heat (or cool) air or water to the HVAC system.
Heat recovery ventilator (HRV)	Heat exchanger.
Hydrophilic	Means "water loving". A hydrophilic material absorbs water due to its polarity.
Microporous	A material with pores usually less than 2 nm. The material lets tiny water vapour molecules pass through while bigger molecules cannot pass through.
Moisture transfer resistance	The resistance of a material to let water vapour pass through it.
NTU	Number of transfer units. A dimensionless unit used in the effectiveness-NTU method to predict the effectiveness of a heat exchanger.
Permeability	The ability of a material to let water vapour pass through it.
Relative humidity (RH)	The amount of water vapour in air. Given as the percentage ratio between partial pressure of water vapour to the saturated vapour pressure at the same conditions (temperature, pressure).
ZEB	The Zero Emission Buildings Research Centre

Chapter 1

Introduction

1.1. Background

In the Nordic countries the population spend most of the time inside buildings. To feel comfortable the indoor air has to be within a specific temperature range (Novakovic et al., 2007). This is done by either heating in cold outdoor conditions or cooling in warm outdoor conditions. Acclimatisation of buildings requires a huge amount of energy per year. The energy efficiency of the acclimatisation systems in buildings have improved through the last decades. However, still more research is needed to continue the improvement. The Zero Emission Buildings Research Centre (ZEB) was initiated by the Research Council of Norway in 2009 as one of eleven national centres of Environment-friendly Energy Research (FME). Hosted by the Faculty of Architecture and Fine Art the research centre shall coordinate the collaboration between several partners ranging from manufacturing companies to architects and several different research and teaching institutions. The aim of the ZEB project is to:

"Over the next eight years, the FME-Centre ZEB will develop competitive products and solutions for existing and new buildings that will lead to market penetration of zero emission buildings related to their production, operation and demolition. " [1]

The ZEB includes both research on building features as facade materials, heating systems and research on the end interplay between the end user and energy efficient buildings. This thesis is based on a project connected to the work package 3 of the ZEB-project: "Energy Supply Systems and Services". The project is cooperation between SINTEF and NTNU.

Heat recovery is an important part of the air handling unit in buildings to lower the energy usage due to heating (and cooling) of the supply air. The heat recovery unit does usually include a heat exchanger where the hot exhaust air exchanges heat with the cold supply air (or opposite for cooling purposes). In the Nordic countries flat plate heat exchangers have been the dominating heat recovery system in buildings with several living units and centralised air handling systems. Different from the more energy efficient heat recovery wheels these heat exchangers will not cause the problems of leakages of pollutants from the exhaust to the supply air (Zhang, 2012). However, the aluminium or plastic based flat plate heat exchangers have quite low

---

[1] «About ZEB», Published: 12.08.11, Quoted:12.05.12, http://www.sintef.no/Projectweb/ZEB/About-ZEB/

annual energy recovery efficiency due to the energy needed for the frost protection systems which are required in low temperature areas (Drivsholm et al., 2005).

Condensation and frost problems in flat plate heat exchangers may be avoided if the exhaust air is dehumidified before the temperature reaches the saturation temperature for humid air. In warm and humid areas where cooling and dehumidifying of supply air is required to meet the desired indoor air quality special enthalpy exchangers have been developed. These exchangers utilise membranes to separate the fresh supply air and the exhaust air. The differences in temperature and moisture content on the different sides of the membrane make heat and moisture transfer from the warm and humid side to the cool and dry side by passive transport mechanisms.

In a preliminary work by the author the membrane based heat exchanger was found to be able to decrease the frost protection temperature compared to a conventional flat plate heat exchanger. This could lead to great energy savings in Nordic residential buildings with several living units and centralised air handling systems. A method to predict the temperature efficiency and the energy recovery efficiency for a given heat exchanger geometry was derived. The necessary moisture transfer efficiency to avoid freezing problems was also found. The results showed that for the Oslo climate a 70% moisture transfer efficient heat exchanger was needless of a frost protection system and its heat recovery efficiency would reach 90%. This means that if such moisture transfer efficiency is obtainable it can reduce the energy used in frost protection and still the indoor air quality will be improved without increased total costs. This is important for new airtight buildings. (Aarnes, 2011)

However, the research on how the flat plate membrane based heat exchanger performs in cold climate conditions is limited. Actually no available research articles were found about the theme. Nevertheless, several manufacturers sell this type of exchangers targetting the cold climate market and claim their good performances. [2] [3]

---

[2] «Case Study: Natural Resources Canada (NRCan) - Canadian Centre for Housing Technology (CCHT) in Ottawa, Ontario.», Quoted: 12.05.12, http://www.dpoint.ca/energy-recovery-ventilator-cores/casestudy-ccht.php

[3] «Mitsubishi Electric: Canada, Energy Recovery and Ventilation, Benefits.», Quoted: 23.05.12, http://www.mitsubishielectric.ca/en/hvac/erv/benefits.html

1.2.   Objective

Stated above, the membrane based heat and moisture exchanger may have great potential as an energy saver compared to a plastic based heat exchanger. However, this statement was based on the assumption that the membrane will elude the problems concerning condensation and frost formation in the exhaust air channels in the exchanger at low temperatures. Several manufacturers produce membranes that could be suitable to use in a membrane based heat exchanger. Since experimental testing takes a lot of time and effort, a method to predict the moisture transfer effectiveness from available data given by the manufacturers is preferable. Available calculation methods found in the literature includes membrane properties only found through special laboratorial testing. The objectives of the work presented in this thesis are to:

- Develop a method to predict the moisture transfer effectiveness in a membrane based heat exchanger. The input values should not require other properties than the ones usually given in the producers' datasheets.

- Build a test rig to compare plastic based heat exchangers against a membrane based moisture and heat exchanger due to water condensation and frost formation.

- Evaluate the membrane based heat exchanger prototype's appropriateness for heat recovery in cold climate areas.

The mathematical method derived was put into a simple program run in *Microsoft Excel*. The program should be suitable for further investigation in the suitability of different membranes for use in membrane based heat exchangers.

A heat exchanger prototype was developed and a test rig was built in the lab at the *Department of Energy and Process Engineering* at *NTNU* to be able to compare different heat and moisture transferring materials. The experimental results will be compared to the results of the mathematical model.

1.3. Literature

The available documentation regarding experimental testing of membrane based heat exchanger performance in cold climates is limited. Nevertheless, there were found two commercial producers of membrane based flat plate heat exchangers designed for cold climate. Both manufactures are operating in North-America. The "Japanese paper total heat exchanger" was invented in 1969 and patented in 1972. The advantages were that this type of heat exchanger could transfer both humidity and heat and without the size and complexity of the energy wheels. (Yoshino & Hashimoto, 1973) These exchangers are still sold under the name *Lossnay* from *Mitsubishi Electric Corporation*. The manufacturer claims that this exchanger will work very well without freezing problems in cold climate areas.[3] Both the temperature efficiency and the moisture transfer efficiency is claimed to reach 70%. The membranes in this exchanger are micro porous.[4] However, no available documented research on the cold weather performance of this exchanger was found. Another commercial membrane based heat exchanger was developed in Canada by *dPoint*. This firm patented a method to produce a water permeable laminated hydrophilic membrane in 2010 (Huizing, 2010). The *dPoint ERV Core* was tested in Canadian winter conditions and compared to a standard *Coroplast HRV core.* The results are only shortly mentioned on the *dPoint* website and the report is confidential.[2] However a very similar experiment was done in summer conditions at the same research centre; *the Canadian Centre for Housing Technology* and this experiment was published (Ouazia et al., 2006). It is therefore reason to believe that the winter condition experimental tests were performed after the same procedure as in the article of Ouazia (2006). The winter test showed, according to the manufacturer's website, that the *ERV Core* had no need of drainage and were 10% more efficient than the *standard HRV core.* The manufacturer claims that the *ERV Core* has 80 % temperature efficiency and 40% moisture transfer efficiency. The heat exchanger was working down to a supply air temperature at -19ºC without frost protection systems.[2]

Articles on the sensible and latent effectiveness for different air flow rates(Nasif et al., 2005; Zhang, 2010) temperatures, flow patterns or geometry(Vali et al., 2009; Zhang, 2010) and humidity levels (Kadylak et al., 2009; Niu & Zhang, 2000) were found in the literature. Zhang (2010) used a modified $\varepsilon - NTU$ method to predict the moisture transfer effectiveness and compared different heat exchanger geometries by the resulting effectiveness. He found that a quasi-counter flow geometry was both possibly to build and superior to the cross flow geometry regarding effectiveness. He did also perform a CFD analysis to see the flow pattern inside such an exchanger (Zhang, 2010). The result is reprinted below:

---

[4]«Mitsubishi Electric: Canada, Energy Recovery and Ventilation, Features.», Quoted: 23.05.12, http://www.mitsubishielectric.ca/en/hvac/erv/features.html
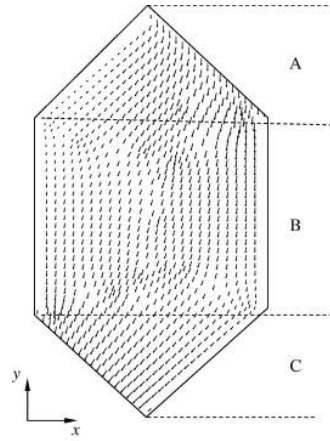
Figure 1.1. *Flow pattern in a quasi-counter heat exchanger. Reprint from (Zhang, 2010).*

Condensation will occur at the heat exchanger plate surface if the surface temperature of gets lower than the saturation line for the moist air flowing over it. The saturation temperature for a given absolute humidity, ω was given as (Aarnes, 2011):

$$T_{sat} = \frac{5427}{\ln\left(\dfrac{10^7}{\omega * 6.19}\right)} \qquad (1.1.)$$

If the surface temperature is below 0°C the condensate will form ice crystals. The surface temperature in the heat exchanger in a given point may be assumed to be:

$$T_f = \frac{T_E + T_S}{2} \qquad (1.2.)$$

The condensation and frost problems in heat exchangers are strongly linked to the exhaust air humidity. Kalamees et al. (2009) studied the outdoor and indoor humidity and temperatures in 170 Finnish residential buildings over a whole year. The connection between the outdoor temperature and indoor relative humidity may be seen in the reprinted figure below.
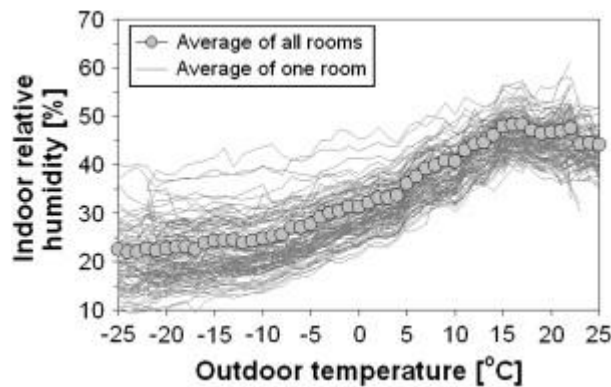
Figure 1.2. *The coherence between the outdoor temperature and indoor relative humidity for Finnish residential buildings. Reprint form Kalamees et al. (2009).*

Frost formation on a cold flat plate with moist warm air flowing over it was shown to grow in different forms of different humidity and temperature levels. For quite warm surface temperatures (close to 0°C) and low humidity levels the frost was found to be dense and had a smooth surface. For colder surfaces and high humidities the frost grew as crystals. These ice crystals increased the surface roughness and actually increased the heat transfer coefficient between the plate and the flowing air in the beginning of the experiments. (Yun et al., 2002) The results from the experiments are shown in a reprinted figure below:
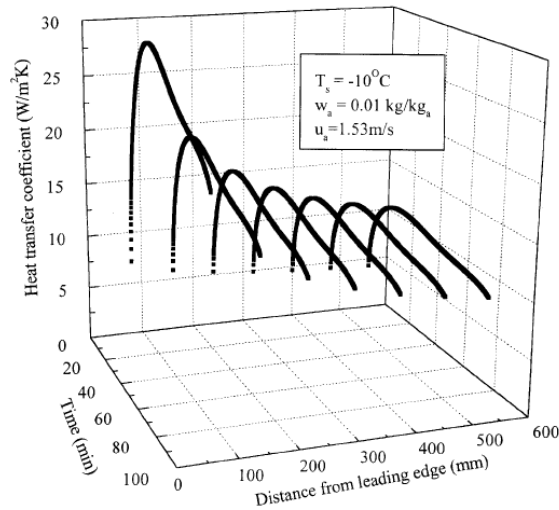
Figure 1.3.   Reprint from (Yun et al., 2002). Frost formation on a horizontal cold plate. Heat transfer coefficient dependency on time and distance from leading edge.

The moisture transfer efficiency of the membrane based heat exchanger will depend on the ability of the membrane material to transport water vapour (or the resistance to let the water molecules diffuse through it). Two main models exist to describe permeation of species through a membrane:

1) The pore-flow model
2) The solution-diffusion model

The pore flow model describes the transport phenomena when a partial pressure difference at different membrane sides makes a convective driven flow of species from one side to the other through tiny pores in the membrane. The pore size acts like a sieve to sort out the different species.(Mukhopadhyay & Midha, 2008) The solution-diffusion model was described in a review of Wijmans and Baker (Wijmans & Baker, 1995). Shortly, the model states that a permeant is dissolved (absorbed) in the membrane material and then diffuses through the membrane. The rate of absorption and diffusion is dependent on the concentration gradient. The permeability, P, is then defined as the diffusion multiplied with the solubility:

$$P = DS \qquad\qquad\qquad (1.3.)$$

To find the permeability experimental test may be done. To find the solubility gravimetric test is usually made(Modesti et al., 2004). There exist several types of vapour transmission and permeability tests. McCullough (2003) compared 26 different commercial fabrics tested according to five different standard methods. When comparing the water transmission flux for the different tests huge differences were found. Some of the differences can be explained by the differences in test methods; some have large humidity gradients and other smaller. In some test a resistance due to a stagnant air layer appears. Some test let the membranes come in contact with water and others have a great temperature gradient as well as a humidity gradient. (McCullough et al., 2003) This implies that when using available test results to predict the moisture transfer resistance of a membrane an understanding of how the tests was conducted is vital to be able to sort out the internal membrane resistance alone.

Henry's law says that the partial pressure, p, is equal to the concentration of the solute, C, multiplied with a constant k_H.

$$p = k_H C \tag{1.4.}$$

Henry's law may also be expressed in terms of the volume fraction, φ (as an alternative to the concentration) and a constant k, describing the water molecules affinity to the membrane material:

$$\varphi = kp \tag{1.5.}$$

The relationship between the volume fraction, φ and the mass fraction, θ is:

$$\theta = \frac{1}{1 + \left(\dfrac{1-\varphi}{\varphi}\right)\left(\dfrac{M_{memb}}{Mw}\right)} \tag{1.6.}$$

Where M_m is the molar weight of the membrane material and M_W is the molecule weight of water. Zhang and Niu (2002) used a general sorption isotherm model derived from Henry's law to describe the relationship between the moisture content in the membrane at different relative humidity levels. The relative humidity is expressed by the partial pressure divided by the vapour pressure at a given temperature. Since the vapour pressure of water at a given temperature is constant this value may be included in the constant k in equation 1.5. and the volume fraction may then be an expression of the relative humidity. This will give the expression given in Zhang and Niu (2002):

$$\theta = \frac{\theta_{max}}{1 - C + \dfrac{C}{\phi}} \tag{1.7.}$$

Where C is a constant, ϕ is the relative humidity and θ is the moisture content in the membrane. θ_{max} is the maximal uptake of water in the material (Zhang & Niu, 2002).

The water molecules unsymmetrical shape gives the molecules a polarity that makes intermolecular bonds between the molecules possible. This polarity makes also water a good solvent and makes the molecules easily bond to other polar molecules, ions or atomic groups. This feature is utilized in hydrophilic membranes. However, the well developed and described Flory-Huggins theory used to describe sorption of solvents into a membrane may not be used if the bonds between the penetrant molecules are stronger than the bindings between the membrane material and the penetrant.(Favre et al., 1993) The bindings between the water molecules make clusters of water inside the membrane. The approach from Favre et al. (Favre et al., 1993) called the ENSIC model (engaged species induced clustering) is described by looking at the membrane surface as a matrix of either cells of polymer or cells of solvent (water vapour). See picture below:
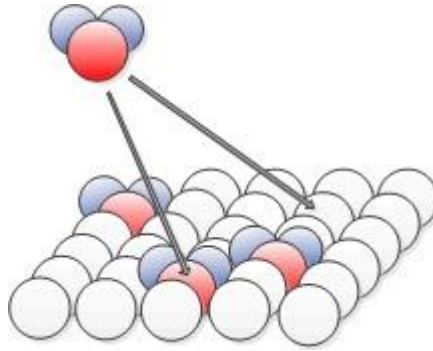
Figure 1.4.   *Water molecules in the gas stream may either bond to polar groups in the polymer membrane surface (white balls) or to other water molecules already absorbed to the surface.*

At equilibrium the membrane has absorbed some water. Water vapour molecules may then either be absorbed by polar groups in the membrane material or by other water molecules already absorbed. If the partial pressure rises the number of water molecules absorbed by the membrane may be assumed to rise. If the total number of molecules in the membrane is assumed to be huge compared to the rise in numbers of water molecules due to the partial pressure rise the total molecule number may be assumed constant. This gives the relation(Modesti et al., 2004):

$$dn_W = (k_{memb}n_{memb} + k_W n_W)dp \qquad (1.8.)$$

The theory may explain why an increase in water content will decrease the moisture transfer resistance of the membrane.

The other factor in the permeability equation in 1.3., the diffusivity, is expressed by Fick's first law (Crank, 1975):

$$F = -D\frac{\partial C}{\partial x} \qquad (1.9.)$$

F is the rate of mass transfer per unit area and C is the concentration of water vapour. Fick's second law is expressed as:

$$\frac{\partial C}{\partial t} = D \frac{\partial^2 C}{\partial x^2} \qquad (1.10.)$$

Fick's first law is derived from the free diffusion theory and does not take into account the changes in molecular structures which play an important role in the transportation of water in a hydrophilic membrane. For porous materials the diffusivity may be considered independent form the change in concentration over the membrane. For hydrophilic materials this are not the case and the water vapour diffusion is shown to change a lot with changing humidity levels. (Gibson, 2000) Modesti et al.(2004) showed that the diffusivity changed with different water activities and could by this not be considered to be a constant value. This differed from the model by Zhang (2012) where the water diffusivity in the membrane was assumed constant for a certain membrane.

Chapter 2

Mathematical Model

In a present work a mathematical model to predict the pressure drop, the temperature effectiveness and the annual heat recovery efficiency for a given frost protection temperature in a flat plate heat exchanger was derived (Aarnes, 2011). The heat transfer in this types of heat exchangers was shown to be independent of the heat exchanger material if the material was sufficiently thin. Hence, the temperature effectiveness is a function of the geometry and the inlet boundary conditions. As written in chapter 1.3. Zhang and Niu (2002) derived a method to find the moisture transfer effectiveness similar to the well-established ε-NTU method for heat transfer. Their method required additional laboratory testing to find the membrane thickness, diffusivity and sorption correlations. In this chapter a method to find the moisture transfer effectiveness without additional testing utilizing the information usually given by the manufacturers is derived. Membranes are often tested in a standardized way. For example the standard ISO 12572: *Determination of water vapour transmission*. The results are the materials permeability (s/m) given by the mass flux and the difference in the vapour partial pressure over the membrane. In addition it is often possible to find properties as thickness, porosity and water content at given humidity levels (often soaked (100%) or 50% RH).

2.1.   Membrane based heat exchanger theory

If the heat of evaporation and the density are assumed to be constant the moisture transfer effectiveness may be expressed as (Zhang & Niu, 2002) :

$$\varepsilon_M = \frac{F}{F_{max}} \cong \frac{\dot{V}_E(\omega_{E,in} - \omega_{E,out})}{\dot{V}_{min}(\omega_{E,in} - \omega_{S,in})} = \frac{\dot{V}_S(\omega_{S,out} - \omega_{s,in})}{\dot{V}_{min}(\omega_{E,in} - \omega_{S,in})} \qquad (2.1.)$$

F is the flow rate of moisture from the exhaust air side to the supply air side (in cold climate). Note that the term efficiency and effectiveness denotes the same feature if the flow rates in each direction are equal. Niu and Zhang (2002) showed that the relationship between the effectiveness and a parameter called the *number of transfer units;* NTU, for moisture transfer followed the same form as for heat transfer. This means that the existing ε-NTU relations for heat transfer in heat exchangers may also be used for moisture transfer. ε-NTU relations for different exchangers are found in Kays and London (1964) or in Incropera and DeWitt (2007).

11

When evaluating moisture transfer with the ε-NTU method the only difference from heat transfer is the definition of the effectiveness given in 2.1. and the NTU-value:

$$NTU_M = \frac{U_M A}{\dot{V}_{min}} \tag{2.2.}$$

Where U_M is the overall moisture transfer coefficient and $\dot{V}$ is the flow rate of air through the exchanger. The relation between the effectiveness and the NTU is given as:

$$\varepsilon_M = f(NTU_M, flow\ arrangement, R) \tag{2.3.}$$

R is the ratio between the minimum and maximum air flow rates.

The relations must be found from experimental investigation and different empirical correlations may be found in the literature. The relation is either to be found as empirical equations or as tabulated values. An empirical relation for a cross flow arrangement is found in Kays and London(1964):

$$\varepsilon_{M,Cross\ flow} = 1 - e^{\left(\frac{1}{R}\right)*NTU_M^{0.22}*\left(e^{-R*NTM_M^{0.78}}-1\right)} \tag{2.4.}$$

For a counter flow arrangement the empirical relation under is found in (Incropera & DeWitt, 2007):

$$\varepsilon_{M,Counter\ flow,R=1} = \frac{NTU_M}{1 + NTU_M} \tag{2.5.}$$

$$\varepsilon_{M,Counter\ flow,\ R<1} = \frac{1 - e^{-NTM_M(1-R)}}{1 - R * e^{-NTU_M(1-R)}} \tag{2.6.}$$

To find the effectiveness for the relevant quasi counter flow arrangement a relation from previous work was used (Aarnes, 2011):

$$\varepsilon_{M,Quasi-counter} = \left(\frac{A_{Counter\ flow}}{A_{tot}}\varepsilon_{M,Counter\ flow} + \frac{A_{Cross\ flow}}{A_{tot}}\varepsilon_{M,Cross\ flow}\right) \tag{2.7.}$$

For a given geometry and air flow rates the effectiveness may be given from the previous equation if the overall moisture transfer coefficient is found. Different form the heat transfer calculation this value will in the moisture transfer case be dependent on the membrane material as the next chapter will show.

2.2.   Heat Exchanger Mass Transfer

The heat exchanger consists of of multiple membranes that separate the supply and exhaust air.
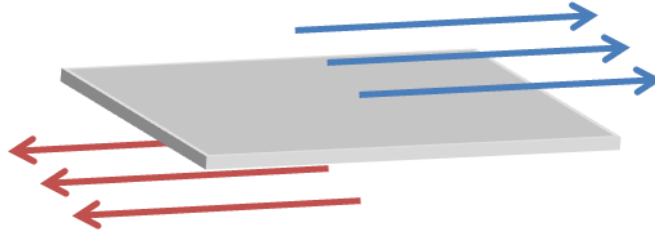
Figure 2.1.   *Flow over membrane.*

The transfer of water from the humid exhaust air side to the dry supply air side (for heating applications) consists of mainly two parts:

(1. Convection to/from the surface from/into the air steams. This part is given by the advection due to the fluid motion over the surface and the diffusion of water molecules in the air streams.
(2. Transport mechanisms inside the membrane material.

These two parts may be added in an overall mass transfer coefficient U_M:

$$U_M = [R_{conv} + R_{memb}]^{-1} \tag{2.8.}$$

Where R_{conv} is the mass transfer resistance connected to the convection and R_{memb} is the mass transfer resistance inside the membrane.

2.2.1. Convective moisture transfer

Convection may be divided into two main groups: forced convection and free convection. If the heat convection coefficient h is found, the mass transfer convective coefficient h_M may be found from the mass-heat analogy as described in Incropera and DeWitt (2007):

$$\frac{h}{h_M} = \frac{k}{D_{WA} \, Le^n} \tag{2.9.}$$

Where D_{WA} is the water diffusivity in air, k is the thermal conductivity and Le is the Lewis number. n is a constant usually set to 1/3. (Incropera & DeWitt, 2007)

Forced convection will be the combination of advection due to the bulk motion of fluid and diffusion of water molecules in the air. Free convection is mainly diffusion transport, but the same analogy as for forced convection may be used since the diffusion causes a change in density and by that a buoyancy effect. (Incropera & Dewitt, 2007)

In a heat exchanger there will always be a velocity present and the convection of heat and mass will then be a forced type. To find the heat transfer coefficient,h a Nusselt number correlation was used.

$$Nu_{D_h} = \frac{hD_h}{k} \tag{2.10.}$$

D_h is the hydraulic diameter. In fully developed laminar flow in a rectangular channel the forced convection Nusselt number is found from(Aarnes, 2011):

$$Nu_{Dh} = -7.4818 * \alpha^3 + 18.535 * \alpha^2 - 15.663 * \alpha \\ + 8.235 \tag{2.11.}$$

Where α is the aspect ratio (height of channel divided by the width). Using equation 2.10. the heat transfer coefficient h is found and may then be used to find h_M from 2.9.

The resistance R$_{conv}$ in equation 2.1. is then given as:

$$R_{conv} = \frac{1}{h_{M,S}} + \frac{1}{h_{M,E}} \tag{2.12.}$$

2.2.2. Moisture Transport through Membranes

The moisture transport resistance through a membrane is strongly dependent on the membrane material. There exist different classes of water permeable membrane materials. For use in a moisture transferring heat exchanger either a microporous or a nonporous hydrophilic membrane was found to be most favourable (Aarnes, 2011). The flow rate of water transported through a membrane is easily expressed as the total volume flow rate of air multiplied with the water vapour concentration difference from the inlet and outlet sides of the exchanger channels:

$$F = \dot{V}_S \rho_A (\omega_{S,out} - \omega_{S,in}) = \dot{V}_E \rho_A (\omega_{E,in} - \omega_{E,out}) \tag{2.13.}$$

Measurement of the water vapour concentration directly is difficult and there is more convenient to express the relation above in terms of the relative humidity difference.

The relation between concentration and vapour pressure is given by the perfect gas law:

$$pV = n\bar{R}T = \left(\frac{m}{M}\right)\bar{R}T \qquad (2.14.)$$

Where M is the molar weight and m is the mass, $\bar{R}$ is the universal gas constant and T is the temperature in Kelvin. The relative humidity is defined as the vapour pressure divided by the saturation pressure at the same temperature. The water vapour concentration is the mass of water in the air divided by the total volume of the air. If the temperature over the membrane is assumed constant 2.13. may be expressed as:

$$F = \frac{\dot{V}\left(\phi_{E,in} - \phi_{E,out}\right)p_s\,M_w}{\bar{R}T} \qquad (2.15.)$$

If the rate of change of concentration through each channel in the heat exchanger is assumed to be constant the moisture flux may be assumed to be given in terms of an arithmetic mean concentration difference and the overall mass transfer resistance in the membrane (Gibson, 2000):

$$F = \frac{\rho_A A \Delta\bar{\omega}}{R_{memb}} \qquad (2.16.)$$

Since it is more convenient to measure the vapour pressure than the concentrations of water vapour, the permeability constant, P may be introduced:

$$F = PA\Delta p_w \qquad (2.17.)$$

Assuming that the arithmetic mean concentration difference equals the difference over one side combining the equations above gives a relation between the permeability and the resistance. Applying the ideal gas law gives:

$$R_{memb} = \frac{M_w}{\bar{R}TP} \qquad (2.18.)$$

With this relation it will be possible to find the resistance and further the overall moisture transfer coefficient from given values for the permeability. Equation 2.18. shows that the resistance is dependent on temperature. However, the temperature dependency was assessed in an article by Gibson (2000). He investigated the temperature dependency of vapour transport through different membrane materials used in waterproof, breathable clothing. He found that the vapour transport resistance inside the membrane changed very little with temperature in the range from 3 - 40ºC. This may be explained from that the permeability is shown to increase with increasing temperature (Mondal et al., 2006) due to the increase in free volume radius. Looking at 2.18. the resistance will decrease with increasing temperature if

the permeability is constant. By using the permeability test temperature value in equation 2.18. the temperature dependency will be eliminated and the resistance may be assumed to be temperature independent since the partial pressure is dependent on temperature.

2.2.3. Humidity Dependent Resistance

The water vapour transport resistance was showed to be dependent on the mean relative humidity over the membrane. The relative humidity affected the amount of vapour content inside the membrane. And the water content in the membrane will affect the water vapour transport to a great extent. (Gibson, 2000) Since the relative humidity will vary through the membrane based heat exchanger, a mean moisture transport resistance was used to find the overall moisture transfer coefficient U_M. The normal operation area for such an exchanger in the Nordic climate is displayed in the figure below.
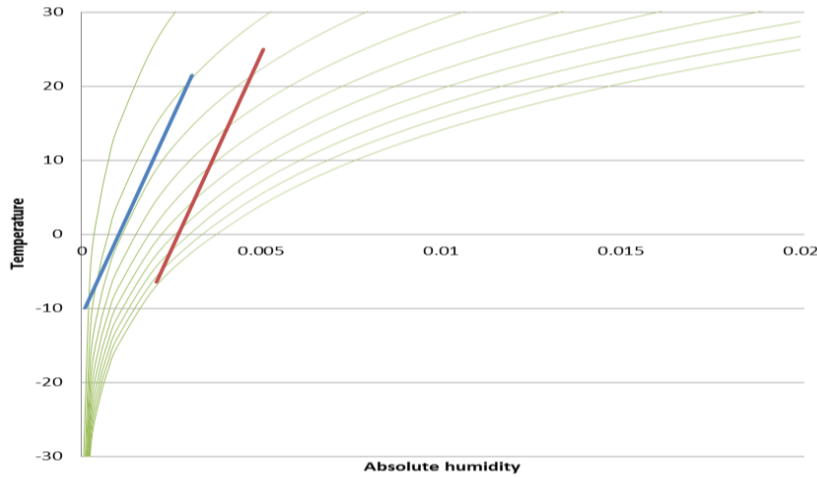
Figure 2.2.   *The normal operation area for a membrane based heat exchanger in cold climate. Green lines are relative humidity lines. The normal middle value is from RH approximately 30% to 80%.*

It was preferable to find a relation between the resistance and the mean humidity for different types of membranes:

$$R = f(\phi, \text{other relavant membrane properties}) \qquad (2.19.)$$

Assuming that the water diffusivity in the membrane material was constant it was possibly to see that the correlation from 2.19 follows the same shape for different materials. The relation between the solubility and permeability is given in 1.2. Results from the literature for different membranes are presented below. The sorption curves are displayed in the same form as the resistance assuming $R(\phi) \sim \frac{1}{S(\phi)}$.
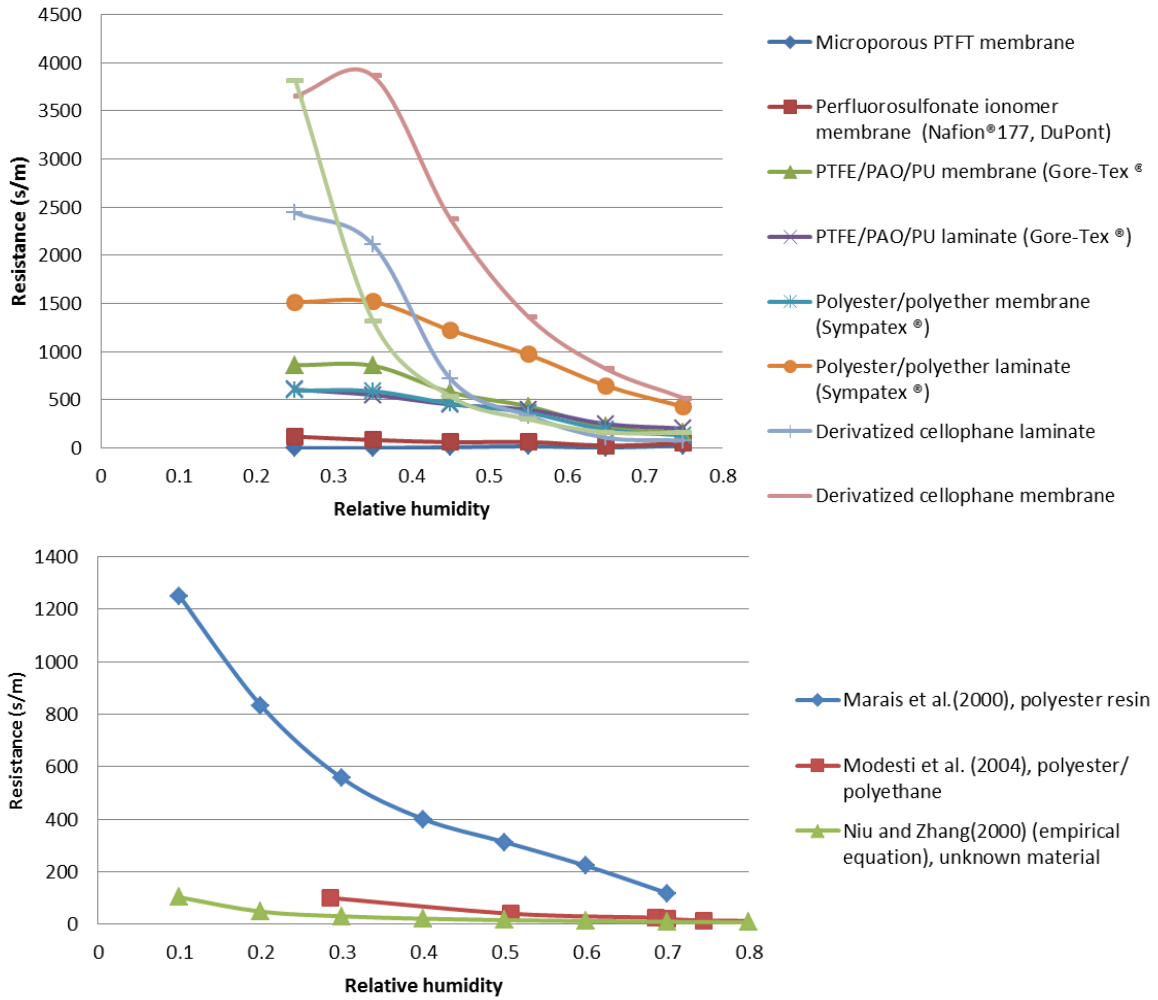
Figure 2.3.   *Upper: Results from Gibson(2000): water vapour transport resistance for different types of membranes for different humidities at 3°C. Lower: Resistance equivalent values from sorption curves from (Marais et al., 2000),(Modesti et al., 2004) and (Niu & Zhang, 2000).*

The literature shows that the relation follows the same form for all different materials, both porous and nonporous hydrophilic ones. As possible to see from the figure above the resistance for a soaked membrane (i.e. RH 100%) does not goes to zero, but an asymptotic value. A correlation of this form will give a good approximation of the relation between the humidity level and he resistance:

$$R(\phi) = A + Be^{-\phi C} \tag{2.20.}$$

However, to find the three constants A, B and C in this correlation three resistances and corresponding humidity levels need to be known. This may be difficult to find and a correlation with only two constants may be more useful. If a reference resistance is found a relation of this form may be used:

$$R = R_{ref}(1 - K + \frac{K\phi_{ref}}{\phi}) \qquad (2.21.)$$

Where K is a constant for a given membrane material. The value may be found from a second reference point.

$$K = \frac{\dfrac{R_{ref2}}{R_{ref1}} - 1}{\dfrac{\phi_{ref1}}{\phi_{ref2}} - 1} \qquad (2.22.)$$

Since only two points are given the resistance outlying from these points would be inaccurate. Especially if the two references are close to each other and the resistance level at interest is at another level than the two. The reference points will give the best result if they are quite far apart in humidity level. However, in most cases the only interesting points is between 30 to 80% RH according to figure 2.2. and there may be assumed that if the first reference point is between 100-60% and the second between 20-50% the results will be good enough for this use. To find the overall moisture transfer coefficient U_M a mean resistance value should be found. The inlet conditions are given in relative humidity. To find the mean humidity level in the exchanger the humidity should be converted to an absolute humidity because this will change linearly through the exchanger different form the relative humidity (see figure 2.2.).

$$\omega_{mean} = \frac{\omega_{E,in} + \omega_{S,in}}{2} \qquad (2.23.)$$

The relation between the absolute and relative humidity is given in Aarnes (2011):

$$\frac{\phi_{mean}}{\omega_{mean}} = \frac{6.19 * e^{\frac{5427}{T}}}{10^7} \qquad (2.24.)$$

The mean resistance is then found from:

$$R_{mean} = R_{ref}(1 - K + \frac{K\phi_{ref}}{\phi_{mean}}) \qquad (2.25.)$$

If a permeability test is run and the permeability is given as in equation 2.17 the reference resistance is given in 2.18. However, permeability test results are not always available, and there is seldom possibly to find more than one reference resistance from permeability tests. This means that there will be preferable to find the resistance from other means as well. For a microporous membrane the resistance is a function of the porosity and the possibility for the water vapour to diffuse through the tiny air filled pores. Since the resistance is dependent on both sorption resistance and diffusion resistance the reference point should be found when the membrane is

soaked (RH 100%) then it is possible to assume that the sorption resistance is zero. The R_{min} may in this case be expressed as:(Yeh & Chang, 2005)

$$R_{min} = \frac{\tau t}{D\varepsilon} \qquad (2.26.)$$

D is the diffusion coefficient or water vapour in air, ε is the porosity, τ is the tortuosity and t is the thickness of the membrane. The tortuosity may be eliminated by a correlation between the porosity and tortuosity (Alves & Coelhoso, 2004):

$$R_{min} = \frac{(2-\varepsilon)^2 t}{D\varepsilon^2} \qquad (2.27.)$$

For a nonporous membrane the R_{ref} must be found from other relations. All models found to predict the water vapour sorption for different materials build on experimental data. For instance the Guggenheim–Anderson–de Boer model (Huang et al., 2004) includes three different constants found from experimental investigation. Another model used in calculations for a membrane based heat exchanger was derived by Niu and Zhang (2000):

$$R = \frac{t10^6 \left(1 - C + \frac{C}{\phi}\right)^2 \phi^2}{D_{wm} e^{\frac{5294}{T}} \theta_{max} C} \qquad (2.28.)$$

The relation between the water content in the membrane and humidity needs to be known to find the sorption constant C. θ_{max} is the maximum amount of water the membrane will hold(kg water/ kg membrane). D_{wm} is the diffusivity of water in the membrane.

If a reference value is found:

$$R_{ref} = \frac{t10^6 \left(1 - C + \frac{C}{\phi_{ref}}\right)^2 \phi_{ref}{}^2}{D_{wm} e^{\frac{5294}{T}} \theta_{max} C} \qquad (2.29.)$$

$$\theta_{ref} = \frac{\theta_{max}}{1 - C + \frac{C}{\phi_{ref}}} \qquad (2.30.)$$

If a sorption test at a second reference humidity is done the resistance for that humidity levels if found from:

$$R_{ref2} = \frac{R_{ref1}}{\left(\frac{\theta_{ref2}}{\theta_{ref1}}\right)^2 \left(\frac{\phi_{ref1}}{\phi_{ref2}}\right)^2} \qquad (2.31.)$$

2.2.4. Evaluation of the empirical relation

The approach derived in the previous chapter used and compared to the results form Gibson (2000). He tested several membranes for the dependency on resistance on relative humidity. See figure 2.3.

McCullough et al. (2003) tested several fabrics after different permeability testing standards. Two of them were *Sympatex®* from *Akzo-Nobel* and *Gore-tex®* from *W.L. Gore & Associates*. The first is a nonporous hydrophilic membrane and the latter is micro porous. The vapour flux found from ASTM E 96 B (ASTM, 2011) and JIS L 1099 (JSA, 1999) in the article by McCullough et al (2003) were used to find two reference resistances at 75% and 100% (soaked membrane) relative humidity respectively. The resistance in the air layer in the ASTM E 96 B-method was approximated after the relation:

$$R_{air} = \frac{d}{D_{wA}A} \approx 500 \; s/m \qquad (2.32.)$$

Where d is the height of the air layer, D_{wA} is the diffusivity of water vapour in air and A is the test cup opening area. The comparison between the proposed method and the result from Gibson is shown below:
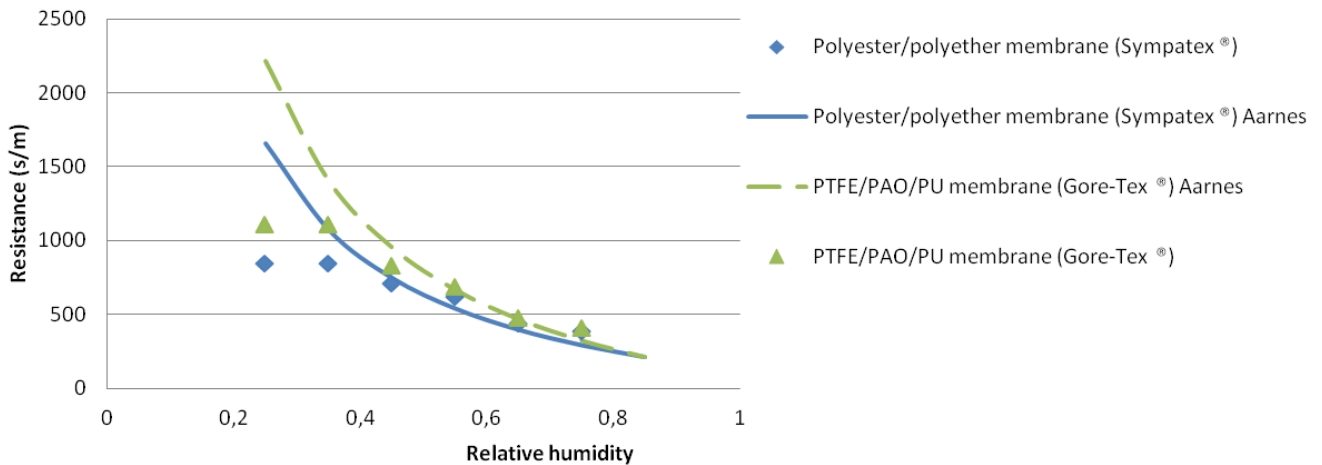
Figure 2.4.   *Comparison between measured values by Gibson(2000) and empirical relations by the author.*

The model seems to fit quite well for humidities over 40% with the results from Gibson (2000).

The porosity of the *Nafion®117* membrane from *DuPont* was showed to be 52±5% (Chen et al., 2008) and was used to find a reference resistance at 100% RH from 2.27. A sorption curve for different humidities was found in (Peron et al., 2010). Values at 20 and 100% RH were used to find a resistance form the sorption model (2.31.).
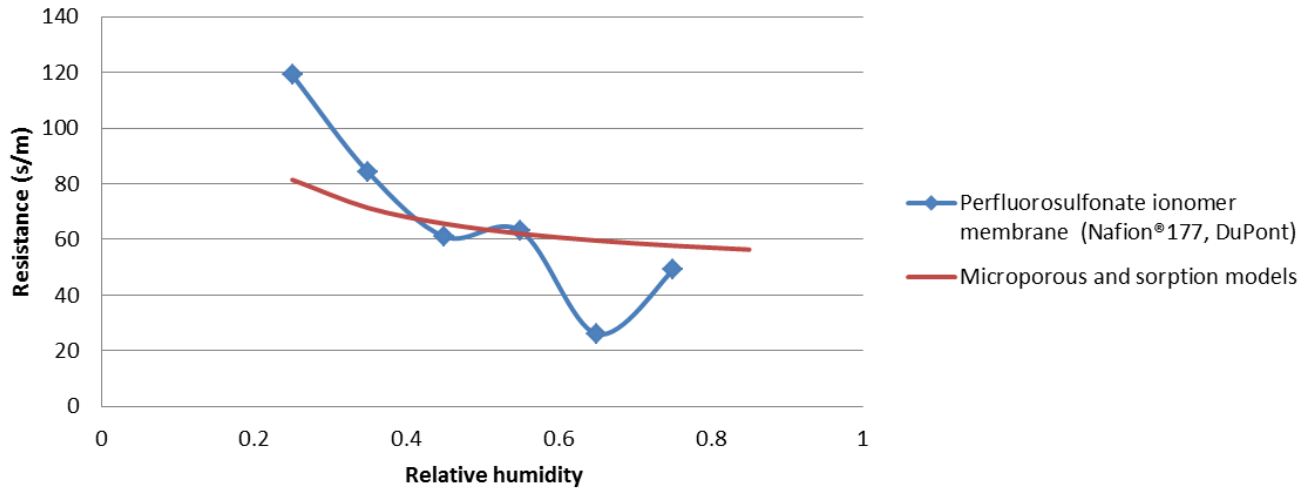
Figure 2.5.   Comparison between measured values by Gibson (2000) and empirical relations by the author.

The model does also in this case fit very well with the results from Gibson (2000) for humidity levels between 40 and 60%.

2.3. Practical use of the mathematical model

For practical use of the model a simple program written in Visual basic language called *HXcalc* was written. The software used was *Microsoft Excel 2010*. This is an extension to the simple program *HXOpt* made in previous work (Aarnes, 2011). The program code is to be found in appendix A.3. The user interface has many dropdown choices for: changing parameter, geometry, membrane resistance calculation method, energy effectiveness weather data location etc. A print screen picture of the input interface is showed here:

Figure 2.6. *User interface of the input sheet in the developed HXCalc program. The white boxes are to be filled in by the user.*

After clicking the "Run simulation!" button the temperature effectiveness, moisture transfer effectiveness (if "Membrane HX?" is set to "Yes") and the annual heat recovery efficiency will be displayed in a separate worksheet named "Results" as graphs where the effectiveness is the y-values and the chosen "Parameter to change" as the x-axis. The results will appear as points. Clicking on a single point will make a

separate window appear. The window includes a drawing of the exchanger with additional information from the conditions given in that point. See example below:
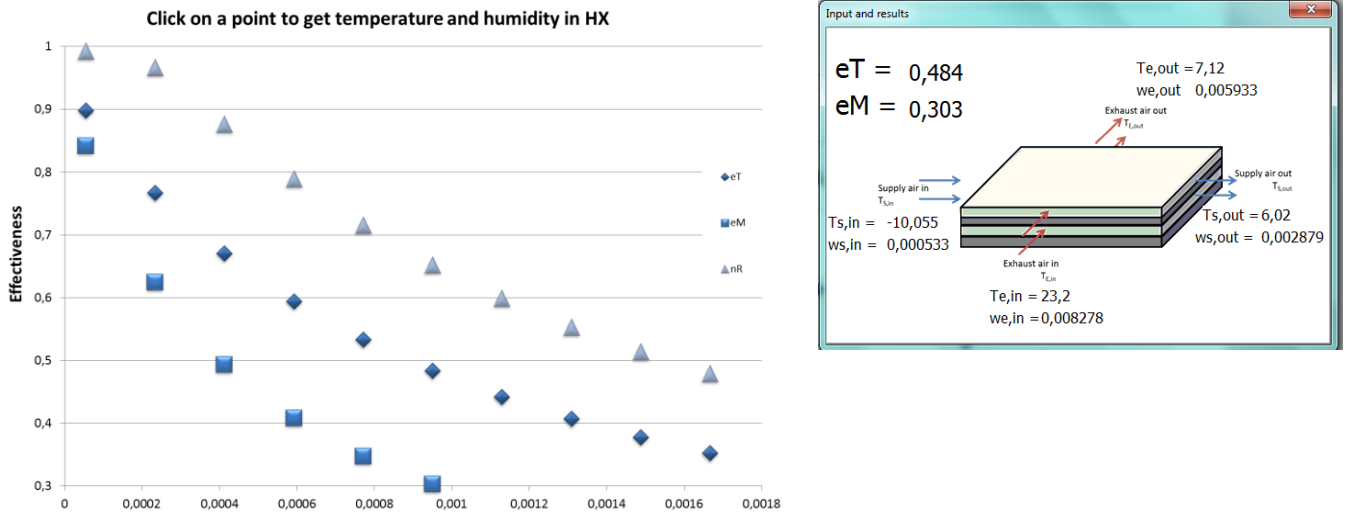
Figure 2.7.   Results sheet after clicking on a single point. An information window appears.

In addition will a second result sheet called "Hum-temp" update when clicking on point in the "Result" sheet. In this chart the input and output temperature and absolute humidities will appear as lines (between inlet and outlet values) in a temperature-humidity diagram. These lines indicate the temperature and humidity development through the exchanger. See picture below for the same case as the picture above:
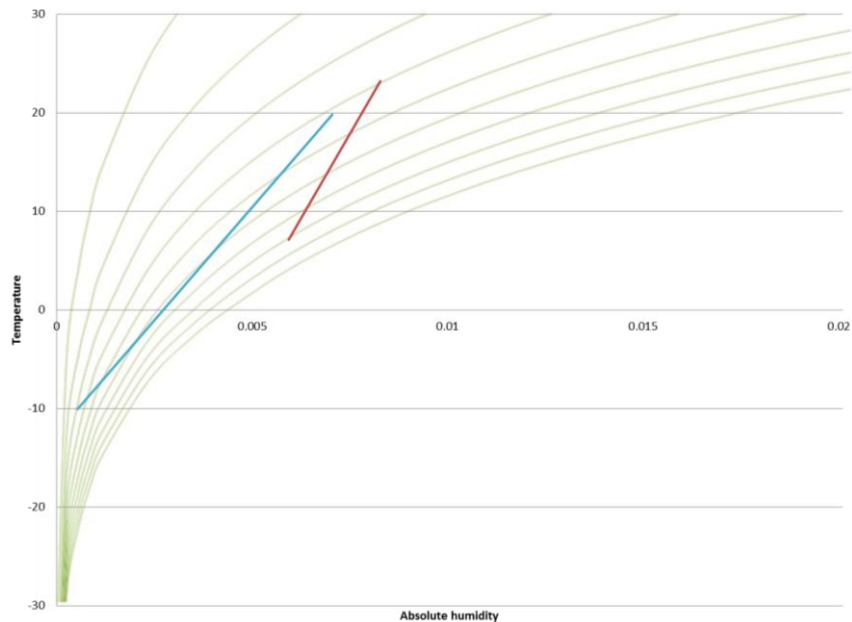
Figure 2.8.   Results sheet after clicking on a single point. An information window appears.

2.4.   Evaluation of the Method in HX Applications

The moisture transfer effectiveness calculation method derived in the previous chapters was compared to the results in an article by (Kadylak et al., 2009). In this case only the moisture transfer effectiveness was addressed hence the article addressed the effectiveness of a humidifier operating in a proton exchange membrane fuel cell. Kadylac et al.(2009) took their starting point in Zhang and Niu's(2002) method to calculate the moisture transfer effectiveness in a flat plate heat and moisture transferring heat exchanger.

Two reference points for the mean resistance values were found from the relation in 2.28. The C value was set to 10. Then the mean resistance was found from equation 2.25. The results comparing to both Kadylac et al. (2009) and Niu and Zhang's (2000) results are displayed below:

Simulation input values:	
LC	0.5m
H	0.145m
Nr of plates	29
D_{WM}	$2.16 * 10^{-8}$
$\dot{V}$	0.039 m^3/s
C	10
$T_{s,in} = T_{E,in}$	70.15 $^{\circ}$C
Θ_{max}	0.23 kg/kg
δ	20 μm
$\Phi_{E,in}$	100%
Le	1.2
k_{air}	0.0263 w/mK
ρ_{air}	1.17 kg/m^3
v_{air}	1.33*10^{-5} m^2/s
cp_{air}	1010 J/kgK
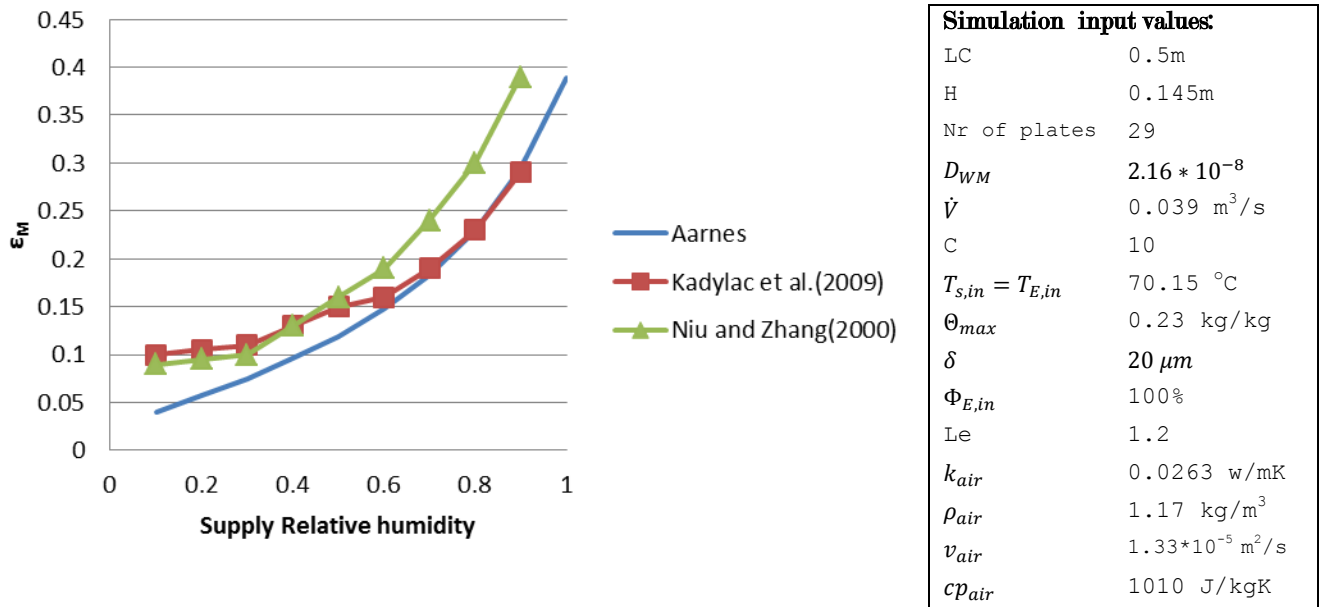
Figure 2.9.   Comparison between the moisture transfer effectiveness calculations methods on changing supply inlet relative humidity from Aarnes, Kadylac et al.(2009) and Niu and Zhang(2000).

As seen the derive method has the same evolution as the results from Niu and Zhang (2000), but the results are a bit lower value. At high humidities the method correlates well with Kadylack at al.'s (method).

Second the dependency on the flow rate was compared to the article by Niu and Zhang (2000). The results are shown below:
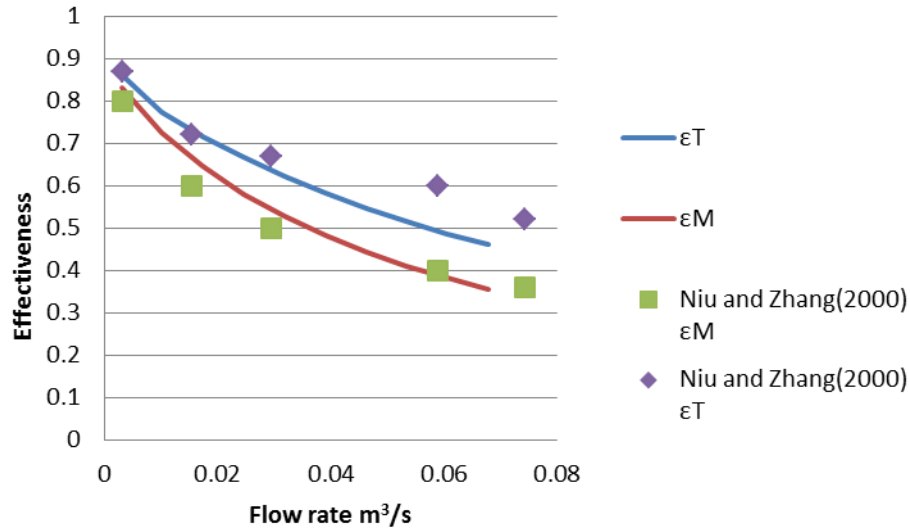
Figure 2.10. *Comparison between the derived model and results from Niu and Zhang (2000) for changing flow rate.*

The results above have the same input values at the previous case. The proposed model correlates well with the model of Niu and Zhang (2000) for this specific example. The temperature effectiveness is not dependent on temperature, different from the moisture transfer effectiveness. A comparison was done, still with the same inputs as over, for different supply inlet temperatures and a supply inlet humidity kept constant at 50%. The results were again compared to the result in the article by Niu and Zhang (2000):
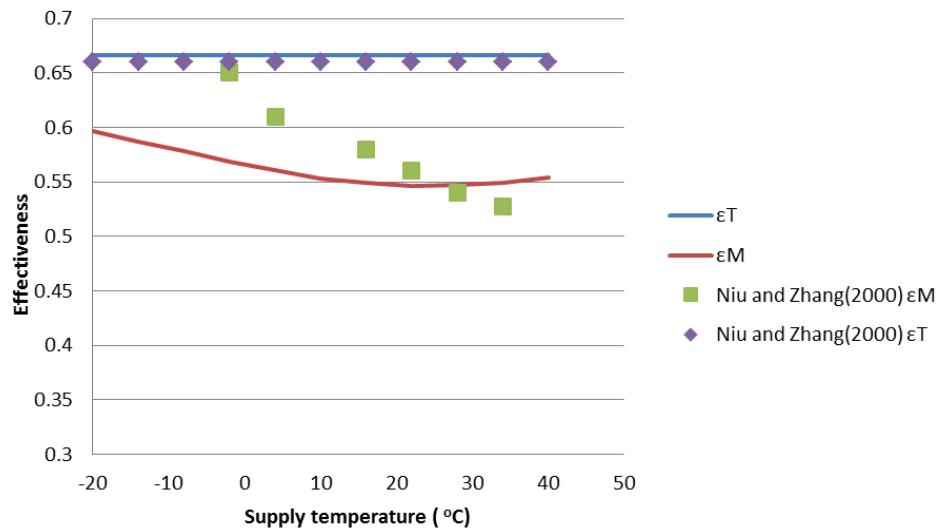
Figure 2.11. *Comparison between the derived model and results from Niu and Zhang (2000) for changing supply inlet temperatue.*

The models do not correlate well regarding the moisture transfer effectiveness dependence on temperature. As seen is the proposed model less sensitive to changes in supply inlet temperatures than the model by Niu and Zhang (2000). The reason is probably that the derived model uses a mean value for the moisture transfer resistance while Niu and Zhangs' (2000) model is iterative and may then take into account differences in humidity through the exchanger.

The annual heat recovery efficiency from the method derived in the previous work by the author (Aarnes, 2011) was included in the program *HXcalc.* Zhang and Niu (2001) derived a method to predict the annual energy savings using a membrane based heat exchanger. A simulation with the same inputs as used in the article by Zhang and Niu (2001) was done. The weather data used was from Hong Kong and was found at the website of the American Energy Department[1]. Under are the results compared when only looking at energy for heating. The two methods seem to correlate very well. The author's model gave a bit higher resulting values; this is probably because the model from Zhang and Niu (2001) did not take into account heating in the summer months as the author's model.
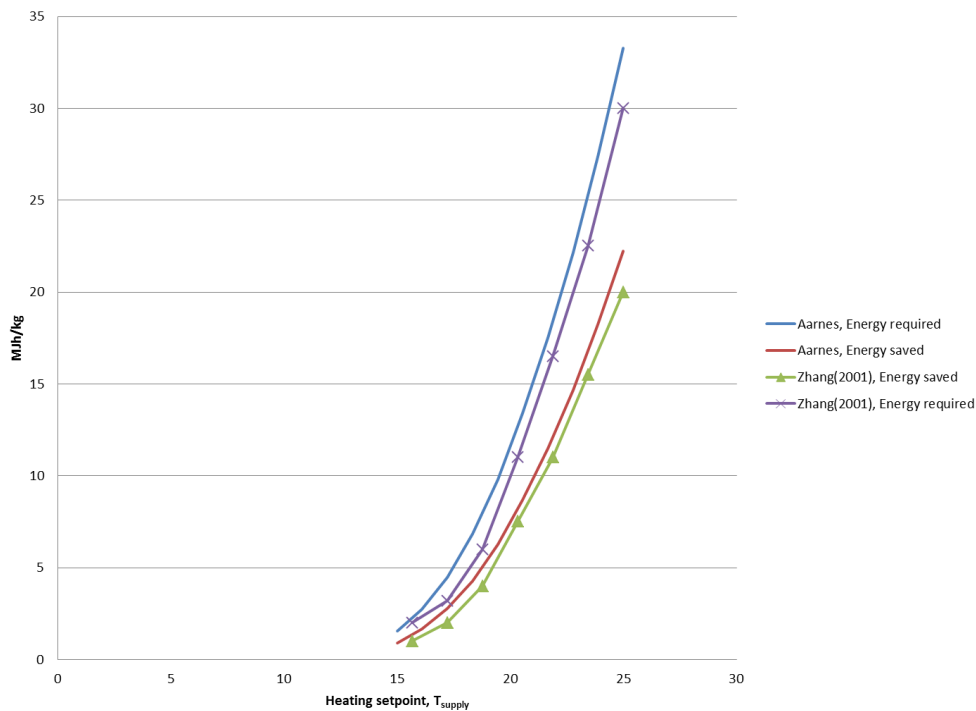
Figure 2.12. *Required and saved energy for heating. Comparison between the derived model and results from Niu and Zhang (2000).*

[1] «Department of Energy: EnergyPlus Energy Simulation Software: Weather Data: China.», Quoted: 06.06.12,
http://apps1.eere.energy.gov/buildings/energyplus/cfm/weather_data3.cfm/region=2_asia_wmo_region_2/country=CHN/cname=China

Chapter 3

Experimental Investigation: Method

The objective of the experimental part of this work was to compare a plastic based heat exchanger to a membrane based heat exchanger due to the problems of condensation and freezing in cold climate conditions. The fundamental hypothesis for the development of the test method was: *When ice and frost is formed inside the exhaust air channels in a heat exchanger the pressure drop over exchanger on the exhaust air side will rice. The pressure drop on the supply air side will remain constant through the test period.*

In addition the test rig was used to perform experiments that could be compared to the mathematical method derived in the previous chapter.

3.1. Development of the Test Rig

A test rig was built to compare the frost formation in two plastic sheets and a membrane based heat exchanger. The test conditions should be as stable as possible over the test periods and it was preferable to have quite large differences in both humidity and temperature level in the supply air and exhaust air sides respectively.

3.1.1. Supply Air Side

The supply air was taken from the lab and blown through the cooling coils with a 12V axial computer fan. The air flow rate was regulated by covering the inlet area to the fan with air tight tape. Two cooling coils in series with glycol as the chilled fluid were used to cool down air on the supply air side. The initial testing of the cooling coils is described in appendix A.1. The glycol was cooled down to -25°C. The long distance between the glycol compressor and the cooling coil gave an immense temperature loss and the coldest outlet air temperature measured at the outlet of the cooling coil was about -15°C. The lack of space in the lab made it necessary to build about 2.5m of ducts from the cooling coil to the heat exchanger. Plastic ducts of 3cm diameter were used and isolated with *Armaflex* (synthetic rubber isolation for ducts) from *Glava*. Due to the very low velocity inside the ducts it was impossible to insulate the ducts well enough to conserve the cold temperature. When reaching the heat exchanger the temperature had riced to about -4 to -10°C depending on the air flow rate. The humidity and temperature probes were placed in square shaped ducts made out of stainless steel plate. The ducts worked also as air straighteners before and after the heat exchanger, supplying the air flow as even distributed as possible.

One centimetre from the channel opening, close to the heat exchanger a thin pipe was welded to the channel and a small hole was drilled through the channel wall. This was used to measure the static pressure over the heat exchanger. Due to ice formation inside the cooling coil the air flow rates decreased after approximately 12 hours. The tests were therefore ended after 12 hours.

3.1.2. Exhaust Air Side

Heating and moisturising of air to simulate the exhaust air side was done inside a "climate chamber" box built of 40mm thick polystyrene plates. By taking some of the cold air from the cooling coil the inlet air to the "climate-chamber" was stable regarding temperature and humidity. A bucket of water with a 300W heating element and a thermocouple coupled to a PID regulator was used to humidify the air. By regulating the water temperature in the water bucket both temperature and humidity were controlled since the inlet temperature and humidity were practically constant. See the picture below.
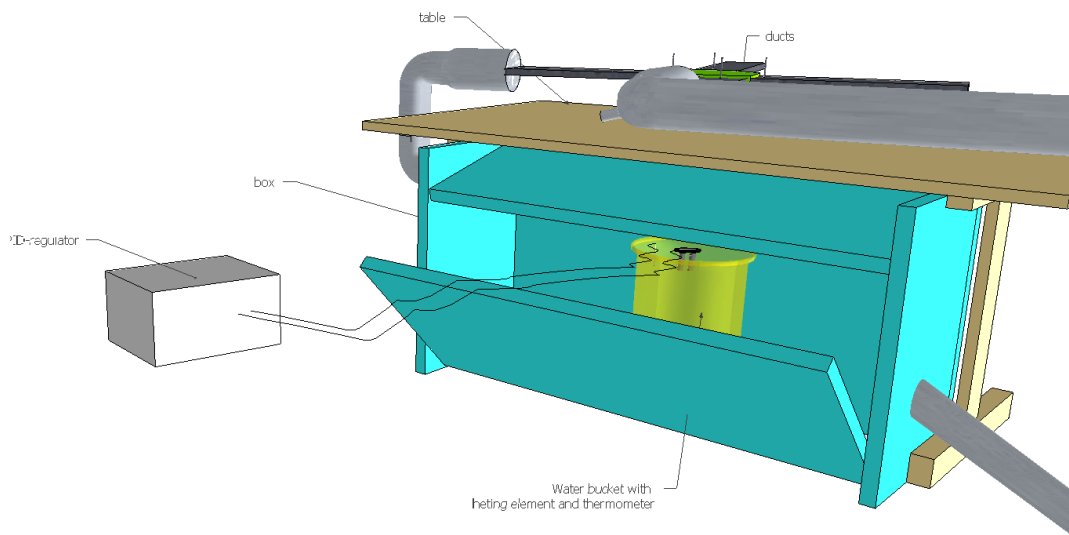
Figure 3.1.   *Drawing made in Google Sketch Up. The exhaust air was heated and humidified in a polystyrene box placed under a table to make the rig as compact as possible. The duct to the lower right was connected to the cooling coil.*

A dimmer was connected to the heating element to regulate the temperature of the water. To get a stable temperature and humidity levels it was preferable to have the same effect from the heating element at all time. The heater was dimmed to give a water temperature at 34ºC. This gave an exhaust temperature at approximately 22 ºC and humidity at approximately 42% RH. The PID-regulator had a set point at 40 ºC to protect the bucket from dry-out. A small axial computer fan with 12V power supply was attached at the inlet of the exhaust air supply duct. This was made out of a 10cm diameter spiro-channel insulated with an aluminium foil covered fibre glass insulation mat from *Glava*. The spiro-channel was attached to a rectangular duct

described in the previous chapter. An identical duct was placed in the opposite side of the heat exchanger.

3.1.3. Small Scale Heat Exchanger Prototype

The heat exchanger was build up with a frame made of two hexagonal shaped 6 mm transparent acrylic plastic plates. Two 3mm bends cut out from a Lexan plate were glued to each hexagonal plate using epoxy glue. Four more bends of 6mm Lexan were also cut out. The first membrane layer was connected to the frame base layer using double sided tape. The construction was built like a sandwich with Lexan bends and membranes as seen in the picture below. For the first test this prototype was used. However, for the rest of the experiments eight new bends, now of 3mm Lexan were made to increase the membrane layers from 3 to 5. The mechanical drawing of the prototype frame is to be found in Appendix A.5.
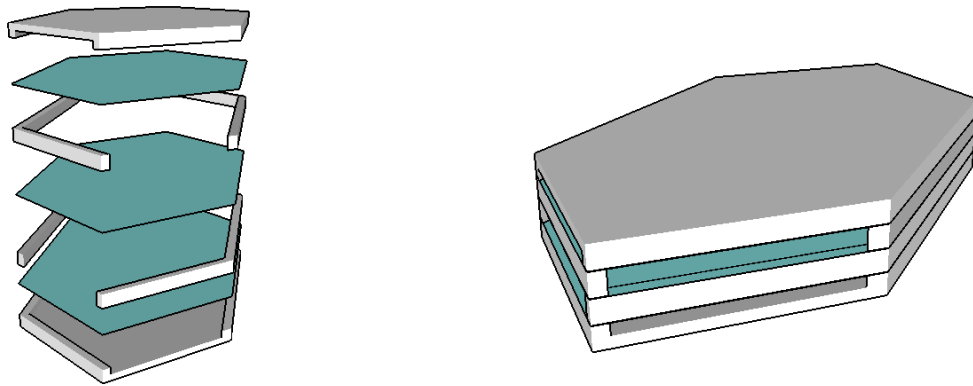
Figure 3.2.   Heat exchanger made of sandwich construction. Drawing of concept in Google Sketch Up. 3 layer prototype.

Three different types of heat exchanger plate materials were tested. Two non-permeable "plastics" and one membrane with high permeability to water vapour. Properties of the materials are shown below:

Table 3.1.   Properties for the different tested plate materials.

Material	Manufacturer	Water permeable	Elastic	Crumples in high humidity
Transparent overhead sheets	*Optimax*	No	No	No
PP	*DuPont*	No	Yes	No
Membrane X	*DuPont*	Yes	Yes	Yes

The transparent overhead sheet from *Optimax* was non-elastic and quite stiff. This made it easy to construct the heat exchanger prototype. The PP-sheets and membrane from *DuPont* were much more difficult to handle in the construction of the prototype exchanger. Results from permeability tests for the membrane were given in datasheets from the manufacturer. These values will not be given in this report due to

29

confidentiality, neither will the actual name of the membrane (therefore is it called *X*). The *PP*-sheets were actually the protection layer for the membrane. This material was used since the appearance was very similar to the membrane. The material was probably polypropylene since it was written *PP* on the sheets. The heat exchanger was placed in a die made from the four rectangular ducts and made air tight with a sealing compound. An isolation mat was placed on top of the heat exchanger under the experiments to minimize the temperature loss to the surroundings. See picture below:
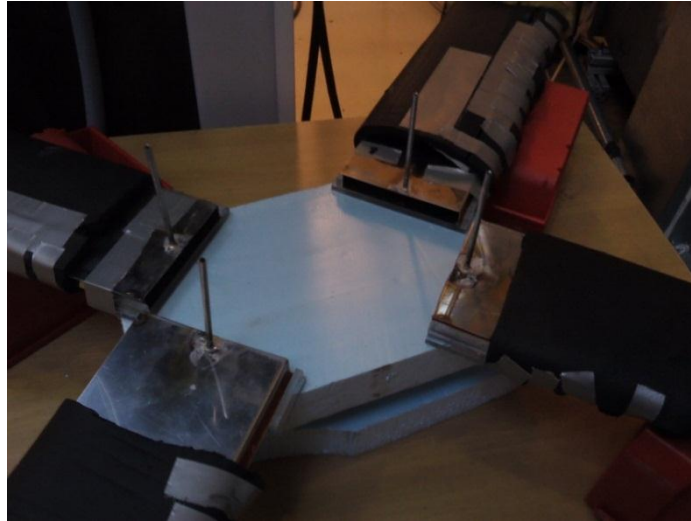
Figure 3.3.   Die for placing of the heat exchanger. The rectangular ducts with pressure measurement pipes are shown.

3.1.4. HSE

A HSE report was written before the experiments were run. The whole report is to be found in Appendix A.6. The biggest risk was connected to the use of the ethylene glycol loop used to chill the supply air (leakages, pipe rupture etc.). The risks were found to be acceptable to run the experiments.

3.2.   Measurement and Instruments

To measure temperature and humidity four instruments from *Vaisala* were used. Three of them were of the type *HMP 233* and the last was of the type *HMT 334*. The probes could measure both humidity and temperature. They were mounted perpendicular to the air streams in each of the rectangular ducts receiving and supplying air from and to the heat exchanger. The pressure drop over the heat exchanger was measured with two micro manometers from *DPM*. The relative humidity and temperature of the surroundings and the supply air outlet velocity were logged with the *TSI Velocicalc 9555-P* instrument. The accuracy of the instruments is shown in the table below:

Table 3.2.   Uncertainty of measurement instruments used in experimental set up.

Manufacturer	Model name	Measurement	Instrument Uncertainty
Vaisala	*HMP 233*	Relative humidity Temperature	±2% (3% for 90-100%RH) ±0.1°C
Vaisala	*HMT 334*	Relative humidity Temperature	±(1+0.008*reading) %RH ±0.2°C (at 20°C), ±0.3°C (at -10°C)
DPM	*TT470s*	Pressure drop	±1% of reading ± 0.1Pa +analogue output: ±0.3%
TSI	*Velocicalc 9555-P*	Relative humidity Temperature Velocity	±3% ±0.3°C ±max(3% of reading, 0.015m/s)

The humidity probes were calibrated with a LiCl-salt solution and against a reference value given by the TSI-instrument in a high humidity chamber (the polystyrene box with the humidity and heating bucket). The most important reason for this calibration was to make sure that the four different humidity probes were calibrated against each other, so that the difference between the inlet and outlet humidity level was as accurate as possible. The instruments were not calibrated for temperature measurements since this accuracy was good in the first place.

The flow rates were not possible to measure with any availiable instruments due to the very low air flow rates. Since velocity measurement by traversing over the ducts with a velocity measurement instrument was found to be to inaccurate a manual method of measuring the air flow rates was used: A plastic bag was hold tight over the air outlet for 10-20 seconds measured with a stop watch. The bag was then quickly removed and the opening twisted. The bag was then put into a bucket of water to find the air volume. The measurements were made several times to find an average value.

The humidity and temperature probes and the two micro manometers were connected to a computer via a serial bus. The program *LabView* was used to transform the analogue signals to preferable variables and log the results. The pressure drop, humidity and temperature were logged every second. The surrounding humidity and temperature were logged by the *Velocicalc* every 10 minutes (averaging by the instrument). *Microsoft Excel* was used to process the outputs into readable charts and averages. The measurement set up is shown in the figures below and at the next page:
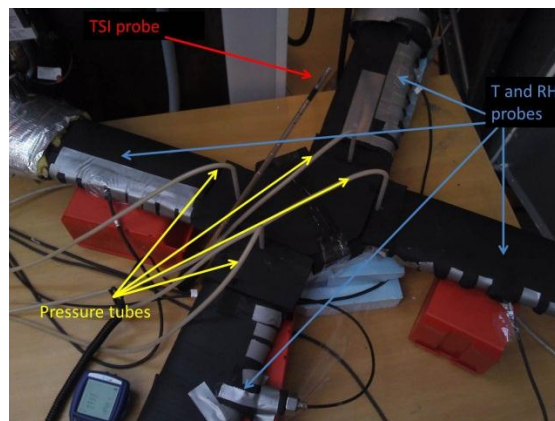
Figure 3.4.   Measurement set up.
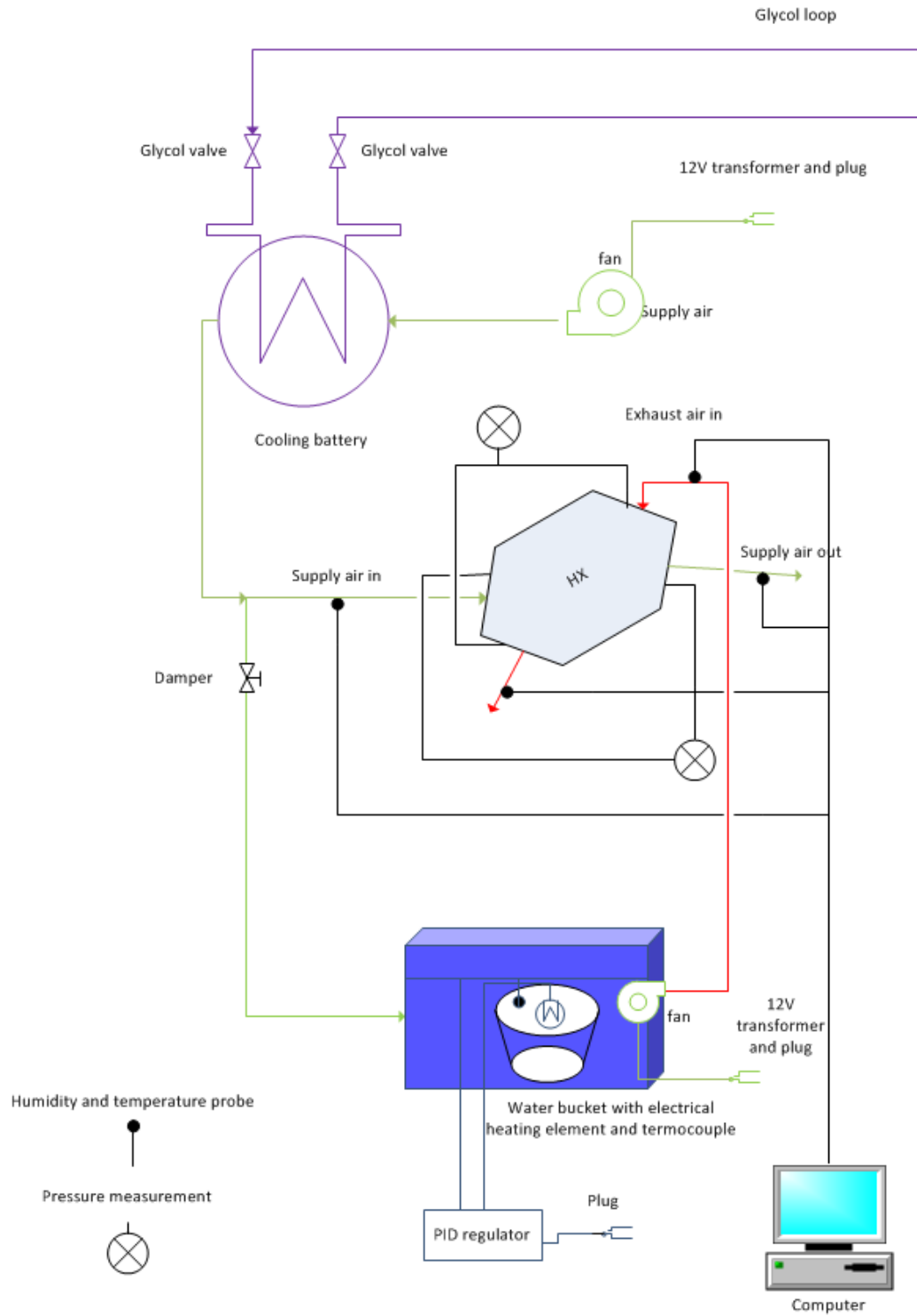
Figure 3.5.   Flow chart of the experimental set up.

3.3. Uncertainty

The uncertainty of the experimental investigation was connected to the reliability and the accuracy of the measurement instruments and the use of them. The relevant uncertainty can be divided into two separate parts(Novakovic et al., 2007):

1) Random uncertainty. Instrument accuracy, influence from other sources etc.

2) Systematic uncertainty- measurement calibration and upset of instruments etc.

An example of random uncertainty is shown in the picture below. The picture shows the pressure drop results, a part of the *LabView* interface during an experiment. The peak shows random uncertainty.
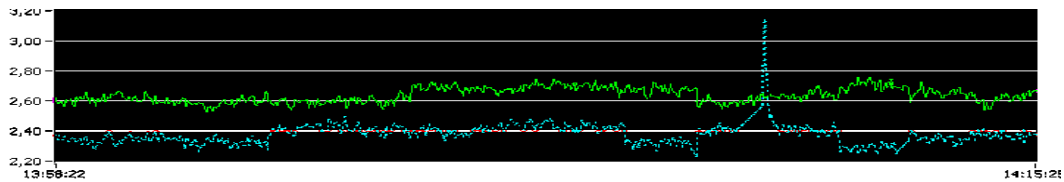
Figure 3.6.   Random uncertainty in the pressure drop measurement. Print screen from LabView Front Panel interface.

The standard deviation tells something about how the measurements will vary about the "true" value. The standard deviation may then be found from:

$$s = \sqrt{\frac{\sum(x - \bar{x})^2}{(n-1)}}$$

(3.1.)

Where $\bar{x}$ is the mean value and n is the number of measurements. Since the pressure drops, especially on the exhaust air side, changed trough the test period (in some experiments) using the variation about a mean value for the pressure drop would lead to a to larger standard deviation for the random uncertainty than it actually was. Therefor was this relation used instead of 3.1.:

$$s = \sqrt{\frac{\sum(x - \tilde{x})^2}{(n-1)}}$$

(3.2.)

Where $\tilde{x}$ is the "true" pressure drop given in a certain time step by a linear trend line describing the increase in pressure drop with time. This trend line is found by the

trend line tool in *Excel.* The supply air and exhaust air side pressure drops are shown in the figure below.
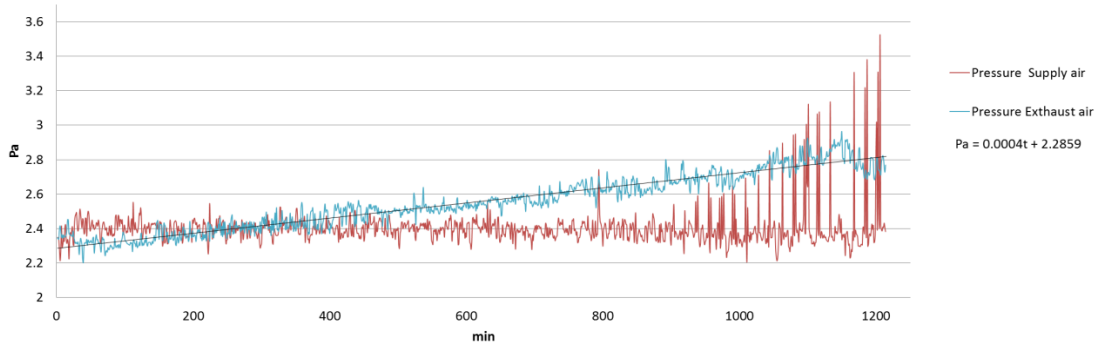
Figure 3.7.   *Pressure drop measurement. A linear trend line equation for exhaust air pressure drop is displayed to the right.*

The pressure drop was logged every second. If the hole time period is taken into account:

- Exhaust air side pressure drop standard deviation: **0.0621 Pa**
- Supply air side pressure drop standard deviation : **0.2228 Pa**

Since the random uncertainty seemed to increase a great deal after 900 min it may only be interesting to look at this first part. If the standard deviation only takes into account the first 900 min:

- Exhaust air side pressure drop standard deviation: **0.0536**
- Supply air side pressure drop standard deviation: **0.0637**

It appeared that the random uncertainty was less for the exhaust air measurement than the supply air measurement. This may be explained by that when the battery capacity was low the analogue output signals from the micro manometers were greater than if the battery was full. This seemed as a reasonable cause seen that the random uncertainty increased with time (ref. figure 3.7.).

Random uncertainty for the mean value is calculated as:

$$U_r = \pm \sqrt{\frac{\sum (x - \bar{x})^2}{(n-1)n}} = \pm \frac{s}{\sqrt{n}} \qquad (3.3.)$$

The systematic uncertainty may consist of different parts. The first is the one that is given by the manufacturer. This uncertainty is given in table 3.2. The systematic uncertainty for the resulting parameters as the efficiency will also be given by the difference in the calibration of the different humidity and temperature probes. This is possibly to see in this picture:
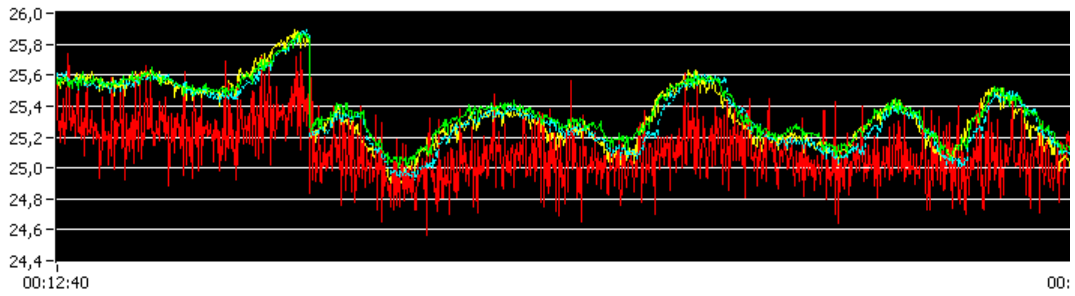
Figure 3.8. *Humidity level measurement. Chart from LabView interface. The graph shows the humidity level at the same sport for the four different Vaisala probes. The HMP3 probe gives a lower value of the humidity than the other probes, about 0.3%.*

The total uncertainty is then:

$$U_T = \pm\sqrt{U_r^2 + U_s^2} \qquad (3.4.)$$

Since the measurements were logged every second and the experiments were run for more than 12 hours the random uncertainty was ignorable compared to the systematic uncertainty for temperature, humidity and pressure as shown in appendix A.4.

For the air flow rate measurement, which was manually done by a plastic bag, a stop watch and a bucket of water, the uncertainty was of the combined type.

$$\dot{V} = \frac{volume\ of\ bag}{time} \qquad (3.5.)$$

Since the volume was manually found from between litre marks on the buckets the systematic uncertainty from manually readings may be set to ±0.2 l. The systematic uncertainty from the time to connect and release the bag from the duct outlet and the start and stop of the stopwatch may be set to ±0.5 sek.

Table 3.3. *Uncertainty of parameters in manual flow measurement method. Numbers from experiment 1.*

Time (s)	$\bar{x}_t = 10.0325$	Volume (l)	$\overline{x_V} = 4.4$
10.17	$s_t = 0.1765$	4.6	$s_V = 0.1414$
9.88	$U_{Rt} = \pm0.088$	4.3	$U_{RV} = \pm0.07$
9.88	$U_{St} = \pm0.5$	4.4	$U_{SV} = \pm0.2$
10.12	$U_t = \pm0.5077$	4.3	$U_V = \pm0.2121$

The uncertainty of an assembled result parameter is given from (Novakovic et al., 2007):

$$U_r = \pm \sqrt{\left(\frac{\partial f}{\partial u_1} \Delta u_1\right)^2 + \left(\frac{\partial f}{\partial u_2} \Delta u_2\right)^2 + \cdots} \qquad (3.6.)$$

For the flow rate measurement:

$$U_{\dot{V}} = \pm \sqrt{\left(-\frac{\bar{V}}{\bar{t}^2} U_t\right)^2 + \left(\frac{1}{\bar{t}} U_v\right)^2} = \pm 0.031 \;{}^{l}/_{sec} \qquad (3.7.)$$

$$= \pm 0.11 \;{}^{m^3}/_{h}$$

The flow rate for the example in table 3.3. is then 1.58 ± 0.11 m³/h.

The relation between the absolute humidity (used to find the moisture transfer efficiency) and the relative humidity was derived for 0°C in the project report by the author. (Aarnes, 2011):

$$\omega = \frac{\phi * 10^7}{6.19 * e^{\frac{5427}{T}}} \qquad (3.8.)$$

$$U_\omega = \pm \sqrt{\left(\frac{\partial \omega}{\partial \phi} U_{T\phi}\right)^2 + \left(\frac{\partial \omega}{\partial T} U_{TT}\right)^2} \qquad (3.9.)$$

$$U_\omega = \pm \sqrt{\left(\frac{10^7}{6.19 * e^{\frac{5427}{T}}} U_{T\phi}\right)^2 + \left(\frac{\phi * 10^7 * \frac{5427}{T^2}}{6.19 * e^{\frac{5427}{T}}} U_{TT}\right)^2} \qquad (3.10.)$$

For the temperature efficiency the most accurate results were found when the temperature difference at the exhaust air side was used in the temperature efficiency relation. The reason was that the temperature loss to the surroundings was greater on the supply air side than on the exhaust air side. For the moisture transfer efficiency it was assumed to be no loss to the surroundings. The efficiencies for moisture transfer and heat transfer for the exhaust air side are given as:

$$\eta_M = \frac{\omega_{E,in} - \omega_{E,out}}{\omega_{E,in} - \omega_{S,in}} \qquad (3.11.)$$

$$\eta_T = \frac{T_{E,in} - T_{E,out}}{T_{E,in} - T_{S,in}} \tag{3.12.}$$

The uncertainties are found from:

$$U_{T,n_T} = \pm \sqrt{\left(\frac{T_{E,out} - T_{S,in}}{(T_{E,in} - T_{S,in})^2}\Delta T_{E,in}\right)^2 + \left(\frac{-1}{T_{E,in} - T_{S,in}}\Delta T_{E,out}\right)^2 + \left(\frac{T_{E,in} - T_{E,out}}{(T_{E,in} - T_{S,in})^2}\Delta T_{S,in}\right)^2} \tag{3.13.}$$

$$U_{T,n_M} = \pm \sqrt{\left(\frac{\omega_{E,out} - \omega_{S,in}}{(\omega_{E,in} - \omega_{S,in})^2}\Delta \omega_{E,in}\right)^2 + \left(\frac{-1}{\omega_{E,in} - \omega_{S,in}}\Delta \omega_{E,out}\right)^2 + \left(\frac{\omega_{E,in} - \omega_{E,out}}{(\omega_{E,in} - \omega_{S,in})^2}\Delta \omega_{s,in}\right)^2} \tag{3.14.}$$

Where Δ is another term for the total uncertainty of the given parameter.

Chapter 4

Results

In this chapter the results from the mathematical simulations and the experimental investigation will be briefly presented. All results from each experimental investigation may be seen in appendix A.4. Comparison and discussion will be presented in the next chapter. The experimental results are given as temperature and moisture transfer efficiency and not effectiveness since the flow rate measurements were too inaccurate and incomplete. The connexion between the moisture transfer efficiency and effectiveness is shown here:

$$\eta_{ME} = \frac{\omega_{E,in} - \omega_{E,out}}{\omega_{E,in} - \omega_{S,in}} = \varepsilon_M \left(\frac{\dot{V}_{min}}{\dot{V}_E} \right) \tag{4.1.}$$

$$\eta_{MS} = \frac{\omega_{S,out} - \omega_{S,in}}{\omega_{E,in} - \omega_{S,in}} = \varepsilon_M \left(\frac{\dot{V}_{min}}{\dot{V}_S} \right) \tag{4.2.}$$

The relations will be equivalent for the temperature effectiveness/efficiency with replacing ω with T.

4.1. Results from the Mathematical Model

To compare the experimental data with the mathematical model derived in chapter 2 simulations were run in the *HXcalc* program. The input values and results for one run are shown below and on the next page:

Table 4.1. Simulation input values.

LC	0.1264m	v_{air}	$1.33*10^{-5}$ m^2/s
L	0.107m	cp_{air}	1006 J/kgK
W	0.178m	R_1	206.5 s/m
H	0.024m	ϕ_1	39%
Number of plates	5	R_2	76.27s/m
Le	0.8	ϕ_2	100%
k_{air}	0.025 w/mK	$\Delta\phi_2$	45%
ρ_{air}	1.17 kg/m^3		
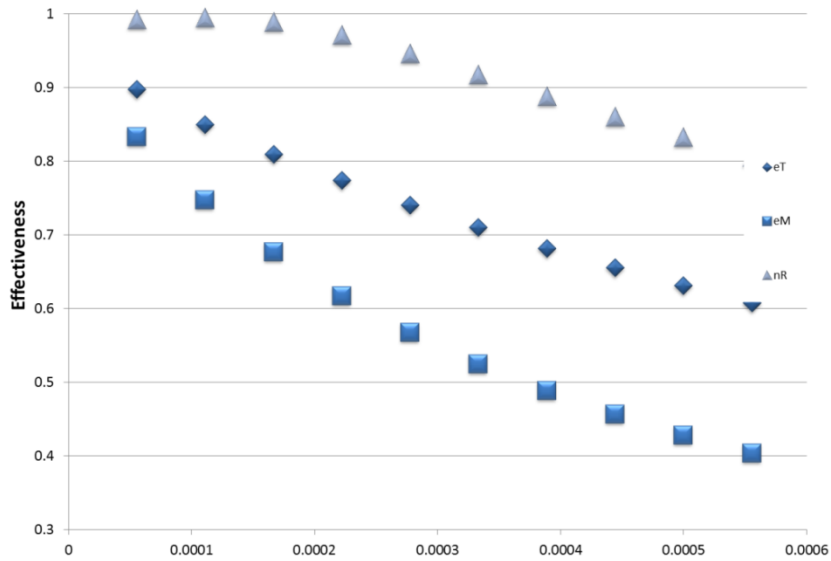
Figure 4.1. *Temperature, moisture transfer and annual heat recovery effectiveness for a set point temperature at 18 °C for different air flow rates(m³/s).*

The same geometry (see Appendix A.5) and input values were used in the simulation as in the experiments. The input properties were -6.4°C and 33.4% RH for supply air and 22.3°C and 43% RH for exhaust air for the case displayed above. These values were the mean input values from all experiments. Two moisture transfer reference resistances for the *DuPont* membrane *X* were found from the permeability test results given in the datasheet from the manufacturer. The reference mean humidities were 39 and 100% respectively from the ASTM E 96B and BW test methods (ASTM, 2011). The air layer resistance for test B was assumed to be 500s/m as in chapter 2.2.4. For flow rates in both directions at 1 m³/h the effectiveness dependence on supply inlet temperatures (all at 33.4% RH) are shown below:
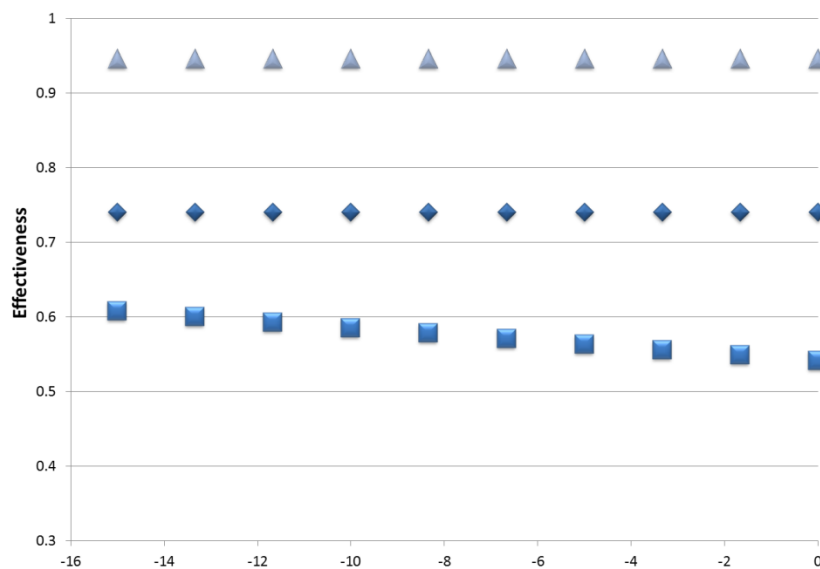
Figure 4.2. *Simulated supply inlet temperature dependence for the efficiencies. Square shapes are the moisture transfer effectiveness and diamonds are temperature effectiveness.*

The figure above was taken directly from the *HXcalc* program. When clicking on the point for -**10**^{o}C this picture appears on the screen:
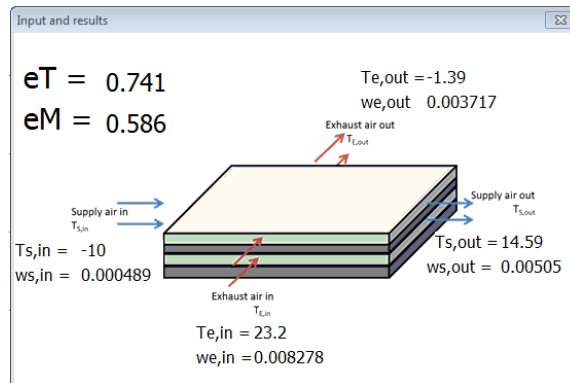
*Figure 4.3.   Popup window from HXcalc for supply air temperature at -**10**^{o}C.*

4.2.   Flow Pattern inside the Heat Exchanger

A heat exchanger with coloured copy paper as heat transfer plates was built to see the flow pattern inside the heat exchanger using a "smoke pen" form *Björnax AB*. A fan was used to pull air through the heat exchanger and the smoke pen was ignited and moved along the inlet end of the heat exchanger. The coloured paper made the smoke visible and it is possible to identify stream lines inside the heat exchanger. Three different picture series were taken starting with the first one with dry paper. After the first series the heat exchanger was exposed to mist form the humidifier for approximately 5 min and a second picture series was taken. After approximately **10** more minutes exposed to mist a third photo series was taken. The paper started to crumple while exposed to humidity and for the last picture series this was clearly visible.
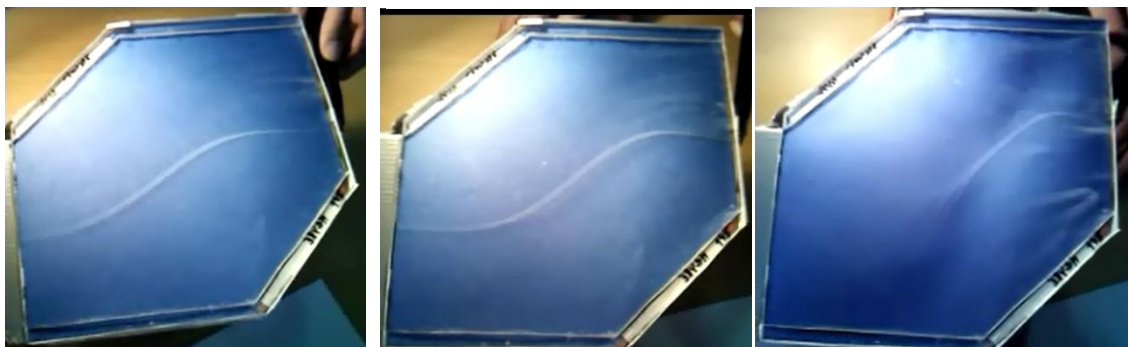
Figure 4.4.   Middle streamline for three different photo series. Picture to the right shows a streamline when the paper was exposed to high humidity.
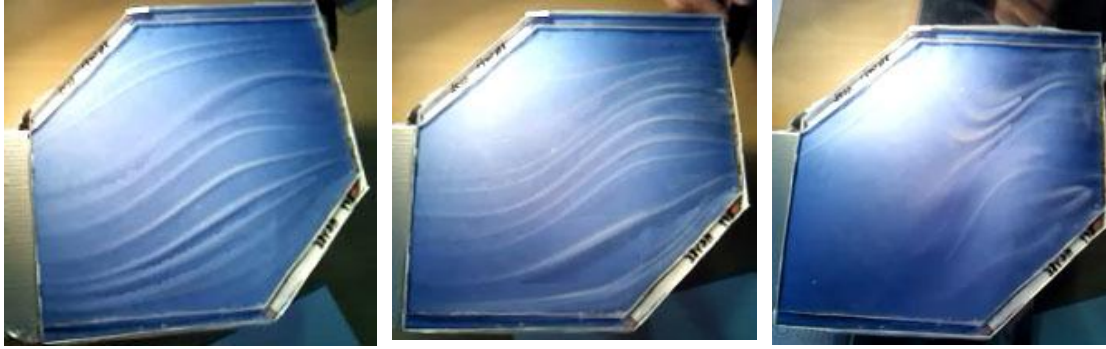
Figure 4.5. *Adobe Photoshop was used to overlay several pictures to see the different streamlines. Dry heat exchanger to the left, exposed to humid air in the middle and wet heat exchanger to the right.*

When the heat exchanger was dry it was possible to see that the air flows over most of the heat exchange area. When the paper started to be wet the flow covered less of the area. This means that there may have been stagnant air in some areas in the heat exchanger.

4.3. Results from the Experimental Investigation

The results from the different experiments are assembled for easier comparison in this chapter. For more results from the individual experiments see Appendix 4. For the experiments the resulting parameter is sown as efficiency given from the exhaust air side, not as the effectiveness given from the *HXcalc* program. Below is a table with the mean results and the name of the heat and moisture transfer plate material for eight different experiments.

Table 4.2. *Overview of all experiments with mean values for inlet temperatures and relative humidity, pressure drops, measured air flow rates and calculated efficiencies based on the exhaust air side.*

	Plate material	$T_{S,in}$ (^0C)	$T_{E,in}$ (^0C)	$\Phi_{S,in}$ (%)	$\Phi_{E,in}$ (%)	ΔP_S (Pa)	ΔP_E (Pa)	$\dot{V}_S$ (m^3/h)	$\dot{V}_E$ (m^3/h)	η_T	η_M
1	Optimax	-5.27	23.81	27.4	43.6	2.40	2.55	1.58*	1.58	0.27	
2	Optimax	-8.05	20.85	33.6	39.3	3.95	5.79	1.66	1.05	0.37	
3	DuPont X	-4.96	21.25	27.1	42.86	9.248	8.96	0.74	1.38	0.41	0.37
4	DuPont PP	-8.41	21.04	35.17	46.15	6.16	6.73	1.38	1.30	0.35	
5	DuPont X	-0.23	22.91	39.02	45.25	10.47	9.85	1.53	1.33	0.54	0.49
6	DuPont X	-4.32	22.77	29.54	43.27	11.13	10.48	1.55	1.20	0.54	0.58
7	DuPont X	-10.5	23.21	41.04	37.27	27.19	25.60	2.6	0.6**	0.60	0.91
8	DuPont X	-9.62	22.90	34.22	46.60	25.25	24.80	1.4*	0.6**	0.61	0.88

*) *Flow rates not measured, but assumed from velocity and humidity-temperature diagram lines.*

The temperature efficiencies for the different experiments are shown below. The temperature efficiencies are quite stable over time for all experiments except experiment two where the temperature efficiency first rice and then sinks.
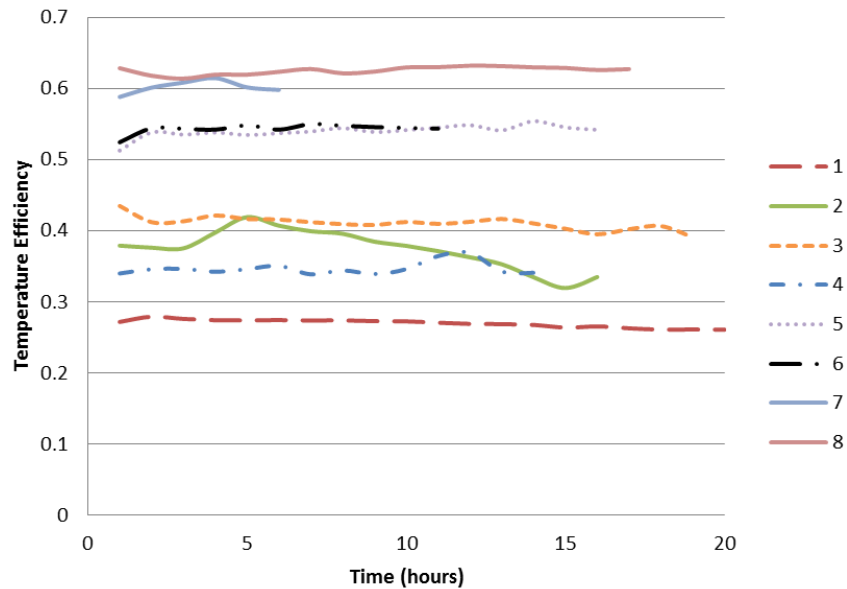
Figure 4.6.   Temperature efficiency for all experiments.

The development of the pressure drops are shown in the figure below for the experiment one to six. The two last experiments had much higher pressure drop and are therefore displayed in a separate figure:
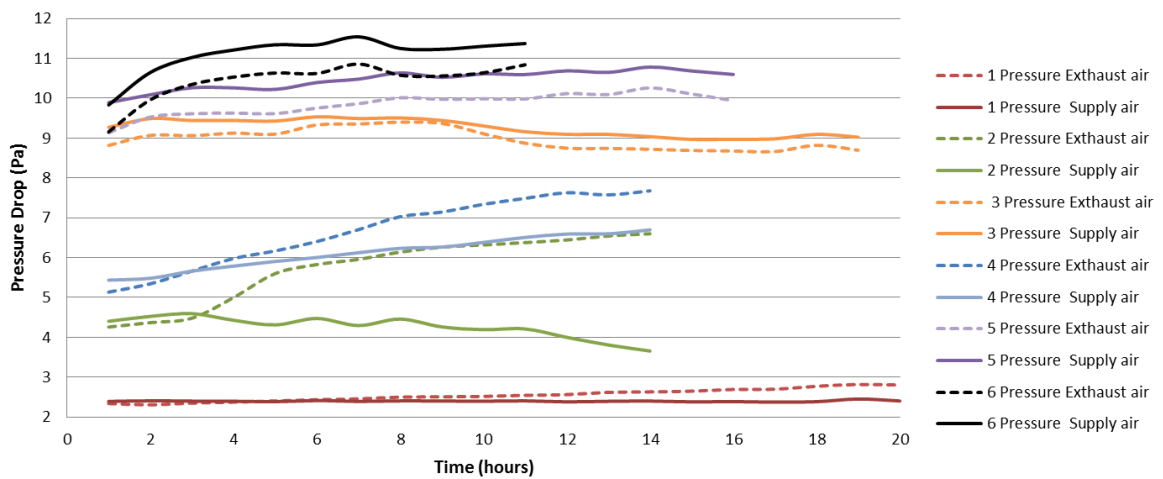
Figure 4.7.   Pressure drop for all experiments except 7 and 8.Experiement 1,2 and 4 were plastic based while 3,5,6,7 and 8 were membrane based.
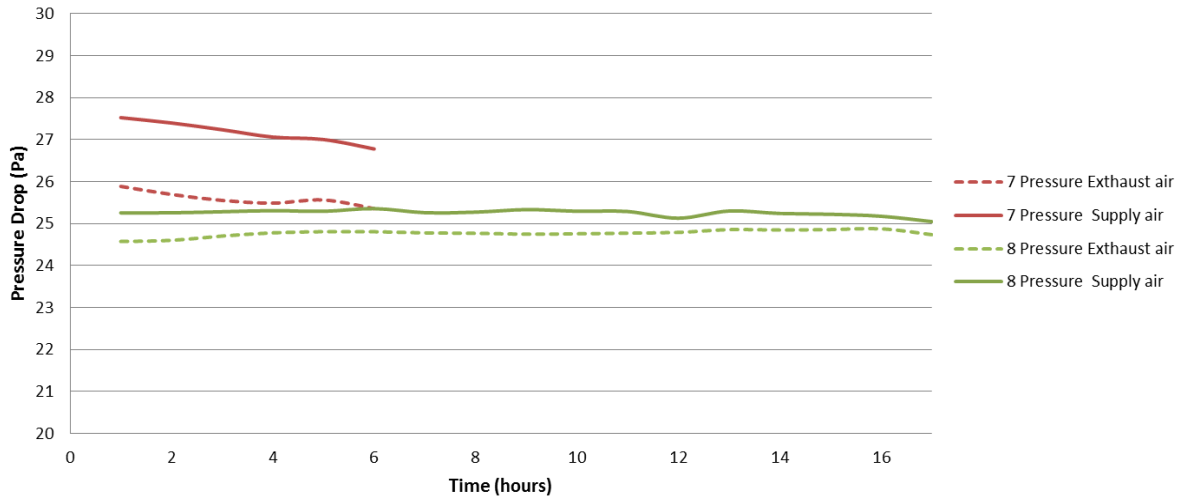
Figure 4.8. *Pressure drop for experiment 7 and 8.*

The start pressure drops changed quite much between the different experiments as possible to see in the figures above. However, a significant difference between the plastic based heat exchangers and the membrane based one is to be easily recognised. While the difference in pressure drop between the two air steams was quite constant over time for the membrane based heat exchanger in experiment 3,5,6 and 7 the difference increased quite significantly with time for the plastic based heat exchanger prototypes in experiment 1,2 and 4. A tiny decrease in the pressure drop difference happened in experiment 8. Since the supply air pressure drops were not stable as expected an equation to elude the changes in supply air pressure drop to see the changes at the exhaust air side was set up:

$$\frac{\Delta \bar{P}}{\Delta t} = \frac{\left(\Delta P_E(t) - \Delta P_S(t)\right) - \left(\Delta P_E(t_0) - \Delta P_S(t_0)\right)}{t} \qquad (4.3)$$

Below is a table showing the results for the eight experiments using the equation above for hour based averages in hour 2 and 14 (hour 1 and 11 in experiment 6, and 1 and 6 from experiment 7):

Table 4.3. *Difference in pressure drop over time.*

Experiment	$\Delta \bar{P}/\Delta t_{hour}$	$\Delta \bar{P}/\Delta t_{24\ hours}$
1	0.027497	0.934894
2	0.25829	8.781845
3	0.008796	0.299074
4	0.093076	3.16458
5	0.003044	0.103503
6	0.014223	0.483596
7	0.043156	1.467318
8	0.021711	0.738186

The membrane based experiment 2 and 4 stand out with high values. High value was also found for the membrane based experiment 7, but this experiment was only run for six hours.

The moisture transfer efficiency results from the membrane based heat exchanger experiments are displayed here:
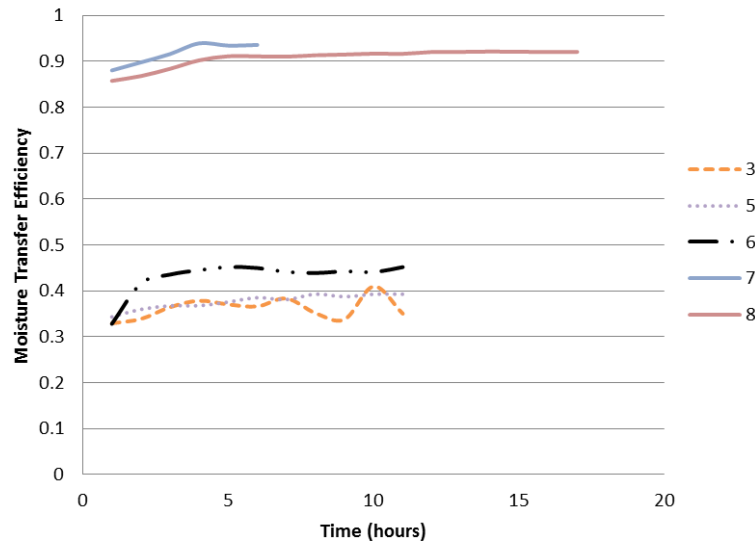
Figure 4.9.   The moisture transfer efficiency dependency on time for the different experiments with membranes.

The results above divide into two groups with experiment 7 and 8 having much higher efficiencies than the other three experiments. This should be seen in connection to the ratio between the flow rates which are much greater in experiment 7 and 8 than in experiment 3,5 and 6.

The moisture transfer efficiency dependence on supply inlet temperature:
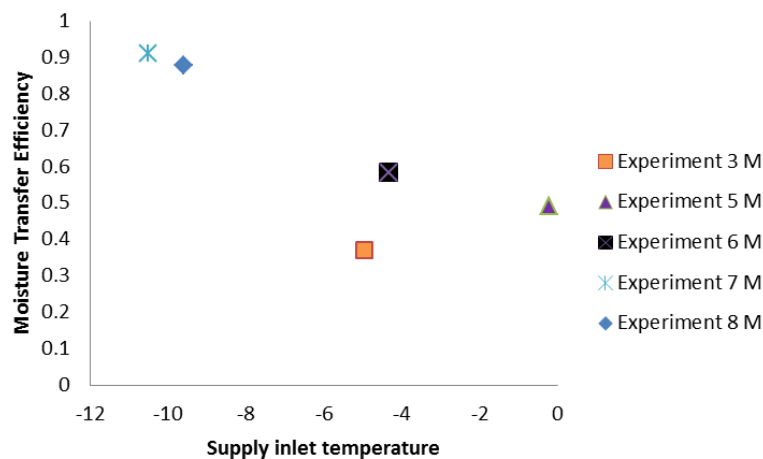
Figure 4.10.   The moisture transfer efficiency on the exhaust air side dependence on time for the different experiments with membranes.

45

The correlation between the temperature and moisture transfer efficiency in experiment 5,6,7 and 8 forms a increasing efficiency trend for lower temperatures. Experiment 3 does not follow this. However the experiment three was the only experiment where the exhaust air flow rate was greater than the supply air flow rate.

Ice and condensed water were found in all plastic exchangers (experiment 1, 2 and 4) plus in the last membrane based experiment (experiment 8). The ice formed in different areas in the plastic based and membrane based exchanger respectively. For the plastic based heat exchangers ice formation occurred in the exhaust air channels near the supply air inlet. In the membrane based heat exchanger the ice formed near the supply air outlet. In the membrane based exchanger the membranes tend to expand and crumple in very humid conditions. This happened in experiment 8 and it was also observed when the cooling coil was turned off between the experiments. However, the membranes tightened when the humidity level went down again.
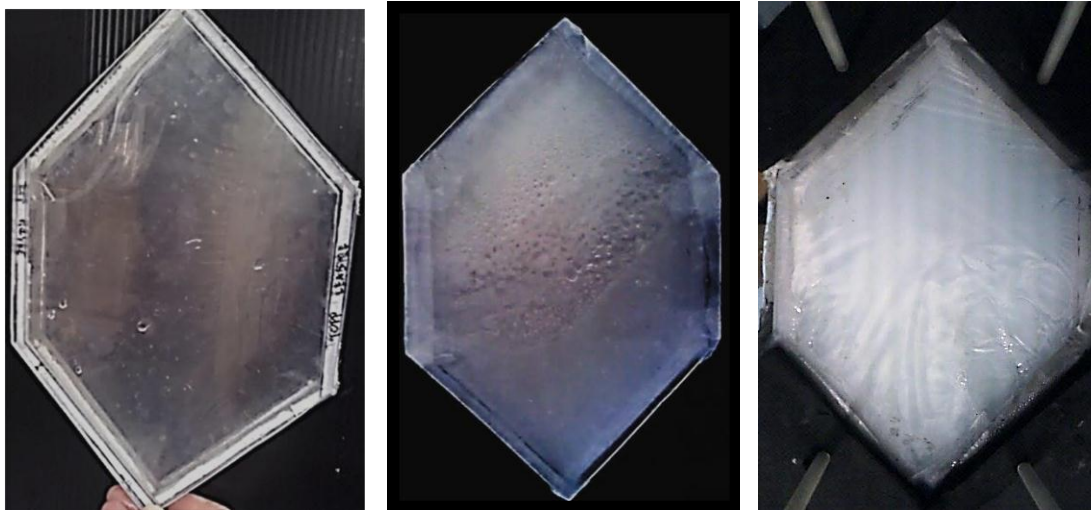
Figure 4.11.   *Ice formation in experiment (from left) 1,4 and 8.*

4.4.   Expansion of the Membrane in High Humidity Conditions

A very simple experiment was done with the membrane based heat exchanger. The exchanger was dipped in water for just a second. The membranes expanded and the membranes stuck together as showed in the picture below. After several hours the membranes dried and were stretched out again as before. Below are two pictures showing the difference between the dry and the wet heat exchanger:
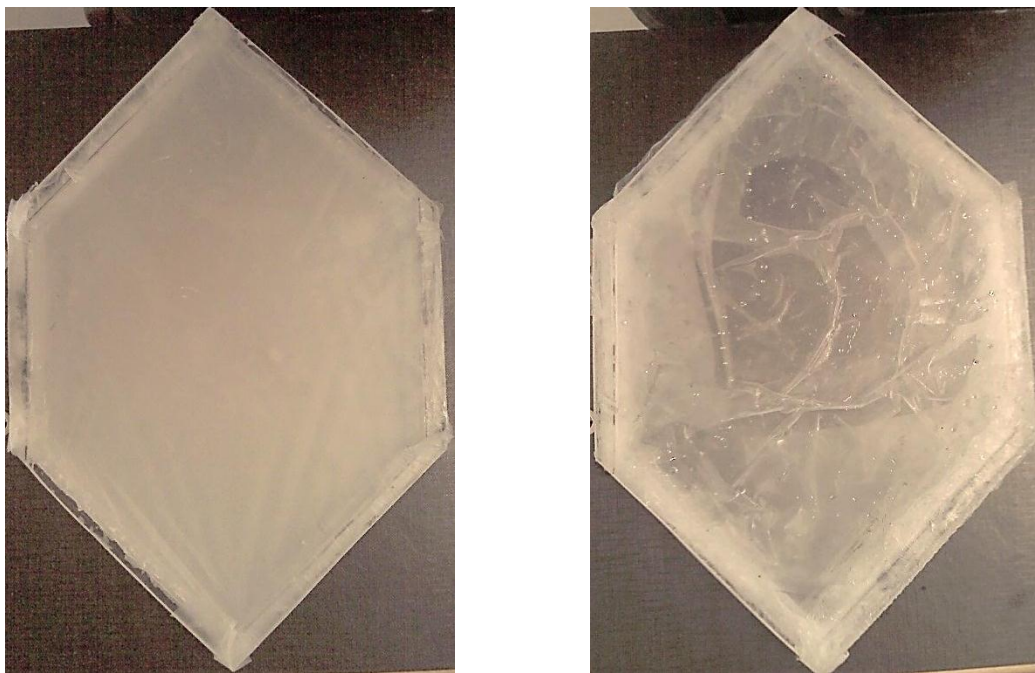
Figure 4.12.   Left: Dry heat exchanger. Right: Wet heat exchanger

Chapter 5

Discussion

The first objective of this work was to make a direct mathematical calculation method to predict the moisture transfer effectiveness. The simulated results and the experimental investigation were compared to see if the proposed method gave reliable results. The second objective was to investigate the difference between the different heat exchanger plate materials regarding condensation and freezing. The change in pressure drop over the heat exchanger was used as an indicator. The heat exchanger prototype top and bottom were made out of transparent acrylic plates. This made it possible to do a visual investigation on if and where ice formation took place.

5.1. Comparison between the Mathematical Model and the Experimental Investigation

A comparison between the proposed mathematical method and the method derived by Niu and Zhang (2000) to predict the heat and moisture transfer efficiency was done in chapter 2.4. The comparison showed that the two methods correlated very well regarding changes in flow rate. However, the proposed method by the author did not correlate with Niu and Zhangs' (2000) method regarding changes in supply temperature.

The HXcalc-program was run with the same inputs (inlet temperatures, humidity, flow rates and geometry) from all experiments (see Appendix A.4). A comparison between the simulated and experimental results for temperature efficiency and moisture transfer efficiency are shown in figures on the next page. Since the results from the simulations were given as effectiveness, while the experimental results were given in efficiency it was necessary with a calculation between the two properties. The correlations are shown in equation 4.1. and 4.2.

49

The two charts show:
Left chart — y-axis "Experimental Temperature Efficincy" (0,2 to 1), x-axis "Simulated Temperature Efficincy" (0,2 to 1), with trend line equation y = 0,3402x + 0,2249.
Right chart — y-axis "Experimental Moisture Transfer Efficiency" (0 to 1), x-axis "Simulated Moisture Transfer Efficiency" (0 to 1), with trend line equation y = 0,9141x + 0,134.
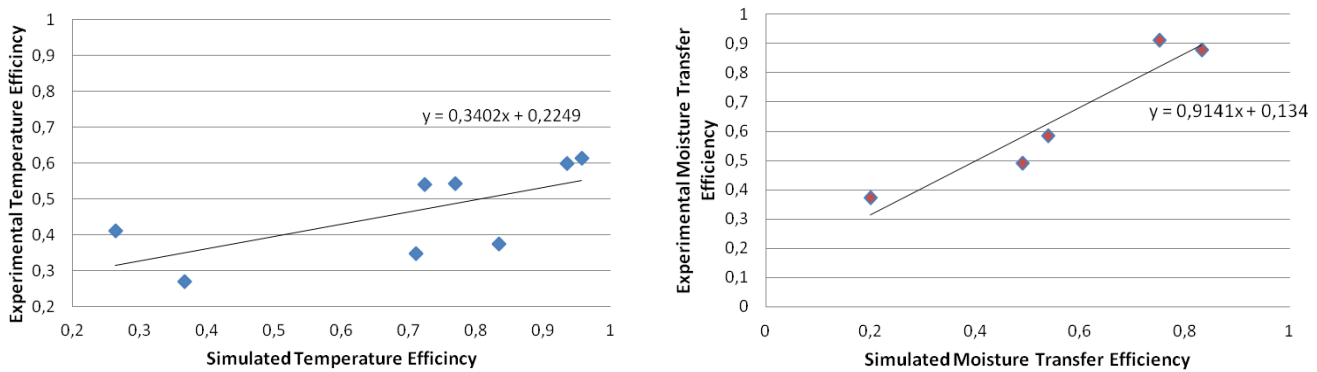
Figure 5.1.   Comparison between the experimental and simulated results for temperature efficiency (left) and moisture transfer efficiency (right). Trend lines equations for the correlation is displayed inside the charts.

For both temperature efficiency and moisture transfer efficiency the correlation of the two set of results is close to a trend line. However, the trend line for temperature efficiency does not have the 1:1 correlation as expected. One explanation why the simulated values for the temperature efficiency were higher than the measured ones may be that the temperature loss to the surroundings from the point where the supply air inlet temperature was measured to the heat exchanger was huge. The supply air inlet temperature was included in the definition of the temperature efficiency (equation 4.1. and 4.2.) and if this measured value was lower than the actual inlet temperature to the heat exchanger the temperature efficiency would be calculated to be too low. The points below the trend line in the figure to the left above were for the lowest supply air inlet temperatures which confirms the theory about temperature loss to the surroundings since the colder the supply air temperature, the higher the loss. The moisture transfer efficiency correlation differs with only 10% between the simulated and experimental results. This is really promising since the mathematical method only takes into account a mean moisture transfer resistance value to calculate the effectiveness. This differs from Niu and Zhangs' (2002) method to calculate the moisture transfer effectiveness which needs a iterative solution method. This result implies that the information given by the manufacturer regarding water vapour permeability was enough information to predict the moisture transfer effectiveness for the given membrane. Nevertheless, as mentioned before, the permeability tests are done in many different ways as stated in the article by McCollough(2003). An understanding on how the tests were performed is vital for good results.

To see if the shape of the heat exchanger worked as intended (counter flow with cross flow headers) the streamlines in the dry exchanger were assumed to be of the same form in both exhaust and supply air streams. The picture below shows the streamlines for both streams overlaid.
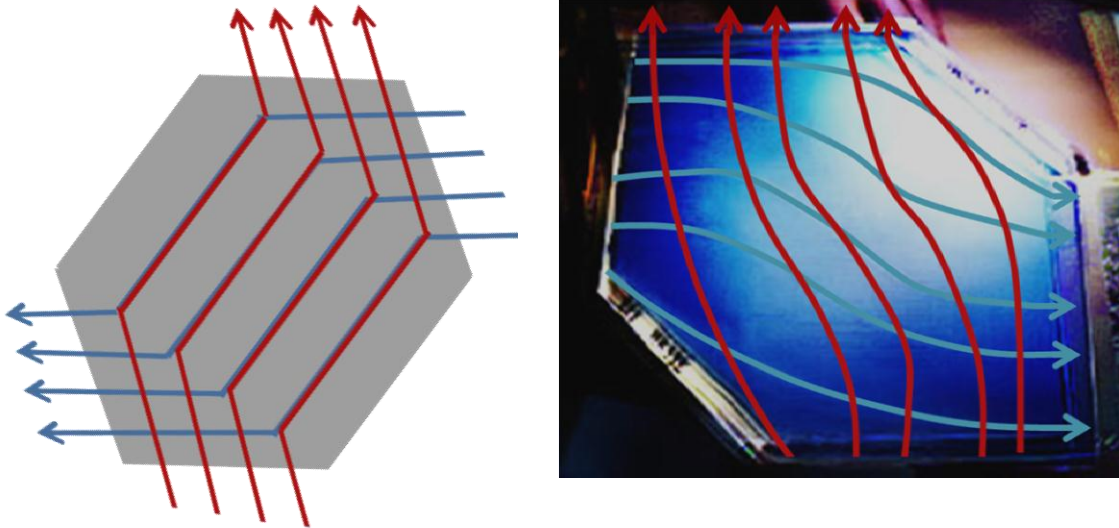
Figure 5.2.   *Idealistic quasi-counter flow heat exchanger flow to the left and the results from the smoke-pen test to the right.*

This small experiment showed that in the cross flow headers the flows were fairly perpendicular, but in the counter flow area the streams were not counter wise but approximately 30°. This means that to predict results as counter flow will probably give over predicted results as for the temperature efficiency in figure 5.1. Compared to Zhang's (2010) CFD-model the streamlines in this experiment were less counter flow angled. However, the geometric shape of Zhang's (2010) exchanger was slimmer than the tested heat exchanger. This may have caused the differences.

5.2. Pressure Drop and Flow Rates through the Exchanger

The *HXcalc* program calculates the pressure drop with this correlation (Aarnes, 2011):

$$\Delta P \ = \frac{1}{2}\rho_{air}V^2\left(\frac{4fL}{D_h} + 0.8775\right) \tag{5.1.}$$

An increase in the flow rate will then cause an increase in the pressure drop. Increasing flow rates will also cause a decrease in the U-value for the heat exchanger. Regarding to the mathematical method this will decrease the efficiency as seen in figure 4.1. This means that an increase in pressure drop should mean a decrease in temperature efficiency. However, the experimental results show the opposite result. There was not found any correlation between the measured pressure drop over the exchanger and the flow rate as seen in the figure below:
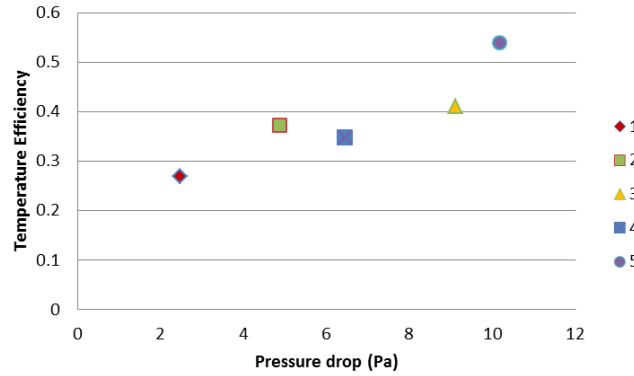
Figure 5.3. Correlation between the temperature efficiency and the mean pressure drop.
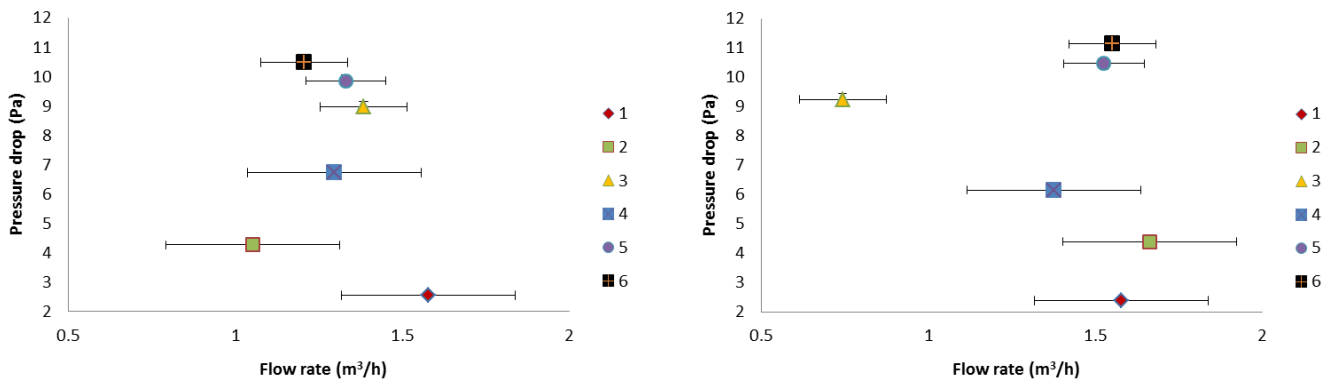
Figure 5.4. Correlation between the exhaust flow rate and the exhaust side pressure drop (left). Correlation between the supply flow rate and the supply side pressure drop (right). Error bars represent the total calculated error. When only one flow rate was measured the error was set to 0.26 m^3/h which was the maximum calculated flow rate error for all tests.

This result may indicate other reasons different from the flow rate that caused the pressure drop. The pressure drop over the supply air side was not stable in all experiments. In experiment 2,3,7 and 8 the supply air side pressure drop decreased, while in experiment 4,5 and 6 it increased. In both experiment 2 and 4 a great amount of ice formation was observed. The test conditions were quite similar in these two experiments. However the pressure drop over the supply air side had opposite developments in these tests. See figure 4.7. A possible reason for the difference may be differences in the material properties. The experiment 2 utilized *Optimax's* quite stiff non-elastic transparent plastic sheets while experiment 4 was utilizing elastic *PP* sheets form *DuPont*. While an ice layer was building up in the PP-exchanger blocking the exhaust air channels and increasing the exhaust air side pressure drop, the elastic material changed the channel height of the supply air side channels as well, increasing the pressure drop also here. This did not happen in experiment 2 using stiff plastic sheets. When the air flow at one side was greater than the other the membrane tend to expand and making the channels with the lowest air flow rate narrower. This caused that the pressure drop at this side increased as well and that the pressure drops were almost equal at both sides. If the side with the highest flow rate decreased the flow rate the other side followed the tendency and the pressure

drop on each side decreased. This may be seen by comparing the figures 4.7. and 4.8. The only experiment that did not follow this was experiment two there inelastic transparent plastic sheets were used. This effect is really a drawback for the membrane from *DuPont* in this application.

5.3. Evaluation of the Test Rig

For simplicity when building the experimental set up, the already installed glycol cooling loop in the lab was used to produce cold air. Since the air flow rates were kept at low levels to increase the temperature efficiency the temperature loss to the surroundings through the distance from the cooling coil to the heat exchanger was huge. This restricted the cold side temperature to about -10.5 $^{\circ}$C for the coldest experiment. Severe difficulties to get the same inlet conditions in the different experiments, especially regarding pressure drop, air flow rates and supply inlet temperatures, made it difficult to compare the results. However, the exhaust air side of the test rig delivered very stable humidity and temperature conditions through the test periods and were found to be almost not affected by changes in the surroundings. The hypothesis that ice formation would create an increase in the pressure drop over the exhaust air side of the heat exchanger was right according to the results. This means that the test rig was suitable to investigate if ice formation problems occurred or not.

The uncertainty of the experimental results was huge, especially concerning the flow rate measurements and the temperature loss to the surroundings. The equipment used for this experimental investigation were not ideal, especially since the cooling coil tended to freeze and the air flow rate on the supply air side therefore decreased with time. The test length was restricted to the time before the cooling coil was filled with ice and blocked the air flow rate. For most experiments this happened after about 800 minutes. Nevertheless, this was enough time to see ice formation in the plastic based heat exchangers. Actually condensation of water was observed to occur after short time in these experiments (1,2 and 4). The differences in pressure drops were also starting to rice at the beginning of these experiments (see figure 4.7.).

If the flow rates are equal, there is no ice formation or condensation, the heat capacity is assumed constant and there are no losses to the surroundings the lines indicating the change in temperature and humidity for the air streams will be of equal length and inclination in the temperature-humidity diagram (as shown in figure 2.2.). In the test rig it was almost impossible to get equal flow rates due to the problems in regulating this, and the difficulty in measuring it as well. The temperature efficiency was calculated based on the exhaust air side as mentioned in chapter 3.3. This lead to that in the case where the exhaust air flow rate was greater than the supply air flow rate, as in experiment 3, the line for the supply air is longer (see figure A.15). When the flow rate for the supply air was greater than the air flow for the exhaust air the line for exhaust air should have been longer than the one for supply air. However, due to experiment 2,4,5 and 6 this was not the case. The supply air lines were still longer (in experiment 4) or of the same magnitude. This may be

53

explained from that the cold supply air experienced a greater temperature loss to the surroundings than the exhaust air. Since the surrounding temperature heated the supply air the line was longer than if it had been no loss. How great this loss was may be found from experiment 4 where the flow rates only differed by approximately 6%. The temperature loss to the surroundings based on the difference in lines length was around **10** ^{o}C for the case when the supply inlet temperature was -8.4 ^{o}C. From the experiment 5 the loss was however below 4°C.

5.4.   Evaluation of the Membrane Based Heat Exchanger Prototype

The plastic based heat exchanger prototypes (both the *Optimax* plastic sheets and the *DuPont PP-*material) were shown to experience water condensation and frost formation in the exhaust air channels. Water droplets were observed through the transparent acrylic top plate in the top exhaust channel already after few hours in these experiments. The frost formation appeared near the supply air inlet (see figure 4.12.) which correlates very well with the CFD analysis of Zhang (2010). Zhang's (2010) analysis shows that the coldest area in the exhaust air channels will be near the supply air inlet. See reprinted figure below:
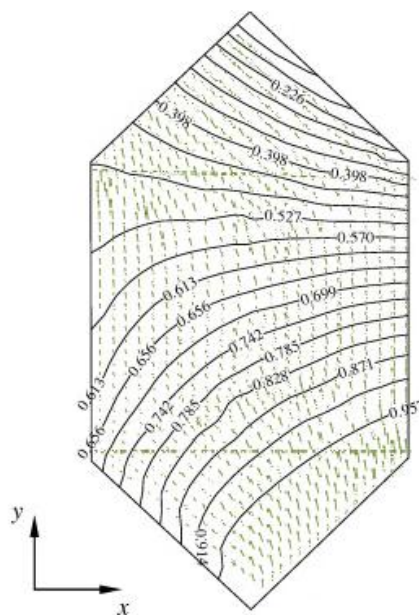
Figure 5.5.   *The dimensionless temperature change and flow pattern in the warm air side through a quasi-counter flow heat exchanger. Reprinted overlaid figures from Zhang (2010).*

The pressure drop difference in these experiments riced significantly through the test periods according to table 4.3.

In the membrane based experiments 3, 5, 6 and 7 neither condensation nor ice formed. The change in pressure drop differences were not significantly (experiment 7 must be disregarded here since the test period was too short). In the last experiment a

54

small amount of condensate water was observed near the supply air outlet in the upper exhaust air channel after 8 hours. The membrane had expanded and was also crumpled in this area in this experiment. The *DuPont X*-membrane material tested was shown to expand in very humid conditions. See figure 4.12. At the end of the experiment ice was found as shown in picture A.41. and 4.12. Since the ice formation appeared in different areas in the plastic based prototypes contra the last membrane based experiment, the ice formation in the latter may have been caused by other means than in the previous. In the plastic based exchanger prototypes the ice formed in the area where the coldest temperature in the exchanger acted; near the supply air inlet. Conversely, the ice in the membrane based heat exchanger appeared near the supply air outlet which actually was the second warmest side of the exchanger.   As shown in the picture series in figure 4.4. and 4.5. the crumpled membrane changed the air flow pattern, making the air in one part of the exchanger area stagnant.

A hypothesis of why ice was formed in this part in the experiment 8 was made: The crumpling of the membrane due to high humidity levels in the exhaust air side made the membrane stuck to the upper and lower heat exchanger frame plates making the exhaust air stagnant. The supply air side cooled the stagnant exhaust air to down to (almost) the temperature of the supply air. Since the moisture transfer efficiency never can be **100%** condensation and freezing occurred.

Zhang's (2010) CFD-analysis showed that the most humid area was on the heat exchangers' lower right side (see figure below) while the ice formation in the experiment was on the lower left side. However, Zhang (2010) showed that the lower left side had a lower velocity than the right side. This can explain why the extensive crumpling and ice formation happened here in the exhaust air side. From figure 5.5. the temperature was also found to be lower in the right side than at the left, increasing the relative humidity.
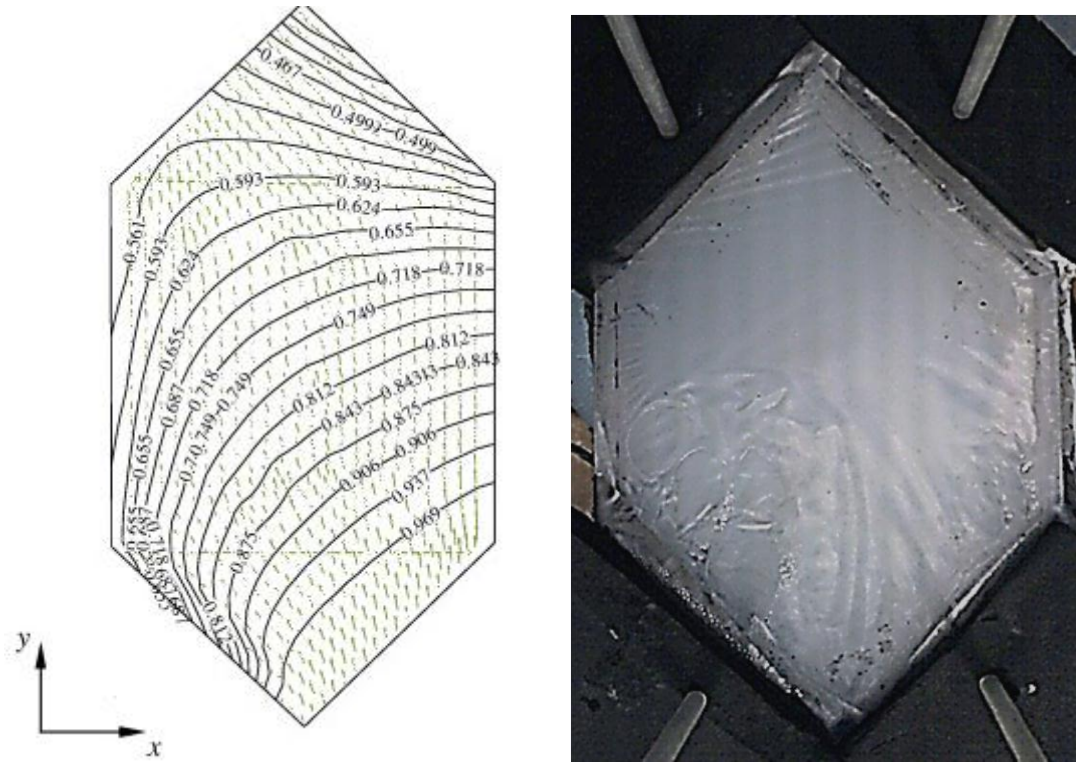
Figure 5.6. *Left: The dimensionless humidity change and flow pattern in the warm air side through a quasi-counter flow heat exchanger. The exhaust air inlet is at the lower rights side. Reprinted overlaid figures from Zhang (2010). Right: the ice formation and crumpling of the tested heat and moisture exchanger. (The picture is mirrored for comparison)*

As neither condensate water nor ice were found in the coldest spot (near the supply air inlet) this may indicate that the expansion of the membrane was the problem that caused the ice formation. Expansion and crumpling were observed when the humidity was high and were experienced in experiment 8 with an exhaust humidity of 46.6% and supply air temperature of -9.6 ℃, but not in experiment 7 with 37.3% and -10.5 ℃.

Experiment 8 had the highest exhaust inlet absolute humidity at 8 g_W/kg_A. The supply air temperature in experiment 7 was colder than in experiment 8, but the exhaust humidity was lower (6.5 g_W/kg_A). Therefore it seems like the temperature and humidity condition that lead to crumpling of the membranes laid somewhere in the range between these two experiments. In the picture below lines are drawn between the exhaust inlet condition and supply inlet condition for the different membrane exchanger experiments in a temperature-humidity diagram. As seen the line for the experiment 8 is much closer to the saturation line than the other experiments. This may explain the expansion of the membrane in this experiment.
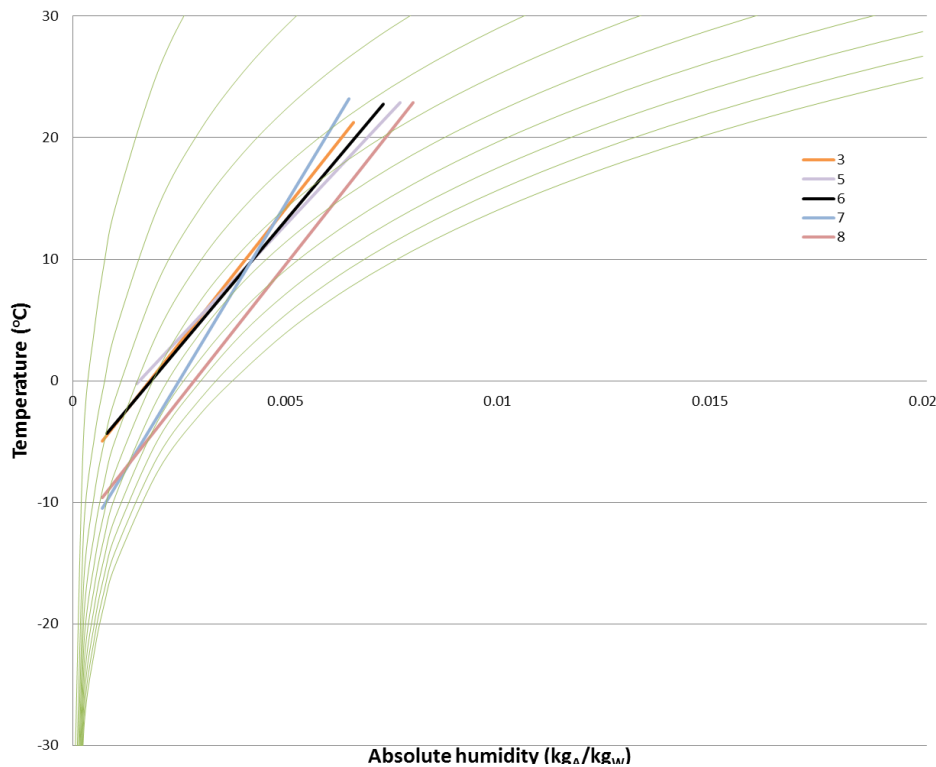
*Figure 5.7.   Lines drawn between the membrane based experiments inlet
                 conditions in a temperature-humidity diagram.*

Since the humidity inside a residential building in winter seldom gets above 40% RH pursuant to Kalamees et al. (2009). See figure 1.3. This means that the tested membrane based heat exchanger may work in even colder supply air temperatures than -10 $^{\circ}$C in normal conditions.

Figure 4.10. shows the relation between the moisture transfer efficiency on the exhaust air side and the supply inlet temperature. The relation follows the effect found in the theory from Niu and Zhang (2000) showed in figure 2.11. The colder the temperature in the supply air inlet was the higher the mean relative humidity close to the membrane. This decreased the mean moisture transfer resistance and increased the moisture transfer efficiency. Since the exhaust air flow rate was much higher than the supply air flow at the two last experiments the measured efficiencies at the exhaust air side reached 90%. This is of course a much higher value than it would have been if the air flow rates were equal. Nevertheless, the correlation shows that an even colder supply inlet temperature may lead to higher moisture transfer efficiency.

It is impossible to define how much better the membrane based heat exchanger would work regarding to energy savings compared to a plastic based exchanger in a residential building use from the test performed in this work. The heat exchanger area and the flow rates were too low to compare this experiment to a "real case". However, the experimental results shows that the freezing and condensation problems were less in the membrane based exchanger. It is need for more investigation to find out at what temperature and humidity levels the membrane based exchanger also will

experience freezing due to the limitation of moisture transfer effectiveness and not because of expansion of the membrane due to humidity levels.

The membrane tested had drawbacks as it was very elastic which made it difficult to get the membranes stretched out when building the heat exchanger prototype. The pressure prop behaviour cause by the elasticity discussed in chapter 5.2 may cause problems if the flow rates are unbalanced. The elastic membranes would probably create an even bigger unbalance and the energy needed for pumping the air through the heat exchanger would increase. The optimal membrane should therefore not expand when soaked in water and should preferably not be elastic due to the problems if the flow rates get imbalanced and the difficulty in building the exchanger.

Chapter 6

Conclusion and Further Work

The mathematical method derived to predict the moisture transfer effectiveness in a membrane based heat exchanger was shown to fit very well with the experimental results. Utilising available permeability test results to find an average moisture transfer resistance were shown to be an appropriate method to find the overall moisture transfer coefficient. The direct computational method was simple to implement in a calculation tool since it did not require any iteration processes or additional testing of the membrane. The calculation tool *HXcalc* made in *Microsoft Excel* may be used for further work to investigate the appropriateness for different membranes in a membrane based heat exchanger.

The experimental tests showed that the heat exchanger prototypes utilizing plastic sheets, as the heat transfer material, experienced condensation and ice formation in the exhaust air channels near the supply air inlet side of the exchanger. In the experiments utilising the hydrophilic membrane *X* from *DuPont* as the heat and moisture transfer material neither condensation nor ice were found near the supply air inlet. However in the experiment with the highest exhaust inlet humidity (46.6% RH) the membrane had expanded and was crumpled near the supply air outlet. Condensate water and ice were found in the exhaust air channels near the supply air outlet in this experiment. The hydrophilic membrane *X* from *DuPont* was therefore found to be superior to the two plastic materials regarding water condensation and frost formation in the heat exchanger prototype when the exhaust air relative humidity was below 37% and the temperature above -10.5 ºC.

The pressure drops over the heat exchanger were found to be strongly influenced by the membrane material's elasticity and were not proportional to the flow rate as expected. The elasticity and the membrane's tendency to expand at high humidity made the tested membrane unsuitable for use in a membrane based heat exchanger. Methods to support the membrane to decrease the elasticity should be investigated. Lamination of the membrane to a supporting fabric may be a solution that should be tested. Other types of membranes should also be tested.

The experimental investigation was restricted to a supply air temperature at about -10 ºC at the lowest. The membrane based heat exchangers performance at even lower temperatures should be investigated to see if the membrane based heat exchanger could work in extreme winter conditions without defrosting systems (frost guards etc).

A plastic based heat exchanger should be tested more carefully to find the lowest exhaust air humidity and warmest supply air temperature that would lead to

condensation and ice formation respectively. Then the two types of heat exchangers may be compared to find the possible energy savings from replacing plastic sheets with membranes.

If the built test rig is to be used for further testing the axial fans should be replaced with centrifugal fans to make sure that the flow rates are stable even if the pressure drop over the exchanger changes due to condensation and ice formation. The heat exchanger prototypes should also be rebuilt with an increased number of heat exchanger plates to be able to increase the air flow rates still remaining high efficiency. Higher air flow rates will decrease the temperature loss to the surroundings and there will be possible to test the heat exchanger at colder supply inlet temperatures.

The membrane should also be tested for durability and pollution transfer to decide if the technology is suitable for use in residential buildings with several living units.

References

Aarnes, S. 2011. *Energy-Efficient Ventilation Solutions for ZEB*. Project Thesis, NTNU, Trondheim.

Alves, V. D., & Coelhoso, I. M. 2004. Effect of membrane characteristics on mass and heat transfer in the osmotic evaporation process. *Journal of Membrane Science*, 228(2): 159-167.

ASTM. 2011. E96/96M-10 **Standard Test Methods for Water Vapor Transmission of Materials**. West Conshohocken, PA: ASTM International.

Chen, L.-C., Yu, T. L., et al. 2008. Nafion/PTFE and zirconium phosphate modified Nafion/PTFE composite membranes for direct methanol fuel cells. *Journal of Membrane Science*, 307(1): 10-20.

Crank, J. 1975. *The mathematics of diffusion*. Oxford: Clarendon Press.

Drivsholm, C., Olsen, H., Larsen, C. G., Jensen, J. S., Nielsen, T. R., Kragh, J., & Svendsen, S. 2005. **Udvikling af energiøkonomisk ventilationsløsning med varmegenvinding til boliger**: BYG-DTU.

Favre, E., Clement, R., Nguyen, Q. T., Schaetzel, P., & Neel, J. 1993. Sorption of organic solvents into dense silicone membranes. Part 2.-Development of a new approach based on a clustering hypothesis for associated solvents. *Journal of the Chemical Society, Faraday Transactions*, 89(24).

Gibson, P. W. 2000. Effect of temperature on water vapor transport through polymer membrane laminates. *Polymer Testing*, 19(6): 673-691.

Huang, J., Cranford, R. J., et al. 2004. Sorption and transport behavior of water vapor in dense and asymmetric polyimide membranes. *Journal of Membrane Science*, 241(2): 187-196.effectiveness

Huizing, R. N. 2010. **Coated Membranes for Enthalpy Exchange and Other Applications**. US Patent and Trademark Office. US Patent PCT/CA2010/000735

Incropera, F. P., & DeWitt, D. P. 2007. **Fundamentals of heat and mass transfer**: John Wiley.

ISO. 2001. NS-EN ISO 12572: **Hygrothermal performance of building materials and products**- Determination of water vapour transmission properties. Oslo, Norway: Standard Norge.

JSA. 1999. JIS L 1099: *Testing Methods for water Vapour Permeability of Clothes.* Tokyo, Japan: Japanese Standard Association.

Kadylak, D., Cave, P., et al. 2009. Effectiveness correlations for heat and mass transfer in membrane humidifiers. *International Journal of Heat and Mass Transfer,* 52(5-6): 1504-1509.

Kalamees, T., Korpi, M., Vinha, J., & Kurnitski, J. 2009. The effects of ventilation systems and building fabric on the stability of indoor temperature and humidity in Finnish detached houses. *Building and Environment,* 44(8): 1643-1650.

Kays, W. M., & London, A. L. 1964. *Compact heat exchangers.* New York: McGraw-Hill.

Marais, S., Métayer, M., et al. 2000. Permeametric and microgravimetric studies of sorption and diffusion of water vapor in an unsaturated polyester. *Polymer,* 41(7): 2667-2676.

McCullough, E. A., Myoungsook, K., & Huensup, S. 2003. A comparison of standard methods for measuring water vapour permeability of fabrics. *Measurement Science and Technology,* 14(8): 1402.

Modesti, M., Dall'Acqua, C., et al. 2004. Mathematical model and experimental validation of water cluster influence upon vapour permeation through hydrophilic dense membrane. *Journal of Membrane Science,* 229(1–2): 211-223.

Mondal, S., Hu, J. L., et al. 2006. Free volume and water vapor permeability of dense segmented polyurethane membrane. *Journal of Membrane Science,* 280(1–2): 427-432.

Mukhopadhyay, A., & Midha, V. K. 2008. A Review on Designing the Waterproof Breathable Fabrics Part I: Fundamental Principles and Designing Aspects of Breathable Fabrics. *Journal of Industrial Textiles,* 37(3): 225-262.

Nasif, M. S., Morrison, G. L., & Behnia, M. 2005. *Heat and Mass Transfer in Air to Air Enthalpy Heat Exchangers.* 6th World Conference on Experimental Heat Transfer, Fluid Mechanics, and Thermodynamics. April 17-21, 2005, Matsushima, Miyagi, Japan

Niu, J. L., & Zhang, L. Z. 2000. Membrane-based Enthalpy Exchanger: material considerations and clarification of moisture resistance. *Journal of Membrane Science,* 189(2): 179-191.

Novakovic, V., Hansen, S. O., Thue, J. V., & Gjerstad, F. O. 2007. *ENØK i bygninger: effektiv energibruk.* Oslo: Gyldendal undervisning.

Ouazia, B. K., Swinton, M. C., Julien, M., & Manning, M. 2006. *Assessment of the enthalpy performance of houses using energy recovery technology*. Paper presented at the 2006 Winter Meeting of the American Society of Heating, Refrigerating and Air-Conditioning Engineers, ASHRAE, January 21, 2006 - January 25, 2006, Chicago, IL, United states.

Peron, J., Mani, A., et al. 2010. Properties of Nafion® NR-211 membranes for PEMFCs. *Journal of Membrane Science*, 356(1–2): 44-51.

Vali, A., Simonson, C. J., Besant, R. W., & Mahmood, G. 2009. Numerical model and effectiveness correlations for a run-around heat recovery system with combined counter and cross flow exchangers. *International Journal of Heat and Mass Transfer*, 52(25-26): 5827-5840.

Wijmans, J. G., & Baker, R. W. 1995. The solution-diffusion model: a review. *Journal of Membrane Science*, 107(1–2): 1-21.

Yeh, H. M., & Chang, Y. H. 2005. Mass transfer for dialysis through parallel-flow double-pass rectangular membrane modules. *Journal of Membrane Science*, 260(1-2): 1-9.

Yoshino, M., & Hashimoto, Y. 1973. The Lossnay penetration-type total heat exchanger. *Mitsubishi Electric Engineer*(38): 24-27.

Yun, R., Kim, Y., & Min, M.-k. 2002. Modeling of frost growth and frost properties with airflow over a flat plate. *International Journal of Refrigeration*, 25(3): 362-371.

Zhang, L. Z., & Niu, J. L. 2001. Energy requirements for conditioning fresh air and the long-term savings with a membrane-based energy recovery ventilator in Hong Kong. *Energy*, 26(2): 119-135.

Zhang, L. Z., & Niu, J. L. 2002. Effectiveness Correlations for Heat and Moisture Transfer Processes in an Enthalpy Exchanger With Membrane Cores. *Journal of Heat Transfer*, 124(5): 922-929.

Zhang, L.-Z. 2010. Heat and mass transfer in a quasi-counter flow membrane-based total heat exchanger. *International Journal of Heat and Mass Transfer*, 53(23-24): 5478-5486.

Zhang, L.-Z. 2012. Progress on heat and moisture recovery with membranes: From fundamentals to engineering applications. *Energy Conversion and Management*(0). http://dx.doi.org/10.1016/j.enconman.2011.11.033

Appendix

A.1.   Initial Testing of Cooling Coils

Testing of the cooling system already installed in the VVS-lab at EPT was carried out initially to see if the system could be used for the experiment. It was preferable to use the installed system to save time and money.

The cooling coil was first tested with outdoor air and quite high air flow rates given by the natural drag through the ducting system. Extensive frost formation on the cooling coils was experienced and the flow rate was decreased after about 6 hours. After 12 hours the cooling coil outlet was completely blocked with frost. Second another approach was tried with smaller air flow rates through the cooling device. A small fan was placed in front of the inlet duct. Warm indoor air from the lab was used to test the "worst case scenario" of frost formation inside the coil. First the cooling coil was tested for 24 hours. The flow rate was measured with the *Velocicalc 9555-P* instrument from *TSI* by measuring the velocity in three different points in the outlet channel and average the value. The flow rate was adjusted by changing the outlet area of the outlet duct using airtight "duct tape". The *Velocicalc* instrument was used to log the pressure drop over the cooling coil and the temperature and humidity after the cooling coil. After 24 hours no increasing pressure drop was found. The outlet humidity was rising through the test period. Since the inlet humidity and temperature was unknown the reason for increasing outlet humidity was unknown. Another test period of 24 hours was then carried out. The cooling coil and fan was not turned off in the break between the test periods. The two tests may therefore be seen in connection. In the second test period the inlet air humidity and temperature was measured using a *TinyTag* instrument from *Gemini*.
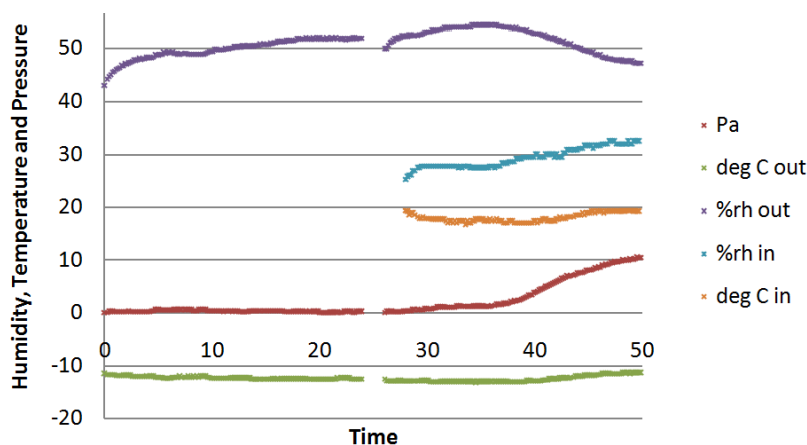
Figure A.1.   *Internal testing of cooling coil. Temperature, relative humidity and pressure were tested for a 24 hour period first. For the second 24 hour period the temperature and humidity in the surrounding room. The outlet temperature was pretty stable at about -12°C and the humidity was between 45-55% through the tests.*

After approximately 38 hours the pressure started to increase. At the same time the outlet temperature started to increase and the outlet humidity started to decrease. The outlet temperature and humidity did not correlate with the fluctuations in the inlet temperature and humidity.

The test showed that the humidity increased through the whole test period until the pressure drop started to increase. Nevertheless since the outlet temperature was quite low the increase in relative humidity will correspond to a very low change in absolute humidity. The inertial testing of the cooling coil seemed therefore promising for tests up to 38 hours. The cooling coil had been turned on for approximately two hours before the measurements begun. Why the humidity didn't draw near **100**% may indicate that the air in fact was colder somewhere inside the cooling coli than at the outlet were the measurement was taken. The small air flow rates may have caused almost stagnant air in the outlet duct witch then may have had a great temperature exchange with the warm surroundings. Insulation of the outlet side of the cooling device was then needed.

A.2. Development of Stable Exhaust Air Conditions

Different attempts were tried out to make warm and humid exhaust air that were stable over a long time. In this appendix is two attempts that were rejected shortly described. The final method is described in chapter 3. A simple system without too many advanced control mechanisms was preferable. A polystyrene box was made to have the heat and humidifier equipment inside. This made it easy to change refill water in the humidifier and the box acted as a small "climate-chamber".

Try-out 1: Electrical humidifier and fan heater.

An "ultrasonic" humidifier was put inside the box together with a 2000 W electrical fan heater with an inbuilt thermostat. Pretesting showed a great fluctuation in the humidity level. The temperature level did also fluctuate to some extent. The temperature and humidity were masured by the *Velocicalc 9555-P* from *Vaisala*.
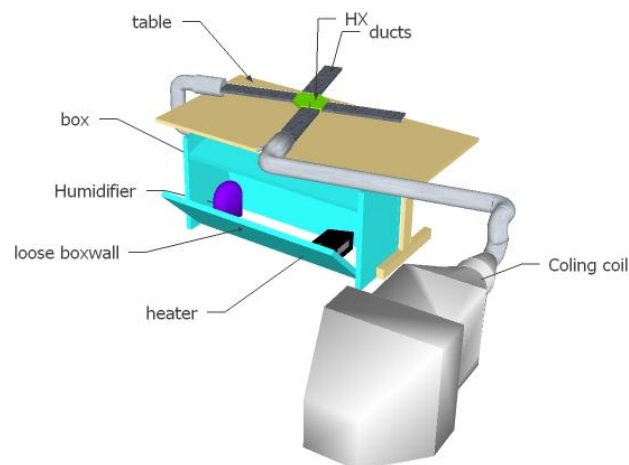
Figure A.2.   Overview of a first attempt to build attest rig. Drawing made in Google Sketch Up. The exhaust air was heated and humidified in a polystyrene box placed under a table to make the rig as compact as possible.
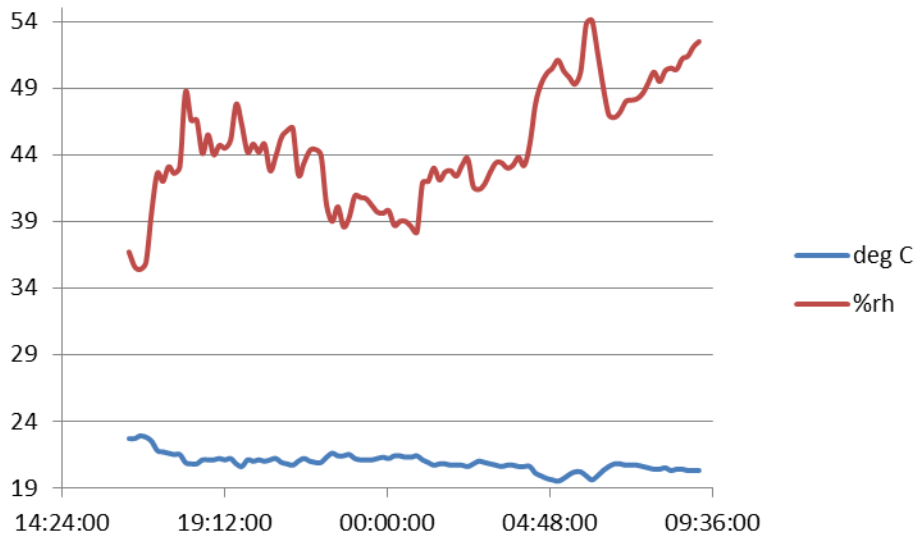
Figure A.3.   *Internal testing of exhaust air side. The temperature seemed quite stable while the humidity level changed greatly through the test period.*

Try-out 2: fan heater and water bracket.

A second approach was tried with an open bracket of water put inside the polystyrene box together with the fan heater. There were still observed fluctuations in the humidity level. This sudden drops in the humidity level corresponded to the on and of switching of the fan heater that probably changed the flow conditions in the polystyrene box a great deal.
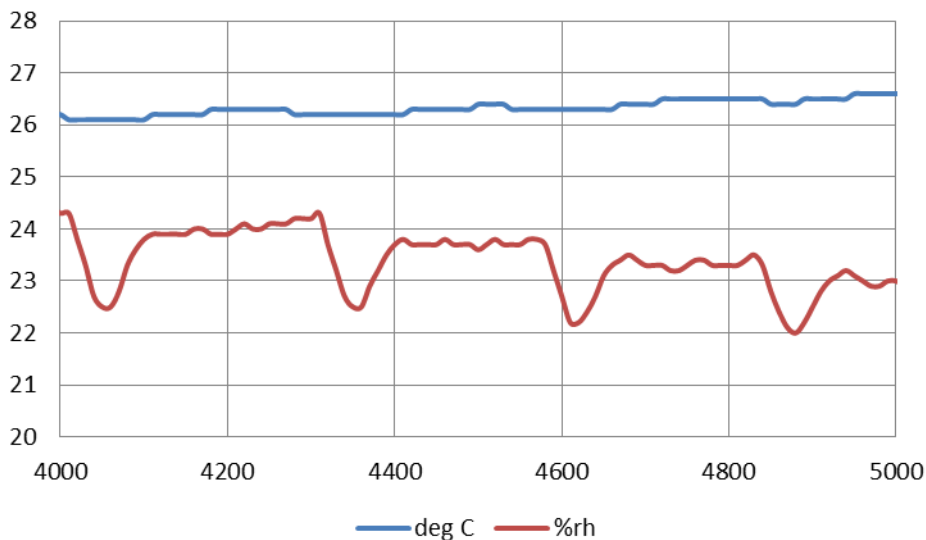
Figure A.4.   *Internal testing of exhaust air side. The temperature seemed quite stable while the humidity level still fluctuating.*

A.3. Program code

Sub inputvar()

```
Call clearsheet2

Min = Worksheets(1).Range("c5")
Max = Worksheets(1).Range("c6")
Begin = Min
If Worksheets(2).Range("d11") = 1 Then
        Worksheets(2).Range("b43").Value = Worksheets(1).Range("c26")
        Worksheets(2).Range("b44").Value = Worksheets(1).Range("c27")
        Worksheets(2).Range("b45").Value = Worksheets(1).Range("c28")
        Worksheets(2).Range("b46").Value = Worksheets(1).Range("c29")
        Worksheets(2).Range("b47").Value = Worksheets(1).Range("c30")
        Worksheets(2).Range("b49").Value = Worksheets(1).Range("c31")
        Ant = (Max - Min) / 2
        Teller = 2
        Varcell = 48

ElseIf Worksheets(2).Range("d11") = 2 Then
         Worksheets(2).Range("b43").Value = Worksheets(1).Range("c26")
        Worksheets(2).Range("b44").Value = Worksheets(1).Range("c27")
        Worksheets(2).Range("b46").Value = Worksheets(1).Range("c29")
        Worksheets(2).Range("b47").Value = Worksheets(1).Range("c30")
        Worksheets(2).Range("b48").Value = Worksheets(1).Range("c21")
        Ant = Worksheets(1).Range("c7")
        Teller = (Max - Min) / (Ant - 1)
        Varcell = 45

ElseIf Worksheets(2).Range("d11") = 3 Then
        Worksheets(2).Range("b43").Value = Worksheets(1).Range("c26")
        Worksheets(2).Range("b44").Value = Worksheets(1).Range("c27")
        Worksheets(2).Range("b45").Value = Worksheets(1).Range("c28")
        Worksheets(2).Range("b47").Value = Worksheets(1).Range("c30")
        Worksheets(2).Range("b48").Value = Worksheets(1).Range("c21")
        Worksheets(2).Range("b49").Value = Worksheets(1).Range("c31")
        Ant = Worksheets(1).Range("c7")
        Teller = (Max - Min) / (Ant - 1)
        Varcell = 46

ElseIf Worksheets(2).Range("d11") = 4 Then
        Worksheets(2).Range("b44").Value = Worksheets(1).Range("c27")
        Worksheets(2).Range("b45").Value = Worksheets(1).Range("c28")
        Worksheets(2).Range("b46").Value = Worksheets(1).Range("c29")
        Worksheets(2).Range("b47").Value = Worksheets(1).Range("c30")
        Worksheets(2).Range("b48").Value = Worksheets(1).Range("c21")
        Worksheets(2).Range("b49").Value = Worksheets(1).Range("c31")
        Ant = Worksheets(1).Range("c7")
        Teller = (Max - Min) / (Ant - 1)
        Varcell = 43

ElseIf Worksheets(2).Range("d11") = 5 Then
        Worksheets(2).Range("b43").Value = Worksheets(1).Range("c26")
        Worksheets(2).Range("b45").Value = Worksheets(1).Range("c28")
        Worksheets(2).Range("b46").Value = Worksheets(1).Range("c29")
        Worksheets(2).Range("b47").Value = Worksheets(1).Range("c30")
        Worksheets(2).Range("b48").Value = Worksheets(1).Range("c21")
        Worksheets(2).Range("b49").Value = Worksheets(1).Range("c31")
        Ant = Worksheets(1).Range("c7")
        Teller = (Max - Min) / (Ant - 1)
        Varcell = 44

ElseIf Worksheets(2).Range("d11") = 6 Then
        Worksheets(2).Range("b43").Value = Worksheets(1).Range("c26")
        Worksheets(2).Range("b44").Value = Worksheets(1).Range("c27")
        Worksheets(2).Range("b45").Value = Worksheets(1).Range("c28")
        Worksheets(2).Range("b46").Value = Worksheets(1).Range("c29")
        Worksheets(2).Range("b48").Value = Worksheets(1).Range("c21")
        Worksheets(2).Range("b49").Value = Worksheets(1).Range("c31")
        Ant = Worksheets(1).Range("c7")
        Teller = (Max - Min) / (Ant - 1)
```

```
        Varcell = 47
End If
Worksheets(2).Cells(Varcell, 2).Value = Begin


For K = 1 To Ant

Call Fmini

Fmin = Worksheets(2).Range("h46")
Fe = Worksheets(2).Range("i46")
Fs = Worksheets(2).Range("j46")

        If Worksheets(2).Range("d32") = 1 Then
                Call geomcross
                If Worksheets(2).Range("d17") = 1 Then
                Call membranecross
                End If
        ElseIf Worksheets(2).Range("d32") = 2 Then
                Call geomcounter
                If Worksheets(2).Range("d17") = 1 Then
                Call membranecounter
                End If
        ElseIf Worksheets(2).Range("d32") = 3 Then
                Call geomcross
                Call geomcounter
                Atot = Worksheets(2).Range("e52") + Worksheets(2).Range("e53")
                nT = (Worksheets(2).Range("e53") / Atot) * Worksheets(2).Range("k53") +
                (Worksheets(2).Range("e52") / Atot) * Worksheets(2).Range("k52")
                Worksheets(2).Range("k54").Value = nT
                DP = Worksheets(2).Range("i52") + Worksheets(2).Range("i53")
                Worksheets(2).Range("i54").Value = DP
                Worksheets(2).Range("e54").Value = Atot

                If Worksheets(2).Range("d17") = 1 Then
                  Call membranecross
                  Call membranecounter
                  nM = (Worksheets(2).Range("e53") / Atot) * Worksheets(2).Range("m53") +
                (Worksheets(2).Range("e52") / Atot) * Worksheets(2).Range("m52")
                  Worksheets(2).Range("m54").Value = nM
                End If
        End If
        'Outoput:
         Tein = Worksheets(2).Range("b43")
         Tsin = Worksheets(2).Range("b46")
         øein = Worksheets(2).Range("b44")
         øsin = Worksheets(2).Range("b47")
         wein = øein * 10 ^ 7 / (6.19 * Exp(5427 / (273.15 + Tein)))
         wsin = øsin * 10 ^ 7 / (6.19 * Exp(5427 / (273.15 + Tsin)))
         Worksheets(2).Range("c44").Value = wein
         Worksheets(2).Range("c47").Value = wsin
         Worksheets(2).Range("b60").Value = xax
          Worksheets(2).Cells(60 + K, 2).Value = Worksheets(2).Cells(Varcell, 2)
          Hxgeom = Worksheets(2).Range("d32")
          Worksheets(2).Cells(60 + K, 3).Value = Worksheets(2).Cells(51 + Hxgeom, 11)
          Worksheets(2).Cells(60 + K, 6).Value = Worksheets(2).Cells(60 + K, 3) * (Tein
        - Tsin) + Tsin
          Worksheets(2).Cells(60 + K, 4).Value = Worksheets(2).Cells(51 + Hxgeom, 13)
          Worksheets(2).Cells(60 + K, 7).Value = -Worksheets(2).Cells(60 + K, 3) * (Tein
        - Tsin) + Tein
          Worksheets(2).Cells(60 + K, 8).Value = Worksheets(2).Cells(60 + K, 4) * (wein
        - wsin) + wsin
          Worksheets(2).Cells(60 + K, 9).Value = -Worksheets(2).Cells(60 + K, 4) * (wein
        - wsin) + wein
          Worksheets(2).Cells(60 + K, 10).Value = Tsin
          Worksheets(2).Cells(60 + K, 11).Value = Tein
          Worksheets(2).Cells(60 + K, 12).Value = wsin
          Worksheets(2).Cells(60 + K, 13).Value = wein
          Tfrost = 5427 / (Log(10 ^ 7 / (6.19 * Worksheets(2).Cells(60 + K, 9)))) - 273
        Ta = Tein - (Tein - Tfrost) / (Worksheets(2).Cells(60 + K, 3))
        Worksheets(2).Cells(60 + K, 14).Value = Ta
        Call recoveryefficiency
        Worksheets(2).Cells(60 + K, 15).Value = Worksheets(2).Cells(51 + Hxgeom, 16)
        Worksheets(2).Cells(60 + K, 5).Value = Worksheets(2).Cells(51 + Hxgeom, 15)
        Worksheets(2).Cells(60 + K, 16).Value = Worksheets(2).Cells(60 + K, 5) *
        Worksheets(2).Cells(60 + K, 15)
        Begin = Begin + Teller
        Worksheets(2).Cells(Varcell, 2).Value = Begin
        Worksheets(2).Cells(60 + K, 20).Value = Worksheets(2).Cells(51 + Hxgeom, 9)
```

```
Next

Worksheets(2).Range("b58").Value = Ant
End Sub
```

Sub geomcross()

```
h = Worksheets(1).Range("e20")
Channelheight = h / (Worksheets(2).Range("b48") + 1)
W = Worksheets(1).Range("f20")
Dh = 2 * Channelheight * W / (Channelheight + W)
L = W
A = Channelheight / W
Atot = L * W * (Worksheets(2).Range("b48"))
Visc = Worksheets(1).Range("c37")
rho = Worksheets(1).Range("c36")
kond = Worksheets(1).Range("c35")
cp = Worksheets(1).Range("c38")
Across = Channelheight * W

Fmin = Worksheets(2).Range("h46")
Fe = Worksheets(2).Range("i46")
Fs = Worksheets(2).Range("j46")
R = Worksheets(2).Range("k46")

Vel = Fmin / ((h / 2) * W)
Re = Vel * Dh / Visc
f = (-50.416 * A ^ 3 + 132.75 * A ^ 2 - 121.22 * A + 95.705) / Re
K = 4 * f * L / Dh
DP = 0.5 * rho * Vel ^ 2 * (K + 0.8775)
Nu = -7.4818 * (A ^ 3) + 18.535 * (A ^ 2) - 15.663 * A + 8.235
Worksheets(2).Range("g42").Value = Nu
hc = Nu * kond / Dh
U = (2 / hc) ^ -1
NTU = U * Atot / (cp * Fmin * rho)
nT = (1 - Exp((1 / R) * (NTU ^ 0.22) * (Exp(-R * (NTU ^ 0.78)) - 1))) / (Fe / Fmin)

Worksheets(2).Range("b52").Value = Dh
Worksheets(2).Range("c52").Value = NTU
Worksheets(2).Range("d52").Value = L
Worksheets(2).Range("e52").Value = Atot
Worksheets(2).Range("f52").Value = A
Worksheets(2).Range("g52").Value = Vel
Worksheets(2).Range("h52").Value = Re
Worksheets(2).Range("i52").Value = DP
Worksheets(2).Range("j52").Value = hc
Worksheets(2).Range("k52").Value = nT
End Sub
```

Sub geomcounter()

```
h = Worksheets(1).Range("e20")
Channelheight = h / (Worksheets(2).Range("b48") + 1)
W = Worksheets(1).Range("h20")
Dh = 2 * Channelheight * W / (Channelheight + W)
L = Worksheets(1).Range("g20")
A = Channelheight / W
Atot = L * W * (Worksheets(2).Range("b48"))
Visc = Worksheets(1).Range("c37")
rho = Worksheets(1).Range("c36")
kond = Worksheets(1).Range("c35")
cp = Worksheets(1).Range("c38")
Fmin = Worksheets(2).Range("h46")
Fe = Worksheets(2).Range("i46")
Fs = Worksheets(2).Range("j46")
R = Worksheets(2).Range("k46")Worksheets(2).Range("f42").Value = R
Across = Channelheight * W
Vel = Fmin / ((h / 2) * W)
Re = Vel * Dh / Visc
f = (-50.416 * A ^ 3 + 132.75 * A ^ 2 - 121.22 * A + 95.705) / Re
K = 4 * f * L / Dh
DP = 0.5 * rho * Vel ^ 2 * (K + 0.8775)
Nu = -7.4818 * A ^ 3 + 18.535 * A ^ 2 - 15.663 * A + 8.235
Worksheets(2).Range("g43").Value = Nu
hc = Nu * kond / Dh
U = (2 / hc) ^ -1
NTU = U * Atot / (cp * Fmin * rho)
If R < 1 Then
```

```
        nT = ((1 - Exp(-NTU * (1 - R))) / (1 - R * Exp(-NTU * (1 - R)))) / (Fe / Fmin)
ElseIf R = 1 Then
        nT = (NTU / (1 + NTU)) / (Fe / Fmin)
End If

Worksheets(2).Range("b53").Value = Dh
Worksheets(2).Range("c53").Value = NTU
Worksheets(2).Range("d53").Value = L
Worksheets(2).Range("e53").Value = Atot
Worksheets(2).Range("f53").Value = A
Worksheets(2).Range("g53").Value = Vel
Worksheets(2).Range("h53").Value = Re
Worksheets(2).Range("i53").Value = DP
Worksheets(2).Range("j53").Value = hc
Worksheets(2).Range("k53").Value = nT
End Sub
```

Sub membranecross()

```
'equation 2.8.
hm = Worksheets(2).Range("j52") / (Worksheets(1).Range("c38") *
(Worksheets(1).Range("c16")) ^ (2 / 3))
Rconv = 2 / (hm)

Fmin = Worksheets(2).Range("h46")
Fe = Worksheets(2).Range("i46")
Fs = Worksheets(2).Range("j46")
R = Worksheets(2).Range("k46")

'reference resistances
R1 = (Worksheets(1).Range("c13"))
r2 = (Worksheets(1).Range("c15"))
Ø1 = Worksheets(1).Range("g12")
T1 = Worksheets(1).Range("f12")
Ø2 = Worksheets(1).Range("g14")
K = (r2 / R1 - 1) / (Ø1 / Ø2 - 1)
øein = Worksheets(2).Range("b44")
Tein = Worksheets(2).Range("b43")
øsin = Worksheets(2).Range("b47")
Tsin = Worksheets(2).Range("b46")
wmax = øein * 10 ^ 7 / (6.19 * Exp(5427 / (273.15 + Tein)))
wmin = øsin * 10 ^ 7 / (6.19 * Exp(5427 / (273.15 + Tsin)))
wref = Ø1 * 10 ^ 7 / (6.19 * Exp(5427 / (273.15 + T1)))
wmean = (wmin + wmax) / 2
Tmean = (Tein + Tsin) / 2
ømean = wmean / (10 ^ 7 / (6.19 * Exp(5427 / (273.15 + Tmean))))
'mean resistance:
Rmem = R1 * (1 - K + K * (Ø1 / (ømean)))
Um = 1 / (Rconv + Rmem)
NTUm = Um * (Worksheets(2).Range("e52")) / (Fmin * Worksheets(1).Range("c36"))
Worksheets(2).Range("n52").Value = NTUm
'moisture transfer efficiency from 2.4
nM = (1 - Exp(NTUm ^ 0.22 * (Exp(-R * NTUm ^ 0.78) - 1) / R)) / (Fe / Fmin)
Worksheets(2).Range("l52").Value = Rmem
Worksheets(2).Range("m52").Value = nM
Worksheets(2).Range("f45").Value = hm
End Sub
```

Sub membranecounter()

```
hm = Worksheets(2).Range("j53") / (Worksheets(1).Range("c38") *
(Worksheets(1).Range("c16")) ^ (2 / 3))
Rconv = 2 / (hm)
Fmin = Worksheets(2).Range("h46")
Fe = Worksheets(2).Range("i46")
Fs = Worksheets(2).Range("j46")
R = Worksheets(2).Range("k46")

R1 = (Worksheets(1).Range("c13"))
r2 = (Worksheets(1).Range("c15"))
Ø1 = Worksheets(1).Range("g12")
Ø2 = Worksheets(1).Range("g14")
T1 = Worksheets(1).Range("f12")
K = (r2 / R1 - 1) / (Ø1 / Ø2 - 1)
øein = Worksheets(2).Range("b44")
Tein = Worksheets(2).Range("b43")
øsin = Worksheets(2).Range("b47")
```

A-10

```
Tsin = Worksheets(2).Range("b46")
wmax = øein * 10 ^ 7 / (6.19 * Exp(5427 / (273.15 + Tein)))
wmin = øsin * 10 ^ 7 / (6.19 * Exp(5427 / (273.15 + Tsin)))
wref = Ø1 * 10 ^ 7 / (6.19 * Exp(5427 / (273.15 + T1)))
wmean = (wmin + wmax) / 2
Tmean = (Tein + Tsin) / 2
ømean = wmean / (10 ^ 7 / (6.19 * Exp(5427 / (273.15 + Tmean))))
Rmem = R1 * (1 - K + K * (Ø1 / (ømean)))
Um = 1 / (Rconv + Rmem)
NTUm = (Um * Worksheets(2).Range("e53")) / (Fmin * Worksheets(1).Range("c36"))
'moiure transfer efficiency from eq 2.5

If R < 1 Then
        nM = ((1 - Exp(-NTUm * (1 - R))) / (1 - R * Exp(-NTUm * (1 - R)))) / (Fe / Fmin)
ElseIf R = 1 Then
        nM = (NTUm / (1 + NTUm)) / (Fe / Fmin)
End If

Worksheets(2).Range("l53").Value = Rmem
Worksheets(2).Range("m53").Value = nM
Worksheets(2).Range("n53").Value = NTUm
End Sub
```

Sub recoveryefficiency()

```
Tsupply = Worksheets(1).Range("c43")
Tein = Worksheets(2).Range("b43")
wein = Worksheets(2).Range("c44")
wsin = Worksheets(2).Range("c47")
V = Worksheets(2).Range("b45") * 3600
Cpair = Worksheets(1).Range("c38")
Rhoair = Worksheets(1).Range("c36")
j = Worksheets(2).Range("d32")

  nM = Worksheets(2).Cells(51 + j, 13)
  DP = Worksheets(2).Cells(51 + j, 9)
  'get nT
  nT = Worksheets(2).Cells(51 + j, 11)
  sumwithout = 0
  DPsum = 0
  summe = 0
  'Set Ta and Tb
  If nM > 0 Then
        weut = -nM * (wein - wsin) + wein
        Else
        weut = wein
  End If

  Tfrost = -8
  Ta = Tein - (Tein - Tfrost) / nT
  If Ta < -273 Then
        Ta = -273
  End If

  Tb = nT * (Tein - Ta) + Ta
 'sums hourly
 place = Worksheets(2).Range("k16")
 For K = 2 To 8761
        Tsupply = Worksheets(1).Range("c43")
          Tsin = Worksheets(2).Cells(K, 16 + place)
          Tc = nT * (Tein - Tsin) + Tsin
        'Set by-pass in summer
        B = 0
        If Tsin > Tsupply Then
        B = 1
        End If
        'find heat needed without recovery
        sumwithout = sumwithout + (1 - B) * Rhoair * V * Cpair * (Tsupply - Tsin)
        'find energy based on pressue drop both air streams. No pressure drop summer
        DPsum = DPsum + 2 * DP * V * (1 - B)
        'Sets Dtfrost
        If (Ta - Tsin) > 0 Then
        DTfrost = Ta - Tsin
        Else
        DTfrost = 0
        End If
        'Sets Dtsupply
```

A-11

```
            If Tsupply > Tc Then
            Dta = Tc
            Else
            Dta = Tsupply
            End If
            If Tb > Dta Then
            Dtb = Tb
            Else
            Dtb = Dta
            End If
            If (Tsupply - Dtb) > 0 Then
            Dtsupply = Tsupply - Dtb
            Else
            Dtsupply = 0
            End If
            'sums Dt values
            summe = summe + DTfrost + Dtsupply
  Next

  'energy for heating rest after rec and frost protection
  Qrec = Cpair * Rhoair * summe * V
'Finds annual heat recovery efficiency
nE = 1 - (Qrec + DPsum) / (sumwithout)
Worksheets(2).Cells(51 + j, 15) = nE
End Sub
```

Sub Fmini()

```
'Flow min
If Worksheets(2).Range("d11") = 2 Then
Fmin = Worksheets(2).Range("b45")
Fe = Fmin
Fs = Fmin
R = 1
Else
 If Worksheets(2).Range("b45") >= Worksheets(2).Range("b49") Then
 Fmin = Worksheets(2).Range("b49")
 Fe = Fmin
 Fs = Worksheets(2).Range("b45")
 R = Fmin / Worksheets(2).Range("b45")
 Else
 Fmin = Worksheets(2).Range("b45")
 Fe = Worksheets(2).Range("b49")
 Fs = Worksheets(2).Range("b45")
 R = Fmin / Worksheets(2).Range("b49")
 End If
End If

Worksheets(2).Range("h46").Value = Fmin
Worksheets(2).Range("i46").Value = Fe
Worksheets(2).Range("j46").Value = Fs
Worksheets(2).Range("k46").Value = R
End Sub
```

A.4.   Results

In this chapter all results from all eight experiments are presented individually. A short description about the performed experiment comes first. Second a table showing the standard deviation, random uncertainty, mean value, systematic uncertainty and the total uncertainty for all measured and calculated results. The mean input and output temperatures and humidity levels are plotted in a humidity-temperature diagram showing the changes through the heat exchangers in each air stream. All relative humidity, temperatures, pressure drop developments and efficiency(ies) with time are displayed. For some experiments the surrounding temperature and humidity level were measures with the *TSI-* instrument, in other experiments the supply outlet velocity were measured with the same instruments. In these cases the results are plotted against time. For experiment 1, 4 and 8 pictures showing the heat exchanger with ice and condensate water are displayed as well. The colours used in the plots are as shown here:
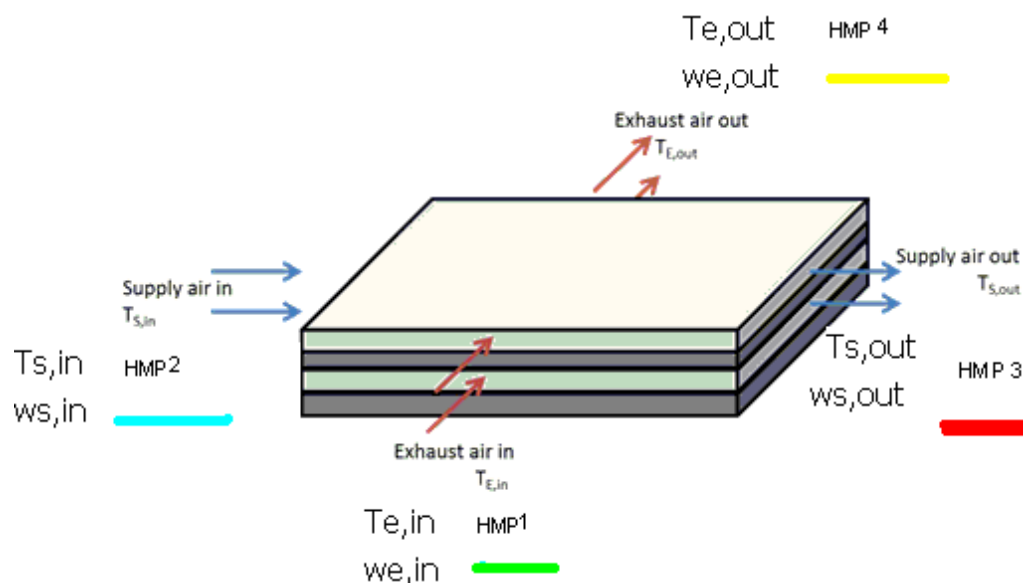
Figure A.5.   *Overview of the Vaisala humidity and temperature probes placement and the air streams. The colour indicates which measurement points that are displayed in the graphs later in this chapter.*

A.4.1 Experiment 1: Three layer *Optimax* plastic sheets

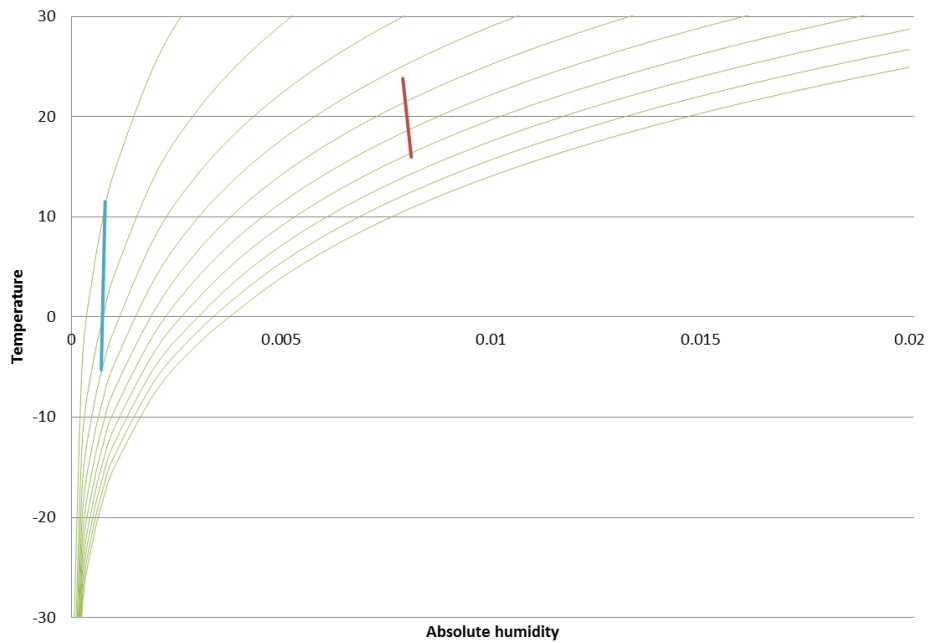The first experiment was done with a three layer plastic sheet exchanger. The plastic sheets used were transparent overhead plastic sheets from *Optifilm*. Only the flow rate on the supply air side was measured. The pressure drop on the supply air side was quite stable while the exhaust air side experienced a linear increase in the pressure drop. After 900 min an increase in the surrounding temperature and decrease in surrounding humidity made the inlet and outlet temperatures increase, while the humidity levels still were quite stable. At the end of the experiment dense ice had built up in the upper exhaust air channel near the supply air inlet. In the middle of the exchanger area condensed water had built up, making the upper and middle plastic sheets sticking together. In the lower channel no ice was found, however water droplets were present.

Table A.1. *Data from experiment 1. Standard deviation, random uncertainty, mean value, systematic uncertainty and total uncertainty are shown.*

	HMP 1 RH	HMP 1 Temp	HMP 2 RH	HMP 2 Temp	HMP 3 RH	HMP 3 Temp	HMP 4 RH	HMP 4 Temp	Pressure Exthaust	Pressure Supply
	%	°C	%	°C	%	°C	%	°C	Pa	Pa
s	3.0150	0.6133	0.6344	0.4696	0.2597	0.6735	4.2812	0.6738	0.0621	0.2065
U_r	0.0112	0.0023	0.0024	0.0017	0.0010	0.0025	0.0159	0.0025	0.0002	0.0008
$\bar{x}$	43.6163	23.8101	27.4885	-5.2667	9.4386	11.5200	71.1096	15.9736	2.5518	2.4006
U_S	2.0000	0.1000	2.0000	0.1000	1.4000	0.2000	2.0000	0.1000	0.1900	0.1900
U_T	2.0000	0.1000	2.0000	0.1000	1.4000	0.2000	2.0001	0.1000	0.1900	0.1900
	n_T	n_M	ω_1	ω_2	ω_3	ω_4	Exhaust flow	Supply flow		
			kg_W/kg_M	kg_W/kg_M	kg_W/kg_M	kg_W/kg_M	m³/h	m³/h		
s										
U_r										
$\bar{x}$	0.2693	0.0132	0.0079	0.0007	0.0008	0.0081	??	1.5789		
U_S										
U_T	0.0044	0.0179	0.0004	0.0001	0.0001	0.0002	??	0.1104		

Figure A.6. *Exhaust (red) and supply (blue) air flows through the heat exchanger (based on inlet and outlet values) in a Humidity-temperature diagram. The green lines are relative humidity lines starting at 10% to the left and 100% (saturation line) at the right.*
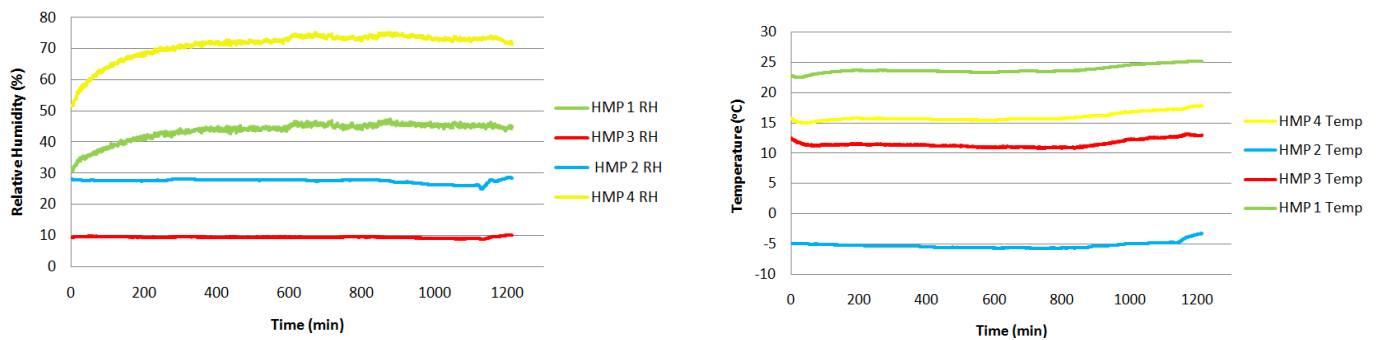
Figure A.7. *Relative humidity (left) and temperature (right) measurements through the test period in all four measurement points.*
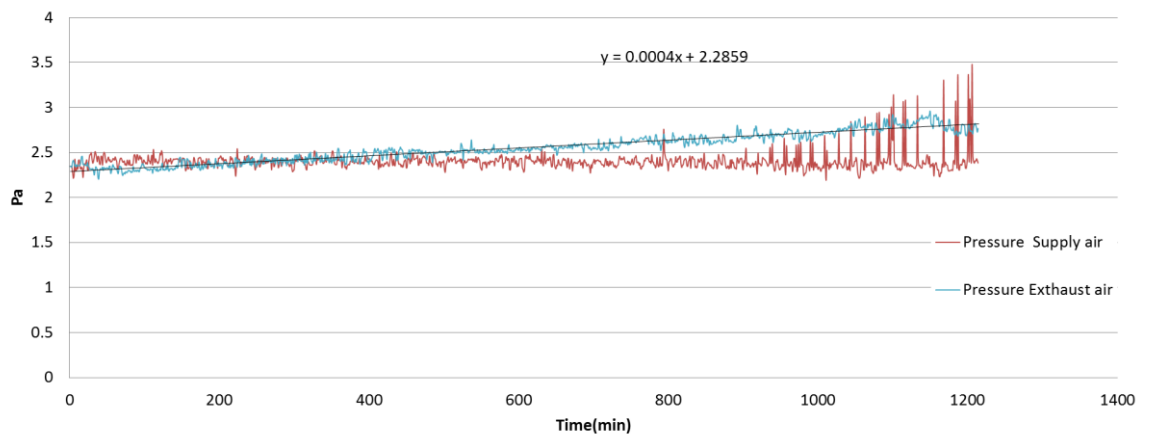
Figure A.8. *Pressure drop for both air flows. Linear trend line for the exhaust air stream is displayed.*
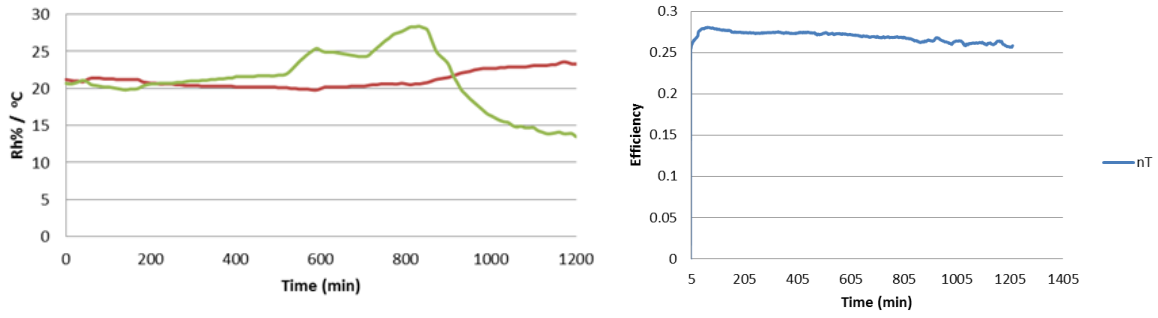
Figure A.9.   *Left: surrounding temperature (red line) and Relative humidity (green line) over the test period. Right: Temperature efficiency.*
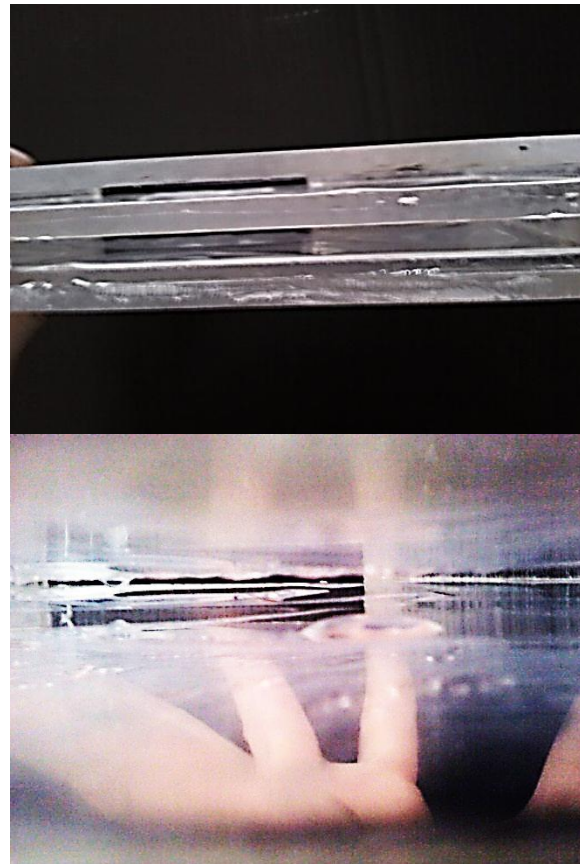
Figure A.10.   *Pictures after experiment. Left: dense ice was found in the upper right part (near the supply air inlet). In the middle a pool of water made the two upper plastic sheets stick together. Upper right: side view of the dry supply air channels. Lower right: picture inside the ice and water filled exhaust air side.*

A.4.2 Experiment 2: Five layer *Optimax* plastic sheets

In the second experiment the heat transfer sheets from experiment 1 were increased to five layers. This were done to increase the temperature efficiency and to see if this increased the ice formation. The flow rate at the exhaust air side were only measured once so no uncertainty were able to be found for that single measurement. Now a more significant ice layer built up in two out of three air channels in the exhaust air side. (Unfortunately no pictures were taken.)

Table A.2.   *Data from experiment 2. Standard deviation, random uncertainty, mean value, systematic uncertainty and total uncertainty .*

|	HMP 1 RH	HMP 1 Temp	HMP 2 RH	HMP 2 Temp	HMP 3 RH	HMP 3 Temp	HMP 4 RH	HMP 4 Temp	Pressure Exthaust	Pressure Supply
	%	°C	%	°C	%	°C	%	°C	Pa	Pa
s	1.3328	0.8945	3.7454	1.6007	2.4531	2.5703	3.7454	1.7966	0.4508	1.2758
U_r	0.0055	0.0037	0.0154	0.0066	0.0101	0.0106	0.0154	0.0074	0.0019	0.0053
$\bar{x}$	39.3434	20.8521	33.6857	-8.0513	16.6964	2.6907	66.7383	10.0383	5.7938	3.9516
U_S	2.0000	0.1000	2.0000	0.1000	1.4000	0.2000	2.0000	0.1000	0.1900	0.1900
U_T	2.0000	0.1001	2.0001	0.1002	1.4000	0.2003	2.0001	0.1003	0.1900	0.1901
	n_T	n_M	ω_1	ω_2	ω_3	ω_4	Exhaust flow	Supply flow		
			kg_W/kg_M	kg_W/kg_M	kg_W/kg_M	kg_W/kg_M	m³/h	m³/h		
s										
U_r										
$\bar{x}$	0.3733	0.0120	0.0060	0.0007	0.0008	0.0051	1.0528	1.6629		
U_S										
U_T	0.0043	0.0146	0.0003	0.0000	0.0001	0.0002	??	0.1096		
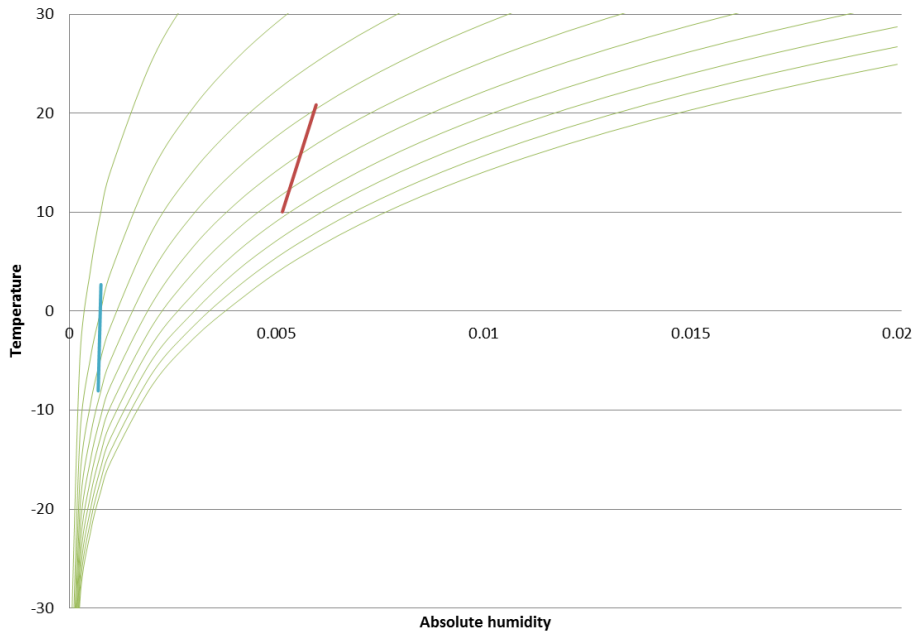
Figure A.11.   *Exhaust (red) and supply (blue) air flows through the heat exchanger (based on inlet and outlet values) in a Humidity-temperature diagram. The green lines are relative humidity lines starting at 10% to the left and 100% (saturation line) at the right.*
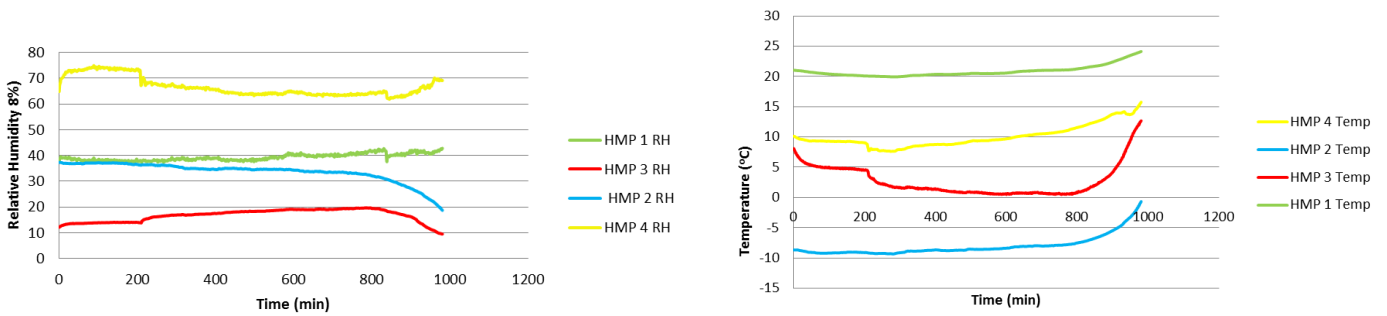

Figure A.12.   *Relative humidity (left) and temperature (right) measurements through the test period in all four measurement points.*
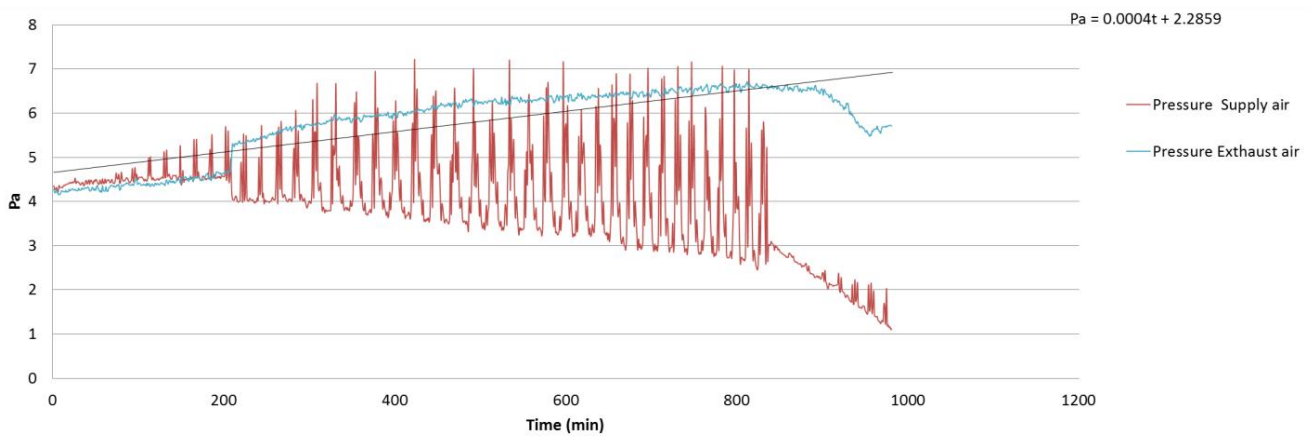
Figure A.13.   *Pressure drop for both air flows. Linear trend line for exhaust air stream is displayed as well.*
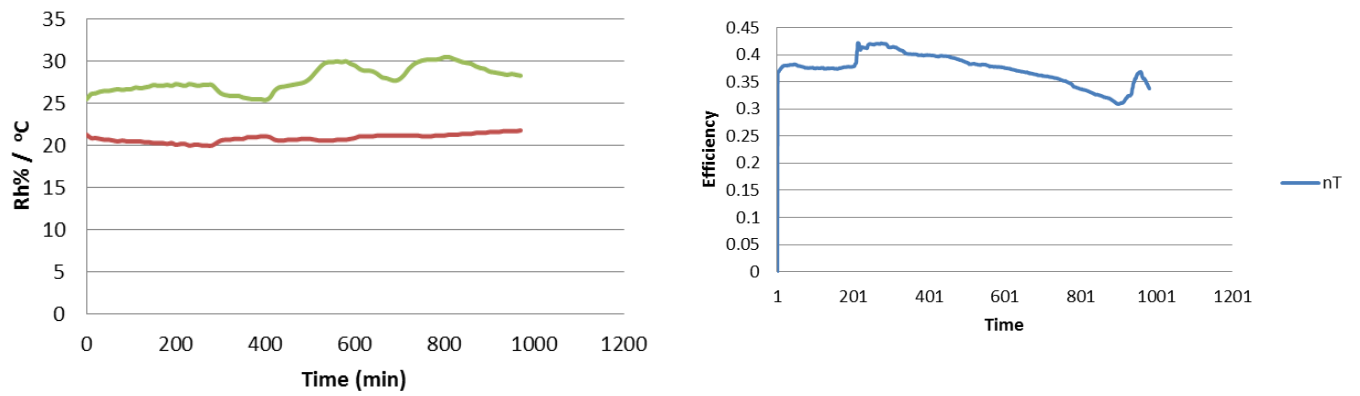
Figure A.14.   *Left: surrounding temperature (red line) and Relative humidity (green line) over the test period. Right: Temperature efficiency.*

A.4.3 Experiment 3: *DuPont* X-membrane

A five layer membrane based heat exchanger utilising a membrane from *DuPont* in this thesis called membrane X was tested. Neither ice formation nor water condensation occurred through the test period.

Table A.3. Data from experiment 3. Standard deviation, random uncertainty, mean value, systematic uncertainty and total uncertainty is shown.

	HMP 1 RH	HMP 1 Temp	HMP 2 RH	HMP 2 Temp	HMP 3 RH	HMP 3 Temp	HMP 4 RH	HMP 4 Temp	Pressure Exthaust	Pressure Supply
	%	$^{\circ}$C	%	$^{\circ}$C	%	$^{\circ}$C	%	$^{\circ}$C	Pa	Pa
s	1.3326	0.3344	0.8330	0.3435	1.8757	0.6351	1.2887	0.2819	0.3535	0.3927
U_r	0.0051	0.0013	0.0032	0.0013	0.0071	0.0024	0.0049	0.0011	0.0013	0.0015
$\bar{x}$	42.8621	21.2534	27.0875	-4.9602	31.5750	16.5439	55.9035	10.4953	8.9637	9.2480
U_S	2.0000	0.1000	2.0000	0.1000	1.4000	0.2000	2.0000	0.1000	0.1900	0.1900
U_T	2.0000	0.1000	2.0000	0.1000	1.4000	0.2000	2.0000	0.1000	0.1900	0.1900

|	n_T	n_M	ω_1	ω_2	ω_3	ω_4	Exhaust flow	Supply flow
			kg_W/kg_M	kg_W/kg_M	kg_W/kg_M	kg_W/kg_M	m^3/h	m^3/h
s								
U_r								
$\bar{x}$	0.4099	0.3721	0.0066	0.0007	0.0037	0.0044	1.3849	0.7439
U_S								
U_T	0.0047	0.0400	0.0003	0.0001	0.0002	0.0002	0.1361	0.0641

Figure A.15.   *Exhaust (red) and supply (blue) air flows through the heat exchanger (based on inlet and outlet values) in a Humidity-temperature diagram. The green lines are relative humidity lines starting at 10% to the left and 100% (saturation line) at the right.*
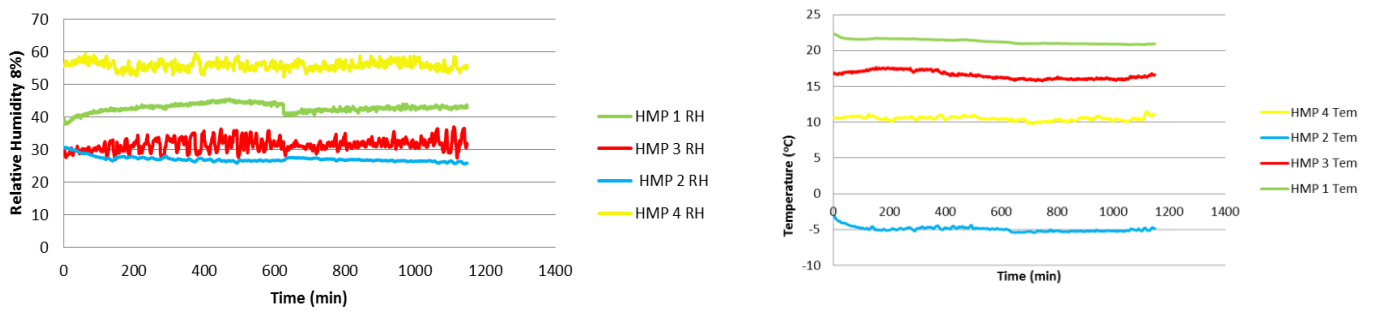
Figure A.16.   *Relative humidity (left) and temperature (right) measurements through the test period in all four measurement points.*
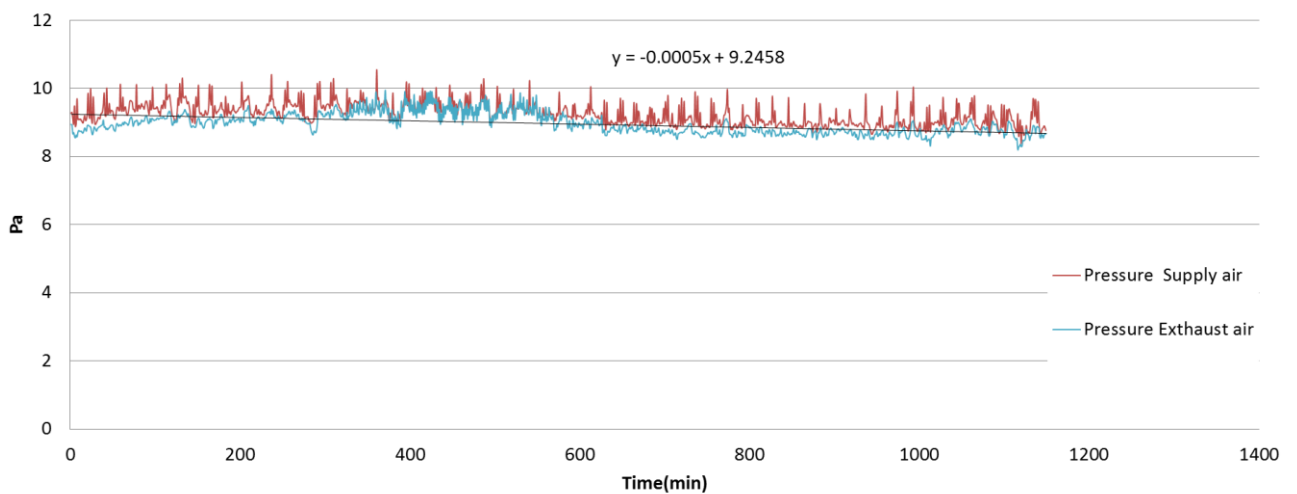
Figure A.17.   *Pressure drop for both air flows. Linear trend line for exhaust air stream is displayed as well.*
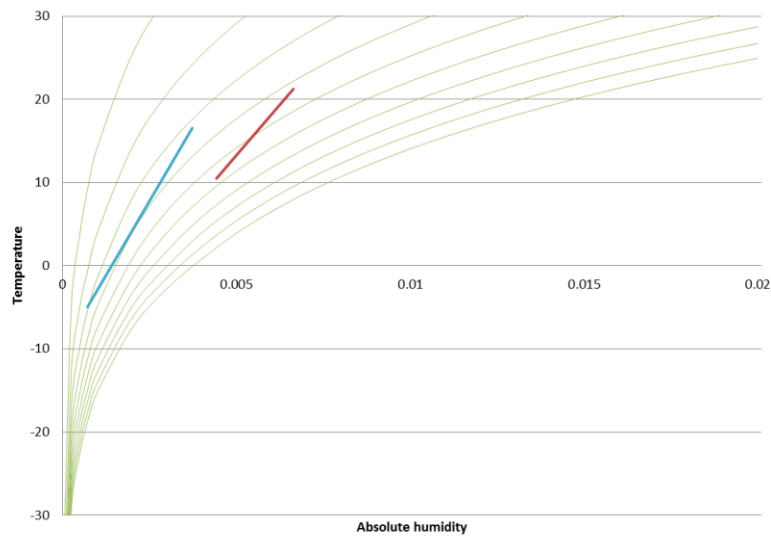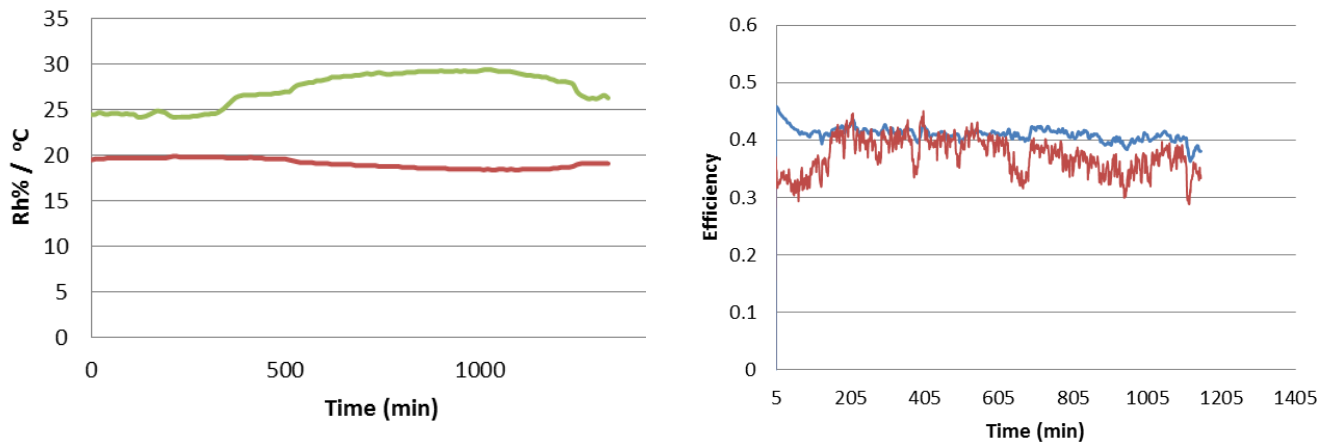
Figure A.18.   Left: surrounding temperature (red line) and Relative humidity (green line) over the test period. Right: Temperature efficiency (blue line and moisture transfer efficiency (red line).

A.4.4 Experiment 4: *DuPont PP*

The poly propylene protection sheet for the *DuPont X* membrane was tested as a second plastic material. The PP-sheet was used since the material was very similar to the membrane material regarding thickness, colour and behaviour as elasticity etc. The heat exchanger had five layers of plastic sheets. In this experiment the *TSI* measurement instrument were used to measure the supply air outlet velocity at the duct exit rather than the surrounding temperature and humidity. Condensed water was observed after a short while in the upper exhaust air channel through the acrylic top plate. At the end of the experiment a lot of ice had formed in the exhaust air side. The supply air channels was observed to be narrower caused by the ice layer in the exhaust air side.

Table A.4.   *Data from experiment 4. Standard deviation, random uncertainty, mean value, systematic uncertainty and total uncertainty.*

|	HMP 1 RH	HMP 1 Temp	HMP 2 RH	HMP 2 Temp	HMP 3 RH	HMP 3 Temp	HMP 4 RH	HMP 4 Temp	Pressure Exthaust	Pressure Supply
	%	$^\circ$C	%	$^\circ$C	%	$^\circ$C	%	$^\circ$C	Pa	Pa
s	2.1919	0.3667	1.4989	0.4807	0.3112	1.2553	1.3578	0.5311	0.4198	0.3427
U_r	0.0094	0.0016	0.0065	0.0021	0.0013	0.0054	0.0058	0.0023	0.0018	0.0015
$\bar{x}$	46.1520	21.0377	35.1761	-8.4142	8.9995	12.5369	75.9515	10.8156	6.7268	6.1573
U_S	2.0000	0.1000	2.0000	0.1000	1.4000	0.2000	2.0000	0.1000	0.1900	0.1900
U_T	2.0000	0.1000	2.0000	0.1000	1.4000	0.2001	2.0000	0.1000	0.1900	0.1900
	n_T	n_M	ω_1	ω_2	ω_3	ω_4	Exhaust flow	Supply flow		
			kg_W/kg_M	kg_W/kg_M	kg_W/kg_M	kg_W/kg_M	m^3/h	m^3/h		
s										
U_r										
$\bar{x}$	0.3466	0.0169	0.0070	0.0007	0.0008	0.0061	1.2982	1.3759		
U_S										
U_T	0.0042	0.0209	0.0003	0.0000	0.0001	0.0002	0.2632	0.1104		

Figure A.19.   *Exhaust (red) and supply (blue) air flows through the heat exchanger (based on inlet and outlet values) in a Humidity-temperature diagram. The green lines are relative humidity lines starting at 10% to the left and 100% (saturation line) at the right.*

Figure A.20.   *Relative humidity (left) and temperature (right) measurements through the test period in all four measurement points.*
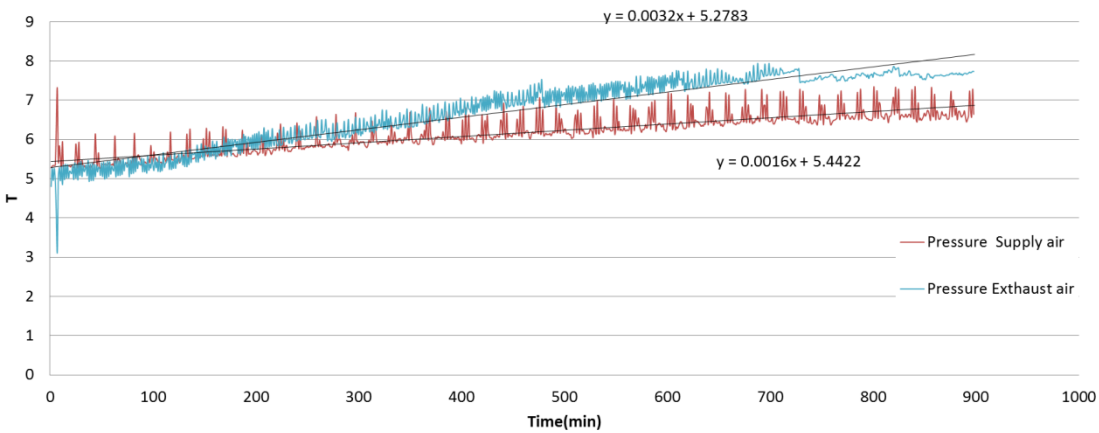
Figure A.21.   *Pressure drop for both air flows. Linear trend line for both air streams are displayed as well.*
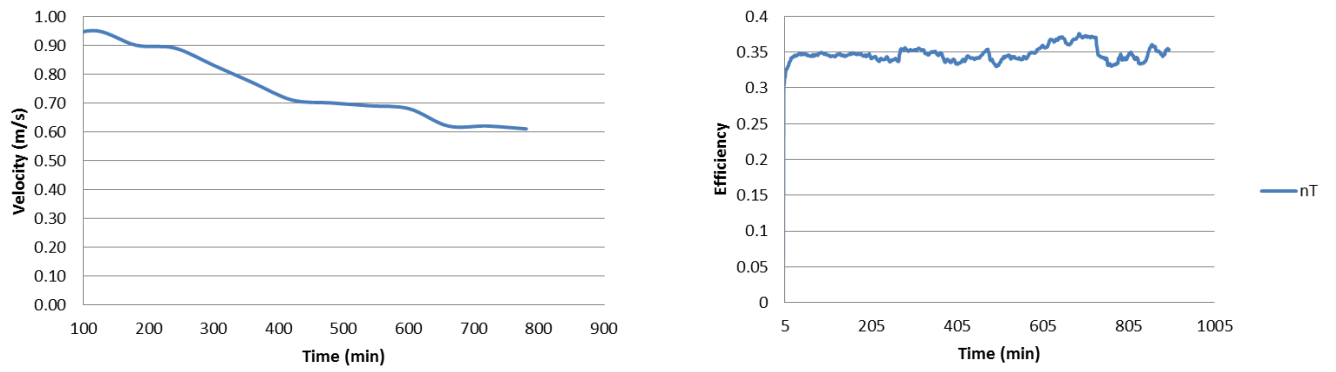
Figure A.22.   *Velocity in one point at the supply air outlet channel exit. Right: Temperature efficiency.*
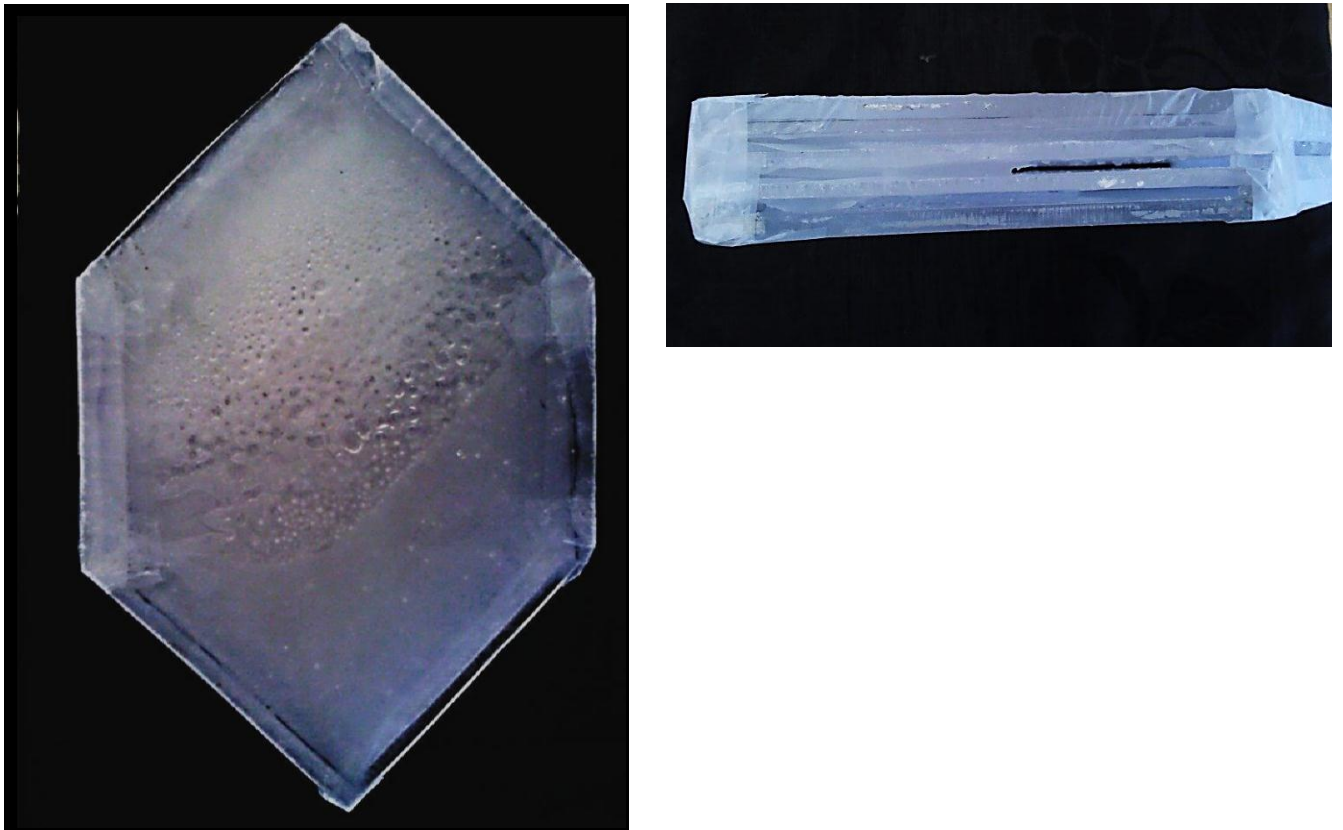
Figure A.23.   *Pictures after experiment. Left: Ice was found in the upper right half (near the supply air inlet). Right: side view of the ice and water filled exhaust air side.*

A.4.5 Experiment 5: *DuPont X*

A second experiment with the membrane from DuPont was done. Now the supply air flow were greater than the exhaust air flow, opposite of the case in experiment 3. The supply air temperature was about 0°C. Neither ice, condensate water nor crumpling of the membrane were observed in this experiment.

Table A.5. *Data from experiment 5. Standard deviation, random uncertainty, mean value, systematic uncertainty and total uncertainty.*

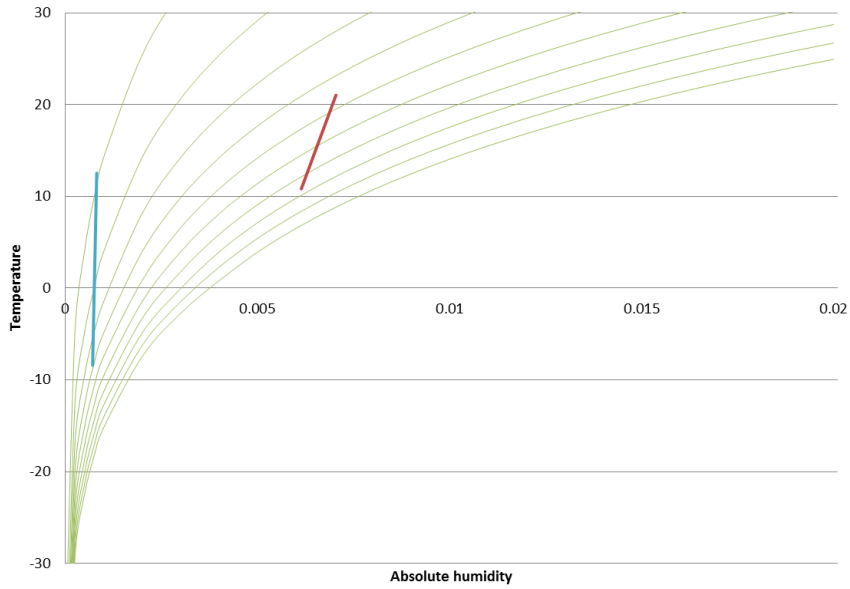|	HMP 1 RH	HMP 1 Temp	HMP 2 RH	HMP 2 Temp	HMP 3 RH	HMP 3 Temp	HMP 4 RH	HMP 4 Temp	Pressure Exthaust	Pressure Supply
	%	°C	%	°C	%	°C	%	°C	Pa	Pa
s	1.5595	0.1760	0.8435	0.1899	1.7984	0.4032	1.9237	0.2700	0.3258	0.4168
U_r	0.0064	0.0007	0.0034	0.0008	0.0073	0.0016	0.0078	0.0011	0.0013	0.0017
$\bar{x}$	45.2467	22.9054	39.0157	-0.2282	36.6576	14.8583	58.9526	10.4258	9.8529	10.4660
U_S	2.0000	0.1000	2.0000	0.1000	1.4000	0.2000	2.0000	0.1000	0.1900	0.1900
U_T	2.0000	0.1000	2.0000	0.1000	1.4000	0.2000	2.0000	0.1000	0.1900	0.1900
	n_T	n_M	ω_1	ω_2	ω_3	ω_4	Exhaust flow	Supply flow		
			kg_W/kg_M	kg_W/kg_M	kg_W/kg_M	kg_W/kg_M	m^3/h	m^3/h		
s										
U_r										
$\bar{x}$	0.5386	0.4914	0.0077	0.0015	0.0039	0.0046	1.3309	1.5261		
U_S										
U_T	0.0053	0.0336	0.0004	0.0001	0.0002	0.0002	0.0922	0.1188		
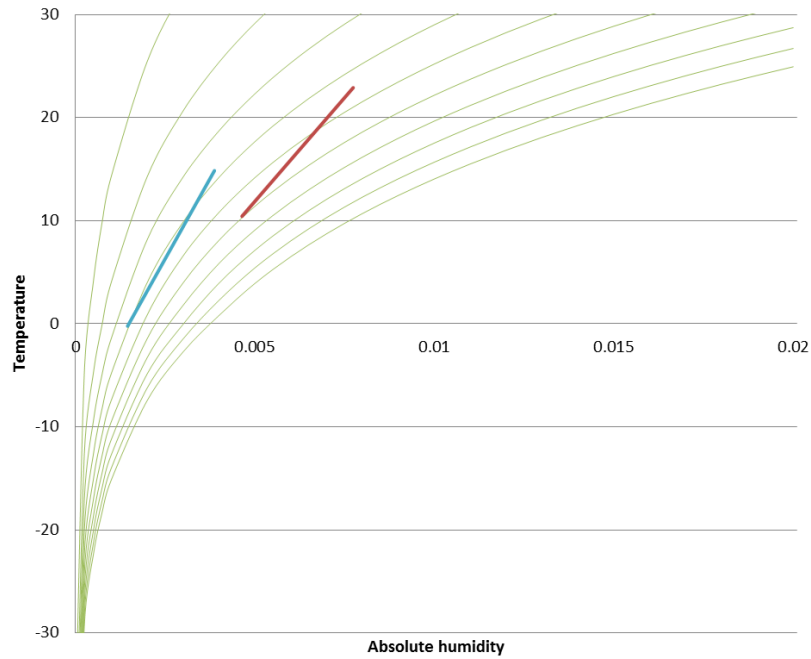
Figure A.24.   *Exhaust (red) and supply (blue) air flows through the heat exchanger (based on inlet and outlet values) in a Humidity-temperature diagram. The green lines are relative humidity lines starting at 10% to the left and 100% (saturation line) at the right.*
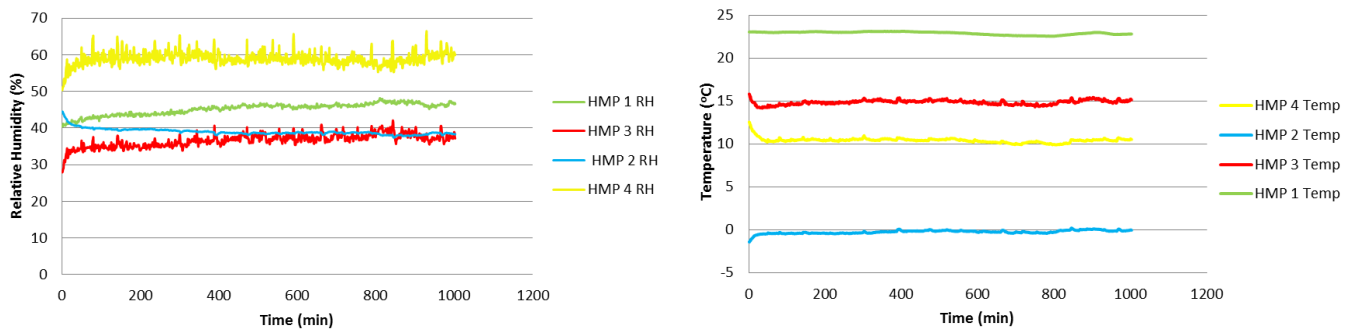
Figure A.25.   *Relative humidity (left) and temperature (right) measurements through the test period in all four measurement points.*
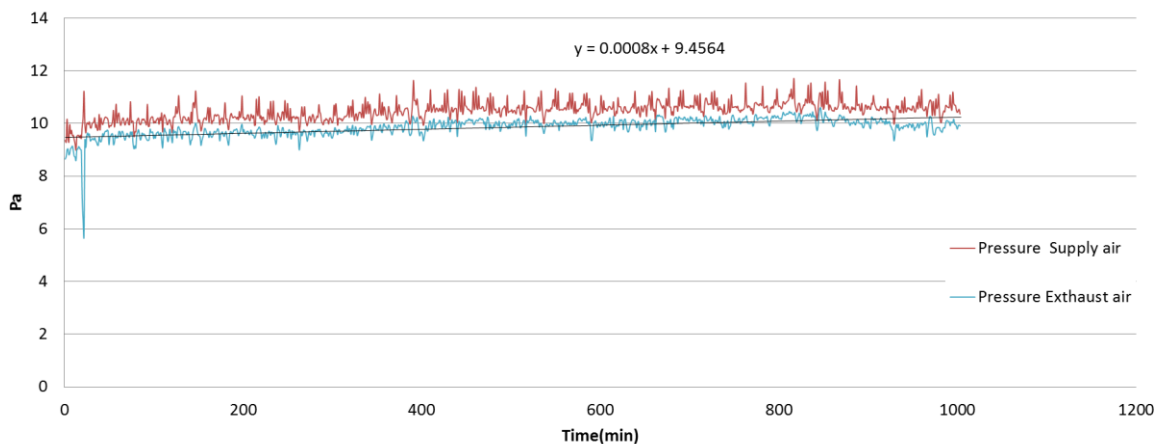
Figure A.26.   *Pressure drop for both air flows. Linear trend line for exhaust air stream is displayed as well.*
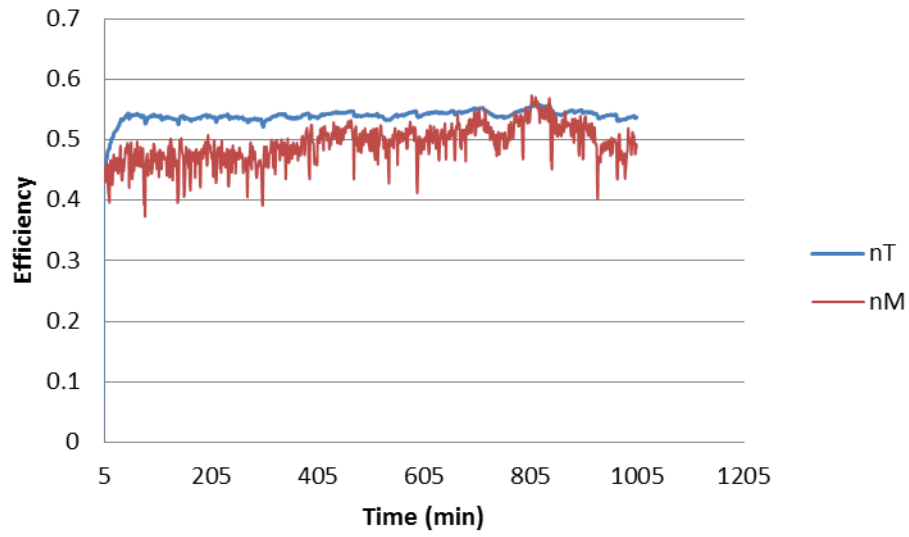
Figure A.27.   *Temperature efficiency (blue line) and moisture transfer efficiency (red line).*

A.4.6 Experiment 6: *DuPont X*

A third experiment with the membrane from DuPont was done. The test conditions were almost the same as for the previous experiment, but the supply inlet temperature was colder. Neither ice, condensate water nor crumpling of the membrane were observed in this experiment.

Table A.6.   Data from experiment 6. Standard deviation, random uncertainty, mean value, systematic uncertainty and total uncertainty.

	HMP 1 RH	HMP 1 Temp	HMP 2 RH	HMP 2 Temp	HMP 3 RH	HMP 3 Temp	HMP 4 RH	HMP 4 Temp	Pressure Exthaust	Pressure Supply
	%	^{o}C	%	^{o}C	%	^{o}C	%	^{o}C	Pa	Pa
s	2.3026	0.2400	2.7213	0.6660	2.5237	1.1290	3.6248	0.4684	0.4611	0.6381
U_r	0.0111	0.0012	0.0132	0.0032	0.0122	0.0055	0.0175	0.0023	0.0022	0.0031
$\bar{x}$	43.2730	22.7717	29.5399	-4.3244	36.3536	14.0723	52.2697	8.0429	10.4779	11.1341
U_S	2.0000	0.1000	2.0000	0.1000	1.4000	0.2000	2.0000	0.1000	0.1900	0.1900
U_T	2.0000	0.1000	2.0000	0.1001	1.4001	0.2001	2.0001	0.1000	0.1900	0.1900

	n_T	n_M	ω_1	ω_2	ω_3	ω_4	Exhaust flow	Supply flow
			kg$_W$/kg$_M$	kg$_W$/kg$_M$	kg$_W$/kg$_M$	kg$_W$/kg$_M$	m^3/h	m^3/h
s								
U_r								
$\bar{x}$	0.5422	0.5839	0.0073	0.0008	0.0037	0.0035	1.2064	1.5509
U_S								
U_T	0.0045	0.0329	0.0004	0.0001	0.0001	0.0001	0.1167	0.1317

Figure A.28.   *Exhaust (red) and supply (blue) air flows through the heat exchanger (based on inlet and outlet values) in a Humidity-temperature diagram. The green lines are relative humidity lines starting at 10% to the left and 100% (saturation line) at the right.*
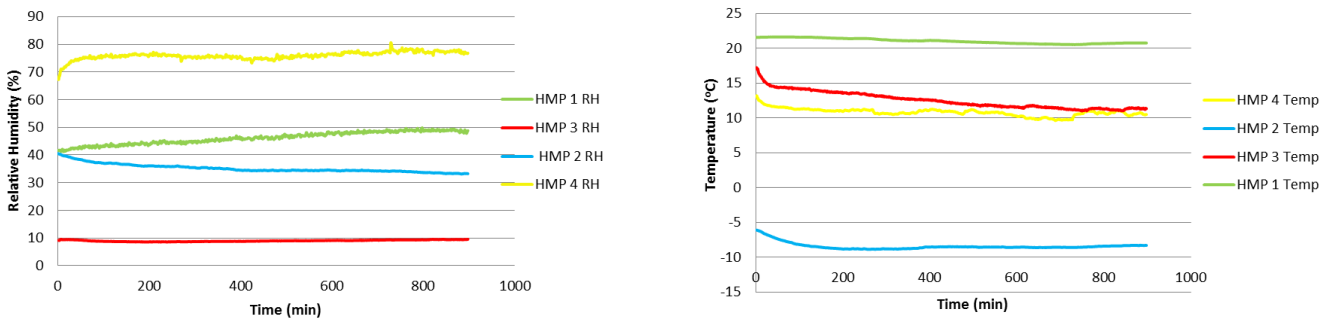

Figure A.29.   *Relative humidity (left) and temperature (right) measurements through the test period in all four measurement points.*


Figure A.30.   *Pressure drop for both air flows. Linear trend line for exhaust air stream is displayed as well.*
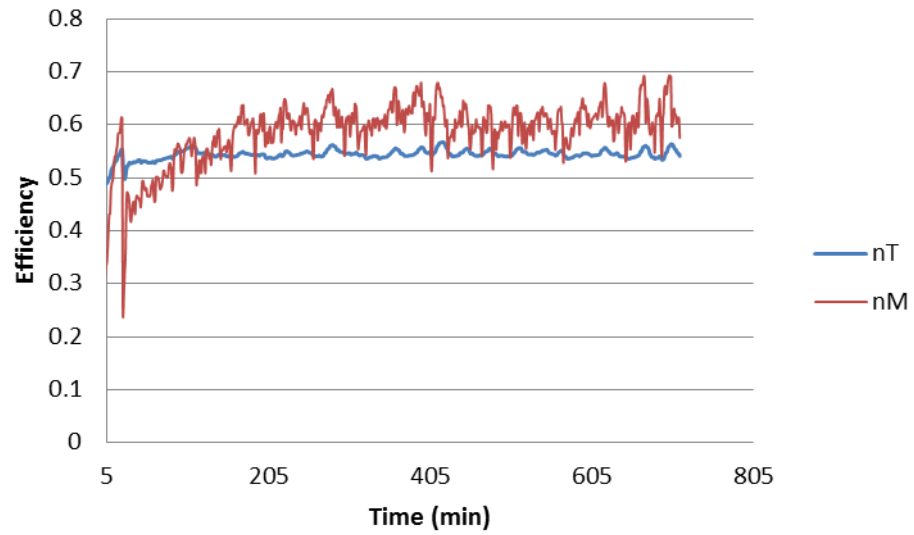
Figure A.31.   *Temperature efficiency (blue line) and moisture transfer efficiency (red line).*

A.4.7 Experiment 7: *DuPont X*

A fourth experiment with the membrane from DuPont was done. Now the test rig was moved closer to the cooling coil and the supply air flow rate was increased to decrease the supply air temperature. The flow rates were not measured, but the supply air flow rate was about three times greater than the exhaust air flow rate. Unfortunately the exhaust air fan stopped working after about 350 min and the result are therefore only displayed for the first 350 min. There were no sign of ice formation in the heat exchanger. A few droplets of condensed water were though found attached to the upper plastic plate. This did however not influence the pressure drop over the heat exchanger.

Table A.7.   *Data from experiment 7. Standard deviation, random uncertainty, mean value, systematic uncertainty and total uncertainty is shown.*

	HMP 1 RH	HMP 1 Temp	HMP 2 RH	HMP 2 Temp	HMP 3 RH	HMP 3 Temp	HMP 4 RH	HMP 4 Temp	Pressure Exthaust	Pressure Supply
	%	^{o}C	%	^{o}C	%	^{o}C	%	^{o}C	Pa	Pa
s	0.4198	0.1208	0.2205	0.0480	0.8949	0.6092	2.4474	0.3560	0.2108	0.3547
U_r	0.0029	0.0008	0.0015	0.0003	0.0062	0.0042	0.0170	0.0025	0.0015	0.0025
$\bar{x}$	37.2678	23.2101	41.0420	-10.5020	35.2069	-3.5668	25.3446	2.9113	25.6146	27.2056
U_S	2.0000	0.1000	2.0000	0.1000	1.4000	0.2000	2.0000	0.1000	0.1900	0.1900
U_T	2.0000	0.1000	2.0000	0.1000	1.4000	0.2000	2.0001	0.1000	0.1900	0.1900

|	n_T	n_M	ω_1	ω_2	ω_3	ω_4	Exhaust flow	Supply flow
			kg$_W$/kg$_M$	kg$_W$/kg$_M$	kg$_W$/kg$_M$	kg$_W$/kg$_M$	m^3/h	m^3/h
s								
U_r								
$\bar{x}$	0.5993	0.9121	0.0065	0.0007	0.0010	0.0012	??	??
U_S								
U_T	0.0037	0.0100	0.0004	0.0000	0.0000	0.0001	??	??

Figure A.32.   *Exhaust (red) and supply (blue) air flows through the heat exchanger (based on inlet and outlet values) in a Humidity-temperature diagram. The green lines are relative humidity lines starting at 10% to the left and 100% (saturation line) at the right.*
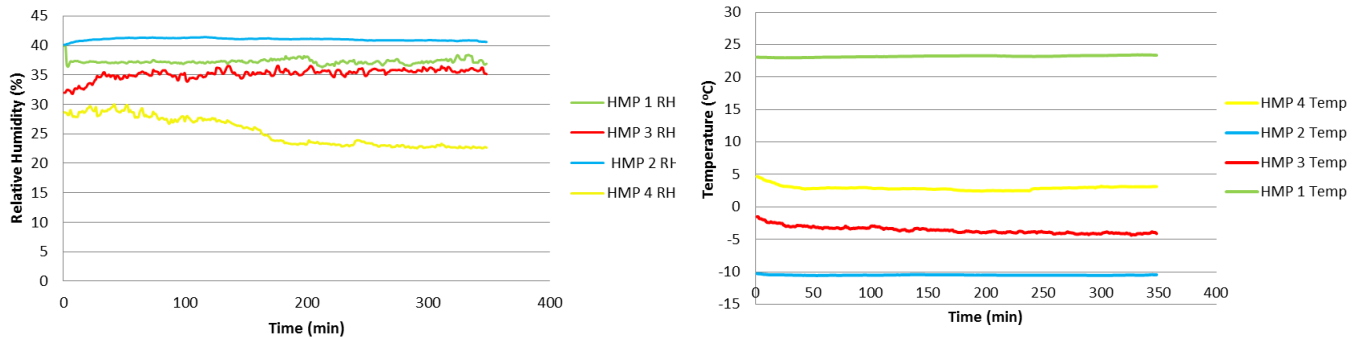
Figure A.33.   *Relative humidity (left) and temperature (right) measurements through the test period in all four measurement points.*
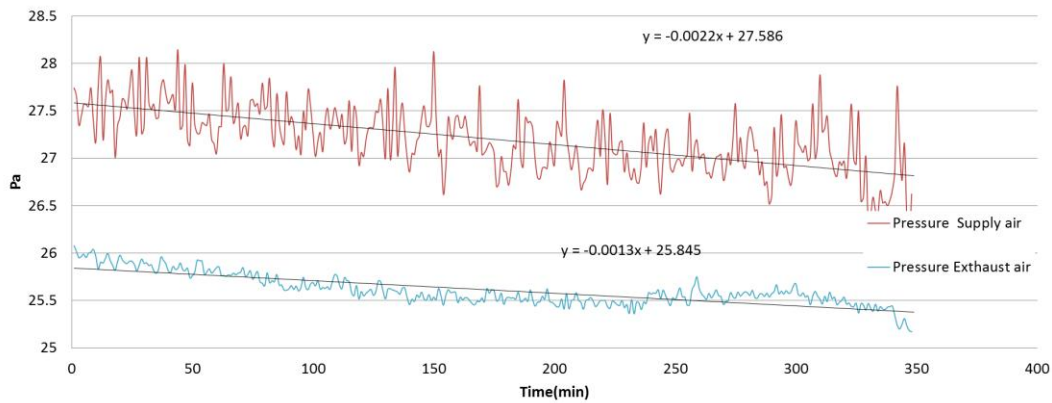
Figure A.34.   *Pressure drop for both air flows. Linear trend lines for the air streams are displayed.*
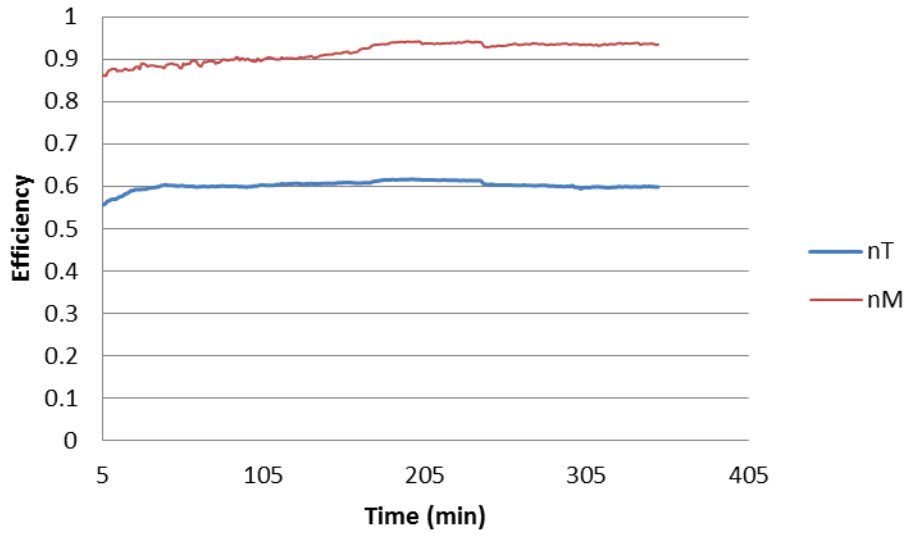
Figure A.35.   *Temperature efficiency (blue line) and moisture transfer efficiency (red line).*
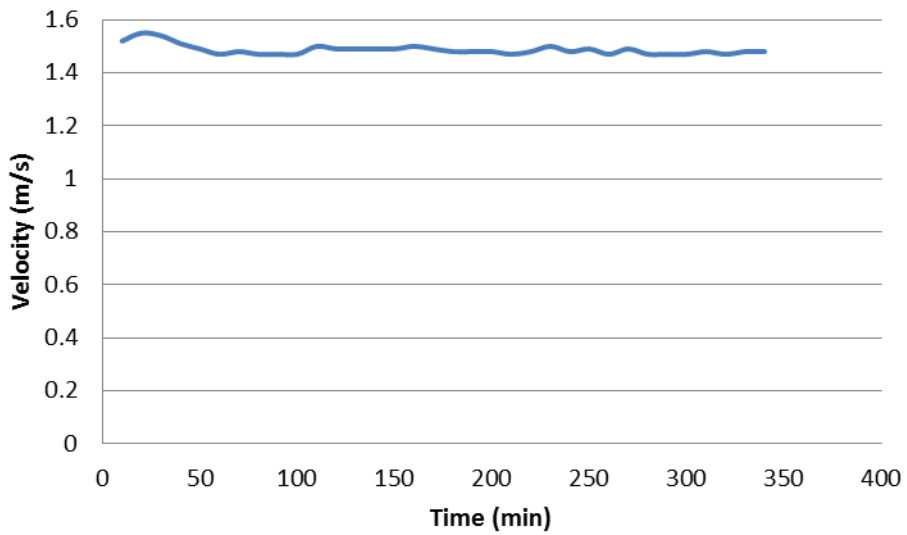
Figure A.36.   *Velocity in one point at the supply air outlet channel exit.*

A.4.8 Experiment 8: *DuPont X*

The membrane based heat exchanger was tested yet another time. The air flow rate on the supply air side was turned down compared to experiment 7. The flow rates were not measured, but the velocity at the supply air outlet was about the half of experiment 7 and at the same level as in experiment 4. The exhaust air humidity were much higher than in experiment 7 (46 to 37% RH). The exhaust air pressure drop experienced a tiny increase compared to the supply air pressure drop. At the end of the test period ice were observed in the exhaust air channels close to the supply air exit. The membrane was also crumbled in this area. No ice was found in the middle exhaust air channel.

Table A.8. Data from experiment 8. Standard deviation, random uncertainty, mean value, systematic uncertainty and total uncertainty is shown.

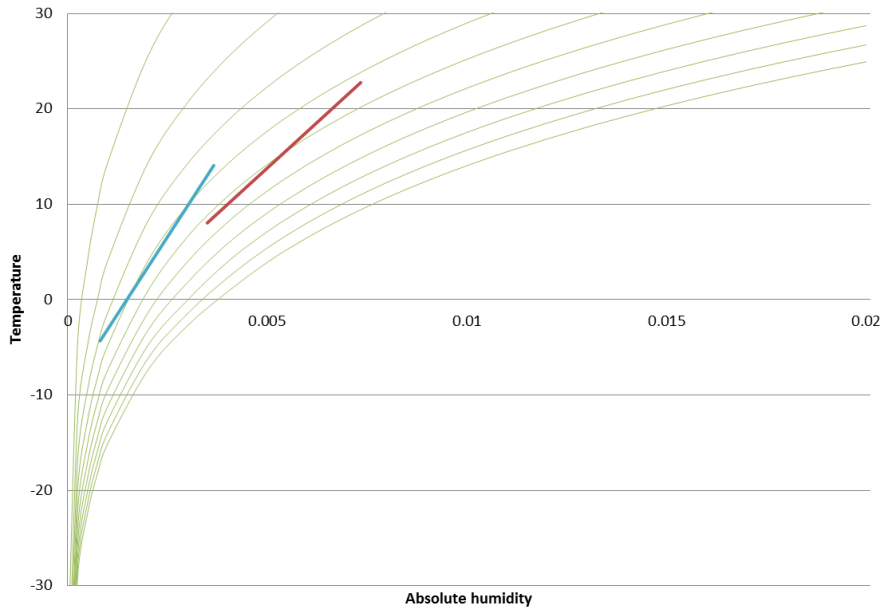|	HMP 1 RH	HMP 1 Temp	HMP 2 RH	HMP 2 Temp	HMP 3 RH	HMP 3 Temp	HMP 4 RH	HMP 4 Temp	Pressure Exthaust	Pressure Supply
	%	$^\circ$C	%	$^\circ$C	%	$^\circ$C	%	$^\circ$C	Pa	Pa
s	0.9636	0.3664	0.4439	0.2078	1.5361	0.6730	0.5425	0.3620	0.4350	0.3284
U_r	0.0046	0.0017	0.0021	0.0010	0.0073	0.0032	0.0026	0.0017	0.0021	0.0016
$\bar{x}$	46.6016	22.8990	34.2201	-9.6160	30.7849	4.1215	27.2570	2.5011	24.8018	25.2476
U_S	2.0000	0.1000	2.0000	0.1000	1.4000	0.2000	2.0000	0.1000	0.1900	0.1900
U_T	2.0000	0.1000	2.0000	0.1000	1.4000	0.2000	2.0000	0.1000	0.1900	0.1900
	n_T	n_M	ω_1	ω_2	ω_3	ω_4	Exhaust flow	Supply flow		
			kg$_W$/kg$_M$	kg$_W$/kg$_M$	kg$_W$/kg$_M$	kg$_W$/kg$_M$	m^3/h	m^3/h		
s										
U_r										
$\bar{x}$	0.6116	0.8782	0.0080	0.0007	0.0019	0.0016	?	?		
U_S										
U_T	0.0038	0.0135	0.0004	0.0000	0.0001	0.0001	?	?		
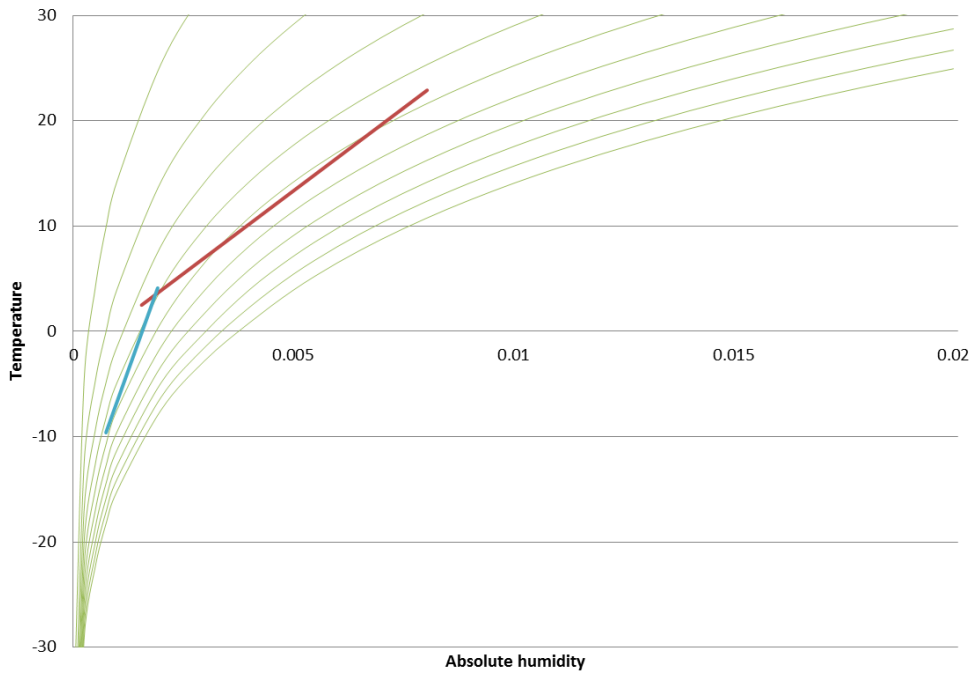
Figure A.37.   *Exhaust (red) and supply (blue) air flows through the heat exchanger (based on inlet and outlet values) in a Humidity-temperature diagram. The green lines are relative humidity lines starting at 10% to the left and 100% (saturation line) at the right.*
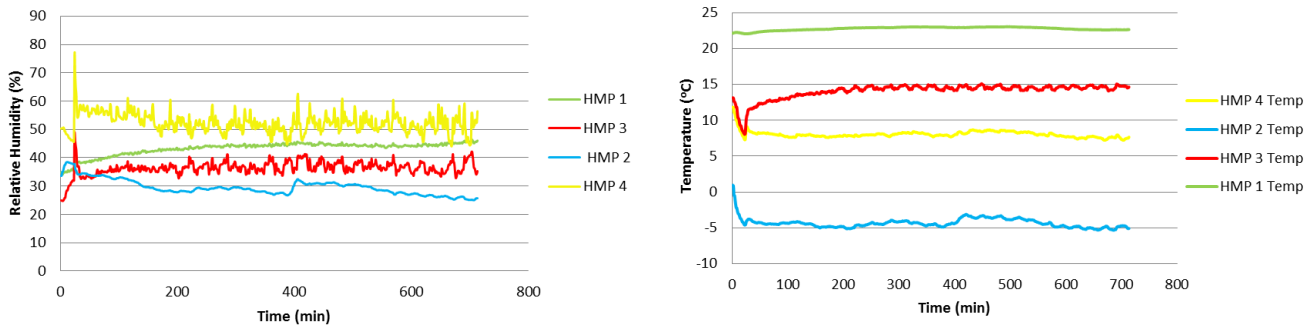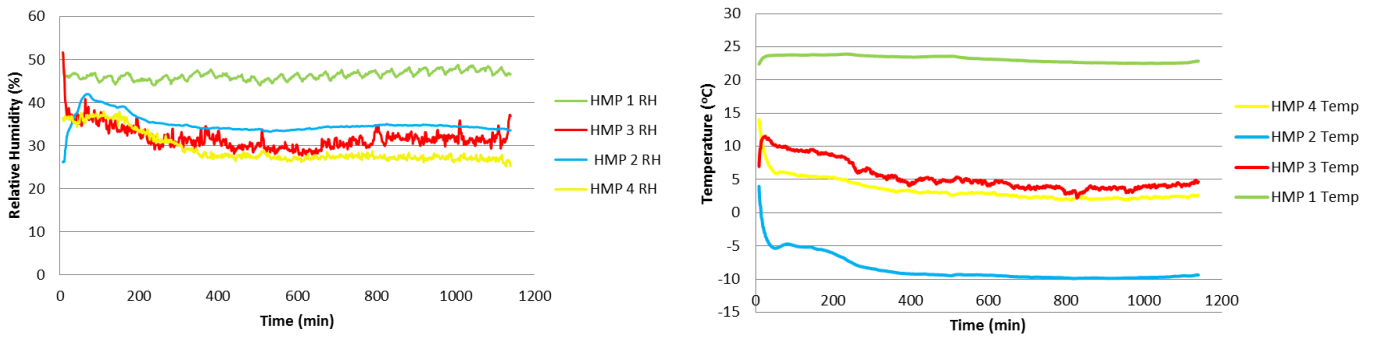

Figure A.38.   *Relative humidity (left) and temperature (right) measurements through the test period in all four measurement points.*
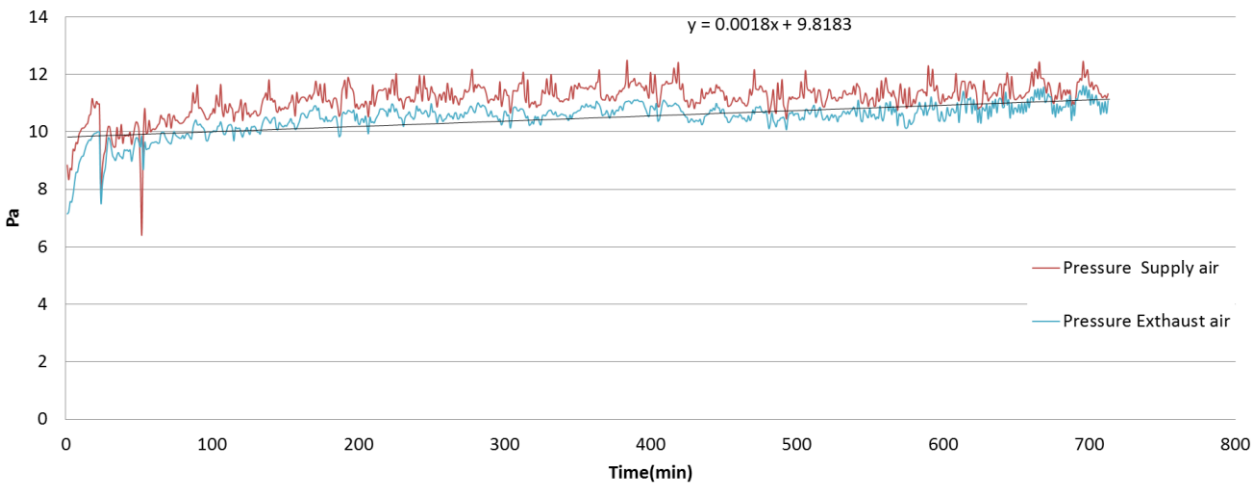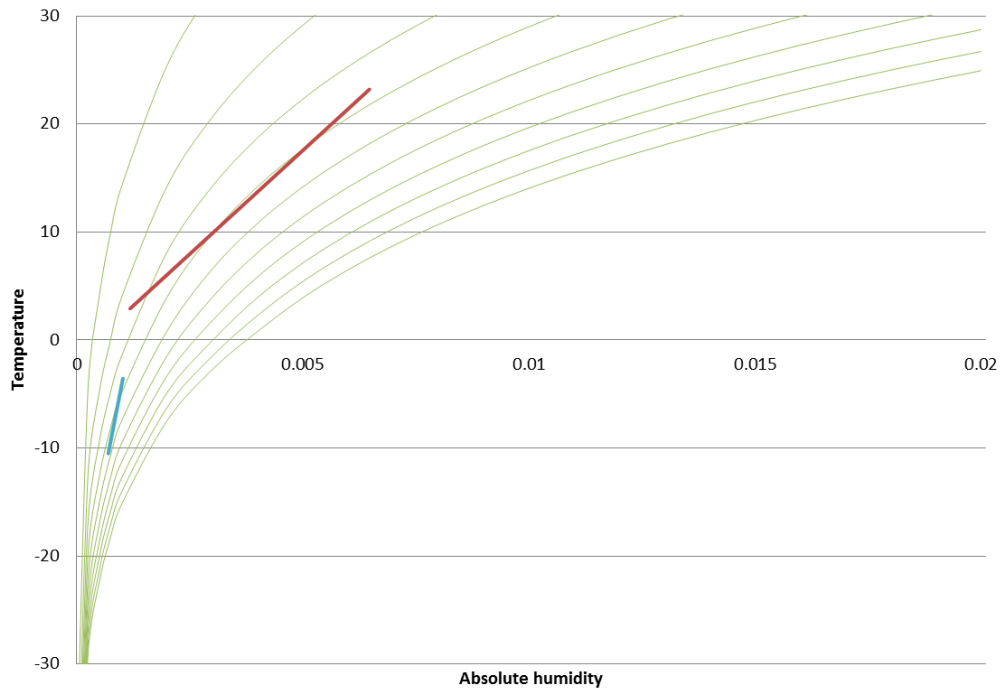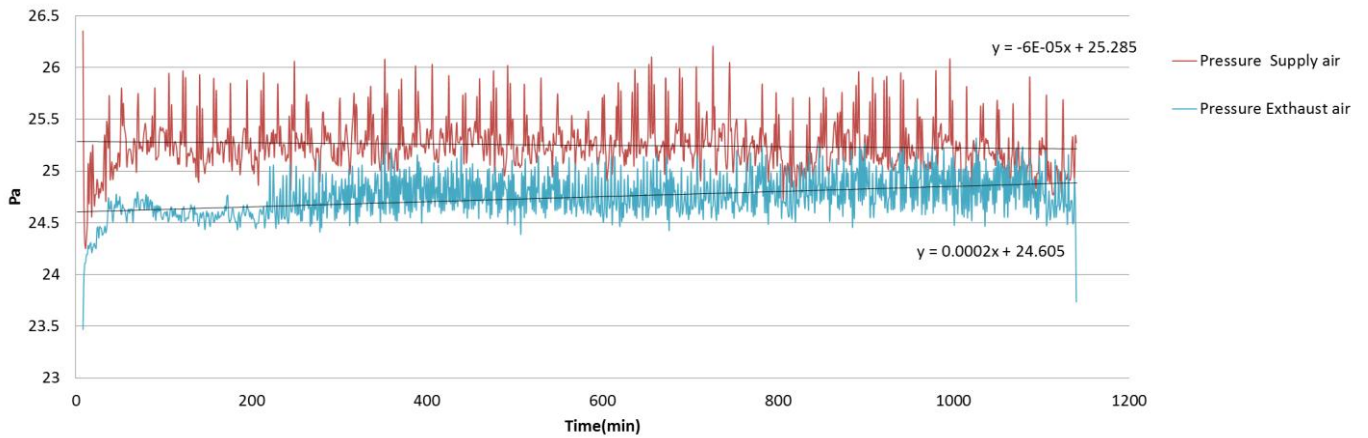

Figure A.39.   *Pressure drop for both air flows. Linear trend lines for the air streams are displayed.*
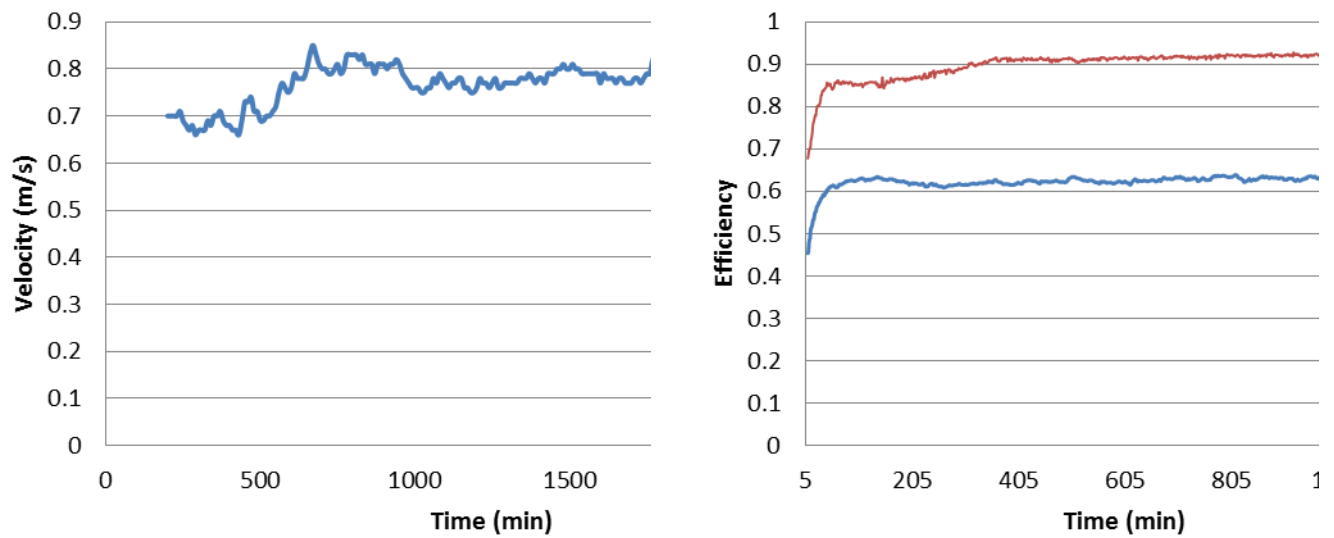
Figure A.40.   *Velocity in one point at the supply air outlet channel exit. Right: Temperature efficiency.*

Figure A.41.   *Pictures after experiment. Left: The membrane had expanded near the supply air outlet (down to the right in the picture) and can be seen as crumpled. In the same area condensed water had formed and stuck the membrane to the upper acrylic plate of the heat exchanger. Right: the heat exchanger was taken out from the set up. The membrane stretched out again after a few minutes. The oval shaped structures in the lower right side in the picture shows ice that stuck the membrane to the upper plate.*

A.5. Heat Exchanger Prototype: Mechanical Drawing

3mm ribs 12X
Material: plexiglas (PMMA) or PC or
other stiff plastic paterial.
Finish: Smooth and clear cuts.

208,5mm

3,0mm

8,5mm

107,0mm

110,5mm

134,2mm

99,1mm

135 deg

6,0mm

Bottom and top plate 2X
Material: plexiglas (PMMA) or PC
or other stiff plastic paterial.
Finish: Smooth and clear cuts.

297,0mm

3,0mm

190,0mm

134,4mm

107,0mm

A.6. HSE Report

NTNU ◎ SINTEF

Risk Assessment Report

Membrane Based Heat Exchanger

Prosjekttittel	Membrane Based Heat Exchanger
Prosjektleder	Håvard Rekstad / Hans Martin Mathisen
Enhet	NTNU
HMS-koordinator	Erik Langørgen
Linjeleder	Olav Bolland
Plassering	VVS-lab
Romnummer	
Riggansvarlig	Håvard Rekstad
Risikovurdering utført av	Sofie Aarnes

NTNU ◎ SINTEF

TABLE OF CONTENTS

NTNU   SINTEF

1 INTRODUCTION

The purpose of the experimental set up is to test the ability for a membrane based heat exchanger compared to a plastic based heat exchanger. Cold air is to be taken from the lab's existing glycol cooling system (cooling battery). Warm and humid air is made by adding heat to a bucket of water with an electrical water heater regulated by a thermocouple and a PID-regulator.

2 ORGANISATION

Rolle	NTNU	Sintef
Lab Ansvarlig:	Morten Grønli	Harald Mæhlum
Linjeleder:	Olav Bolland	Mona J. Mølnvik
HMS ansvarlig:	Olav Bolland	Mona J. Mølnvik
HMS koordinator	Erik Langørgen	Harald Mæhlum
HMS koordinator	Bård Brandåstrø	
Romansvarlig:	Harald Mæhlum	
Prosjekt leder:	Hans Martin Mathisen	
Ansvarlig riggoperatører:	Sofie Aarnes	

3 RISK MANAGEMENT IN THE PROJECT

Hovedaktiviteter risikostyring	Nødvendige tiltak, dokumentasjon	DATE
Prosjekt initiering	Prosjekt initiering mal	24.01.12
Veiledningsmøte Guidance Meeting	Skjema for Veiledningsmøte med pre-risikovurdering	24.01.12
Innledende risikovurdering Initial Assessment	Fareidentifikasjon – HAZID Skjema grovanalyse	May.2012
Vurdering av teknisk sikkerhet Evaluation of technical security	Prosess-HAZOP Tekniske dokumentasjoner	May.2012
Vurdering av operasjonell sikkerhet Evaluation of operational safety	Prosedyre-HAZOP Opplæringsplan for operatører	May.2012
Sluttvurdering, kvalitetsikring Final assessment, quality assurance	Uavhengig kontroll Utstedelse av apparaturkort Utstedelse av forsøk pågår kort	May.2012

4 DRAWINGS, PHOTOS, DESCRIPTIONS OF TEST SETUP

Attachments:
Process and Instrumentation Diagram (PID)
Shall contain all components in the experimental setup
Component List with specifications
Drawings and photos describing the setup.
Where the operator is present, how is the gas bottles, shutdown valves for water / air.

NTNU   SINTEF

5 EVACUATION FROM THE EXPERIMENT AREA

Evacuate at signal from the alarm system or local gas alarms with its own local alert with sound and light outside the room in question, see 6.2
Evacuation from the rigging area takes place through the marked emergency exits to the meetingpoint, (corner of Old Chemistry Kjelhuset or parking 1a-b.)
Action on rig before evacuation:
Shut off electricity supply for electrical heater. Turn off main current switch of glycol system.

6 WARNING

6.1 Before experiments

E-mail with information about the test run duration, (hour) and the involved to HMS koordinator NTNU/SINTEF
    Erik.langorgen@ntnu.no
    Baard.brandaastro@ntnu.no
Project Managers on neighboring units alerted for clarification around the use of the exhaust system without fear or interference of any kind, see rig matrix.

All experiments should be planned and put into the activity calendar for the lab.
Experiment leader must get confirmation that the experiments are coordinated with other activity before start up.

6.2 Nonconformance

FIRE
Fire you are not able to put out with locally available fire extinguishers, activate, the nearest fire alarm and evacuate area. Be then available for fire brigade and building caretaker to detect fire place.
If possible, notifie;

NTNU	SINTEF
Labsjef Morten Grønli, tlf: 918 97 515	Labsjef Harald Mæhlum tlf 930 149 86
HMS: Erik Langørgen, tlf: 91897160	Forskningssjef Mona J Mølnvik tlf 930 08 868
Instituttleder: Olav Bolland: 91897209	

GASALARM
At a gas alarm, close gas bottles immediately and ventilated the area. If the level of gas concentration not decrease within a reasonable time, activate the fire alarm and evacuate the lab. Designated personnel or fire department checks the leak to determine whether it is possible to seal the leak and ventilate the area in a responsible manner.
Alert Order in the above paragraph.

PERSONAL INJURY
• First aid kit in the fire / first aid stations

NTNU ◉ SINTEF

- , Shout for help
- Start life-saving first aid-
CALL 113 if there is any doubt whether there is a serious injury
Other Nonconformance (AVVIK)
NTNU:
Reporting form for nonconformance at:
http://www.ntnu.no/hms/2007 Nettsider/HMSRV0401 avvik.doc

SINTEF:
Synergi

7   ASSESSMENT OF TECHNICAL SAFETY

7.1 HAZOP

The experiment set up is divided into the following nodes:

Node 1	cold air side
Node 2	Glycol loop system (permanent set up in VATL-lab)
Node 3	Heat and humidity supply box (warm air side)

Attachments:, skjema: Hazop_mal
Conclusion: Biggest risk is associated with leakages from the glycol loop in the lab (node 2). This is a part of the lab-infrastructure. According to the MSDS for the chemical used as the cooling liquid is moderately irritating to skin and eyes. It is toxic and deadly if bigger amount (1/2 cups) is consumed. If precautions are done as described in the operating manual the experiment has a very low risk for any hazardous situations.

7.2 Flammable, reactive and pressurized substances and gas

Contains the experiments Flammable, reactive and pressurized substances and gas

| NEI | YES. Explosion document have to be made and or documented pressure test, (See 7.3) |

Attachments:
Conclusion :.The pressure in of node 1 and 3 in the experiment is so low that the pressure is neglected in a HSE perspective. In node 2 the pressure is also low. A safety valve is present in the "glycol room"

7.3 Pressurized equipment

Contain the set up pressurized equipment?

| NEI | YES Equipment have to undergo pressure testes in accordance with the norms and be documented |

Attachments:: Sertifikat for trykkpåkjent utstyr.
Conclusion: The pressures in this experimental set up is so low that there will not exist any risk related to this.

7.4 Effects on the environment (emissions, noise, temperature, vibration, smell)

| NEI | YES |

NTNU ◉ SINTEF

Conclusion: This is not relevant for the experiment.

7.5 Radiation

| NEI | JA, Radiation source need to have an own risk assessment |

Attachments:
Conclusion: No source of radiation in this experiment

7.6 Usage and handling of chemicals.

| NEI | JA, Do a risk assessment of the use |

Attachments: MSDS_GlycoShell
Conclusion: The experiment will only use the chemical in a closed loop. Ethylene glycol "GlycoShell" is used in the cooling coil as the cooling liquid. Due to the possibility of leakages from the closed system protective gloves and goggles should be used when emptying the drainage buckets from under the cooling coil. While running experiments no protective personal equipment is needed. In normal circumstances the leakages will be very limited and no extra precautions needs to be done (the leakages will mix with drainage water and the glycol is very water-soluble. If big leakages (>0,5 l) follow the disposal instructions from the MSDS report and contact lab-personnel. Turn off main current switch in glycol loop when emergency exit.

7.7 El safety (need to deviate from the current regulations and standards.)

| NEI | JA, El safety have to be evaluated |

Her forstås montasje og bruk i forhold til normer og forskrifter med tanke på berøringsfare
Attachments:
Conclusion: Not relevant

8   ASSESSMENT OF OPERATIONAL SAFETY

Ensures that established procedures cover all identified risk factors that must be taken care of through procedures. Ensures that the operators and technical performance have sufficient expertise.

8.1 Prosedure HAZOP

The method is a procedure to identify causes and sources of danger to operational problems.
Attachments:: HAZOP_MAL_Prosedyre
Conclusion: If the proscribed safety equipment is used (gloves and goggles) and the procedure followed the risk of any hazard will be very low.

8.2 Operation and emergency shutdown procedure

The operating procedure is a checklist that must be filled out for each experiment. Emergency procedure should attempt to set the experiment set up in a harmless state by unforeseen events.

NTNU / SINTEF

1	*Leakage of glycol*	3	A	A3
2	*Ignition from overheating in bucket? Danger of fire*	1	D	D1
3	Splashing of glycol into skin or eye	1	C	C1

Conclusion : *Following the operation procedure this experiment is acceptable regarding HSE.*

10 CONCLUSJON

The rig is built in good laboratory practice (GLP).

Experiment unit card get a period of **1 month**
Experiment in progress card get a period of **1 month**

NTNU / SINTEF

Attachments: "Procedure for running experiments
Emergency shutdown procedure: Turn off electricity for electrical heater and air supply fan

8.3 Training of operators

A Document showing training plan for operators
What are the requirements for the training of operators?
• *What it takes to be an independent operator*
• *Job Description for operators*
Attachments:: Training program for operators

8.4 Technical modifications

This work does not need new risk assessment:
▪ Technical modifications made by the Operator
　o (for example: Replacement of components, equal to equal)
　▪ Technical modifications that must be made by Technical staff.
　o (for example, modification of pressure equipment).
　▪

Conclusion: Only changes that will change the total set up will require a new HSE.

8.5 Personal protective equipment

Gloves and protective spectacles when handling drainage buckets under cooling coil because of possible leakage of "glycoShell" mono ethylene glycol from pipes.
▪ Conclusion:.

8.5.1 General Safety

• Experiment can be run unattended for 8 hours the first 12 hours after starting logging. Then it should be looked after every 1 hour into the experiment end. Be sure the water bucked is completely filled before leaving experiment and that the thermometer in bucket are in the right position.
• Conclusion:

Is Operator allowed to leave during the experiment? Yes. See above

8.6 Safety equipment

• Warning signs, see the Regulations on Safety signs and signaling in the workplace

8.7 Special actions.

° Monitoring the temperature in exhaust air side. To warm may indicate that the PID regulator/ thermostat don't work as intended.

9 QUANTIFYING OF RISK - RISK MATRIX

See Chapter 14 "Guide to the report template".
The risk matrix will provide visualization and an overview of activity risks so that management and users get the most complete picture of risk factors.

IDnr	Aktivitet-hendelse	Frekv-Sans	Kons	RV

DOCUMENTATION

- Tegninger, foto, beskrivelser av forsøksoppsetningen
- Hazop_mal
- Sertifikat for trykkpåkjent utstyr
- Håndtering avfall i NTNU
- Sikker bruk av LASERE, retningslinje
- HAZOP_MAL_Prosedyre
- Forsøksprosedyre
- Opplæringsplan for operatører
- Skjema for sikker jobb analyse, (SJA)
- Apparaturkortet
- Forsøk pågår kort

11 REGULATIONS AND GUIDELINES

Se http://www.arbeidstilsynet.no/regelverk/index.html
- Lov om tilsyn med elektriske anlegg og elektrisk utstyr (1929)

Arbeidsmiljøloven
- Forskrift om systematisk helse-, miljø- og sikkerhetsarbeid (HMS Internkontrollforskrift)
- Forskrift om sikkerhet ved arbeid og drift av elektriske anlegg (FSE 2006)
- Forskrift om elektriske forsyningsanlegg (FEF 2006)
- Forskrift om utstyr og sikkerhetssystem til bruk i eksplosjonsfarlig område NEK 420
- Forskrift om håndtering av brannfarlig, reaksjonsfarlig og trykksatt stoff samt utstyr og anlegg som benyttes ved håndteringen
- Forskrift om Håndtering av eksplosjonsfarlig stoff
- Forskrift om bruk av arbeidsutstyr.
- Forskrift om Arbeidsplasser og arbeidslokaler
- Forskrift om Bruk av personlig verneutstyr på arbeidsplassen
- Forskrift om Helse og sikkerhet i eksplosjonsfarlige atmosfærer
- Forskrift om Høytrykksspyling
- Forskrift om Maskiner
- Forskrift om Sikkerhetsskilting og signalgivning på arbeidsplassen
- Forskrift om Stillaser, stiger og arbeid på tak m.m.
- Forskrift om Sveising, termisk skjæring, termisk sprøyting, kullbuemeisling, lodding og sliping (varmt arbeid)
- Forskrift om Tekniske innretninger
- Forskrift om Tungt og ensformig arbeid
- Forskrift om Vern mot eksponering for kjemikalier på arbeidsplassen (Kjemikalieforskriften)
- Forskrift om Vern mot kunstig optisk stråling på arbeidsplassen
- Forskrift om Vern mot mekaniske vibrasjoner
- Forskrift om Vern mot støy på arbeidsplassen

Veiledninger fra arbeidstilsynet
se: http://www.arbeidstilsynet.no/regelverk/veiledninger.html

12 GUIDANCE TO RISK ASSESSMENT TEMPLATE

Kap 7 Assessment of technical safety.
Ensure that the design of the experiment set up is optimized in terms of technical safety. Identifying risk factors related to the selected design, and possibly to initiate re-design to ensure that risk is eliminated as much as possible through technical security.
This should describe what the experimental setup actually are able to manage and acceptance for emission.

7.1 HAZOP
The experimental set up is divided into nodes (eg motor unit, pump unit, cooling unit.). By using guidewords to identify causes, consequences and safeguards, recommendations and conclusions are made according to if necessary safety is obtained. When actions are performed the HAZOP is completed.
(e.g. "No flow", cause: the pipe is deformed, consequence: pump runs hot, precaution: measurement of flow with a link to the emergency or if the consequence is not critical used manual monitoring and are written into the operational procedure.)

7.2 Flammable, reactive and pressurized substances and gas.
According to the Regulations for handling of flammable, reactive and pressurized substances and equipment and facilities used for this:

Flammable material: Solid, liquid or gaseous substance, preparation, and substance with occurrence or combination of these conditions, by its flash point, contact with other substances, pressure, temperature or other chemical properties represent a danger of fire.

Reactive substances: Solid, liquid, or gaseous substances, preparations and substances that occur in combinations of these conditions, which on contact with water, by its pressure, temperature or chemical conditions, represents a potentially dangerous reaction, explosion or release of hazardous gas, steam, dust or fog.

Pressurized : Other solid, liquid or gaseous substance or mixes having fire or hazardous material response, when under pressure, and thus may represent a risk of uncontrolled emissions

Further criteria for the classification of flammable, reactive and pressurized substances are set out in Annex 1 of the Guide to the Regulations "Flammable, reactive and pressurized substances"
http://www.dsb.no/Global/Publikasjoner/2009/Veiledning/Generell%20veiledning.pdf
http://www.dsb.no/Global/Publikasjoner/2010/Tema/Temaveiledning_bruk_av_farlig_stoff_Del_1_p df

Experiment setup area should be reviewed with respect to the assessment of Ex zone
• Zone 0: Always explosive atmosphere, such as inside the tank with gas, flammable liquid.
• Zone 1: Primary zone, sometimes explosive atmosphere such as a complete drain

point
• Zone 2: secondary discharge could cause an explosive atmosphere by accident, such as flanges, valves and connection points

7.4 Effects on the environment
With pollution means: bringing solids, liquid or gas to air, water or ground, noise and vibrations, influence of temperature that may cause damage or inconvenience effect to the environment.
Regulations: http://www.lovdata.no/all/hl-19810313-006.html#6
NTNU guidance to handling of waste:http://www.ntnu.no/hms/retningslinjer/HMSR18B.pdf

7.5 Radiation
Definition of radiation
Ionizing radiation: Electromagnetic radiation (in radiation issues with wavelength <100 nm) or rapid atomic particles (e.g. alpha and beta particles) with the ability to stream ionized atoms or molecules.
Non ionizing radiation: Electromagnetic radiation (wavelength >100 nm), og ultrasound[1] with small or no capability to ionize.
Radiation sources: All ionizing and powerful non-ionizing radiation sources.
Ionizing radiation sources: Sources giving ionizing radiation e.g. all types of radiation sources, x-ray, and electron microscopes.
Powerful non ionizing radiation sources: Sources giving powerful non ionizing radiation which can harm health and/or environment, e.g. class 3B and 4. MR[2] systems, UVC[3] sources, powerful IR sources[4].

[1]Ultrasound is an acoustic radiation ("sound") over the audible frequency range (> 20 kHz). In radiation protection regulations are referred to ultrasound with electromagnetic non-ionizing radiation.
[2]MR (e.g. NMR) - nuclear magnetic resonance method that is used to "depict" inner structures of different materials.
[3]UVC is electromagnetic radiation in the wavelength range 100-280 nm.
[4]IR is electromagnetic radiation in the wavelength range 700 nm - 1 mm.

For each laser there should be an information binder (HMSRV3404B) which shall include:
• General information
• Name of the instrument manager, deputy, and local radiation protection coordinator
• Key data on the apparatus
• Instrument-specific documentation
• References to (or copies of) data sheets, radiation protection regulations, etc.
• Assessments of risk factors
• Instructions for users
• Instructions for practical use, startup, operation, shutdown, safety precautions, logging, locking, or use of radiation sensor, etc.
• Emergency procedures
See NTNU for laser: http://www.ntnu.no/hms/retningslinjer/HMSR34B.pdf

7.6 Usage and handling of chemicals.
In the meaning chemicals, a element that can pose a danger to employee safety and health
See: http://www.lovdata.no/cgi-wift/ldles?doc=/sf/sf-20010430-0443.html

NTNU   SINTEF

Farge	Beskrivelse
Rød	Unacceptable risk Action has to be taken to reduce risk
Gul	Assessment area. Actions has to be concidered
Grønn	Acceptable risk. Action can be taken based on other criteria

---

NTNU   SINTEF

Safety datasheet is to be kept in the HSE binder for the experiment set up and registered in the database for chemicals.

Kap 8 Assessment of operational procedures.

Ensures that established procedures meet all identified risk factors that must be taken care of through operational barriers and that the operators and technical performance have sufficient expertise.

8.1 Prosedure Hazop

Procedural HAZOP is a systematic review of the current procedure, using the fixed HAZOP methodology and defined guidewords. The procedure is broken into individual operations (nodes) and analyzed using guidewords to identify possible nonconformity, confusion or sources of inadequate performance and failure.

8.2 Procedure for running experiments and emergency shutdown.
Have to be prepared for all experiment setups.

The operating procedure has to describe stepwise preparation, startup, during and ending conditions of an experiment. The procedure should describe the assumptions and conditions for starting, operating parameters with the deviation allowed before aborting the experiment and the condition of the rig to be abandoned.
Emergency procedure describes how an emergency shutdown have to be done, (conducted by the uninitiated),
what happens when emergency shutdown, is activated. (electricity / gas supply) and which events will activate the emergency shutdown (fire, leakage).

Kap 9 Quantifying of RISK
Quantifying of the residue hazards, Risk matrix
To illustrate the overall risk, compared to the risk assessment, each activity is plotted with values for the probability and consequence into the matrix. Use task IDnr.
Example: If activity IDnr. 1 has been given a probability 3 and D for consequence the risk value become D3, red. This is done for all activities giving them risk values.
In the matrix are different degrees of risk highlighted in red, yellow or green. When an activity ends up on a red risk (= unacceptable risk), risk reducing action has to be taken

CONSEQUENSES	E1	E2	E3	E4	E5
Svert alvorlig	E1	E2	E3	E4	E5
Alvorlig	D1	D2	D3	D4	D5
Moderat	C1	C2	C3	C4	C5
Liten	B1	B2	B3	B4	B5
Svert liten	A1	A2	A3	A4	A5
	Svert liten	Liten	Middels	Stor	Svært Stor
			PROBABILITY		

The principle of the acceptance criterion. Explanation of the colors used in the matrix

NTNU   **SINTEF**

• **ATTACHMENT A HAZOP MAL**

Project: Node: 1 Cold air side					Page	
Ref #	Guideword	Causes	Consequences	Safeguards	Recommendations	Action	Date Sign
	No flow	Fan stop	No results	monitoring			
	Less flow	Fan stops/ freezing on cooling coil	Bad results Destroyed equipment	Monitoring pressure/flow rate			
	More temperature	Cooling coil out of function/ heating coil out of function	Bad results	Monitoring			
	Less temperature	Cooling coil out of function/ heating coil out of function	Bad results Freezing in HX-destroying HX	Monitoring			

1

SINTEF

NTNU

Attachment to Risk Assessment report

Membrane Based Heat Exchanger

Project name	Membrane Based Heat Exchanger (ZEB project)
Project leader	Håvard Rekstad/ Hans Martin Mathisen
Enhet	NTNU
HMS-koordinator	Erik Langørgen
Linjeleder	Olav Bolland
Rignavn	Membrane based heat exchanger
Plassering	VATL-inneklima lab
Romnummer	
Riggansvarlig	Sofie Aarnes

TABLE OF CONTENTS

NTNU   **SINTEF**

Project:					Page	
Node: 2 glycol loop						
Ref #	Guideword	Causes	Consequences	Safeguards	Recommendations	Action	Date Sign
	No flow	Pump/compressor stops	No cooling. Temperature rise in cold side. Bad results	Monitoring of cold inlet air.	Be sure no abnormal noises from compressor room	Contact lab-personnel	
	More pressure	Plug in glycol loop etc.	Increased leakages. Splashing into room. Toxic if inhaled. Moderate irritating if splashed into skin or eyes.	Safety valve	Be sure no abnormal noises from compressor room when turning the system on.	Contact lab-personnel. Turn of power control switch.	
	More temperature	Cooling system out of function	Bad results.	Monitoring of cold inlet air. Temperature display outside glycol system room.	Check that system is still turned on.	Contact lab-personnel. Turn of power control switch if nothing wrong is found.	
	Less Flow	Fan out of function. Cooling coil blocked with ice.	Bad results	Monitoring cold side outlet temperature.	Check if fan is still on.	Stop logging.	
	Contamination	Leakage of glycol	Moderate irritating if contact with skin or eye. Toxic if inhaled. Environmental hazard if big amount.	Wear protective gloves and goggles when handling drainage buckets.		Contact HSE responsible at lab if huge lekages (more than app. 0,5l)	

2

NTNU   **SINTEF**

Project:					Page	
Node: 3 warm air side						
Ref #	Guideword	Causes	Consequences	Safeguards	Recommendations	Action	Date Sign
	No flow	Fan stopped. Frost formation in Cooling coils	No air flow rate. Bad results	Check that fan is on and that electricity supply is sufficient.			
	More temperature	Temperature regulator out of work	Bad results. Over heating	Monitoring of warm supply air. Check that water bucket is filled before experiment start up and that the thermostat is securely fastened in right place in bucket.		Stop experiment	
	Less temperature	Same as over	Bad results			Stop experiment	
	Ignition	PID regulator out of work and burnable obstacle ignited by electrical heater	fire	PID regulator. Monitoring of warm supply air. Fully filled water bucket before experiment start.		After 6.2	

3

NTNU   **SINTEF**

- **ATTACHMENT F HAZOP TEMPLATE PROCEDURE**

Project: Node: 1							Page
Ref #	Guideword	Causes	Consequences	Safeguards	Recommendations	Action	Date Sign
	Not clear procedure	Procedure is to ambitious, or confusingly					
	Step in the wrong place	The procedure can lead to actions done in the wrong pattern or sequence					
	Wrong actions	Procedure improperly specified					
	Incorrect information	Information provided in advance of the specified action is wrong					
	Step missing	Missing step, or step requires too much of operator					
	Step unsucessful	Step has a high probability of failure					
	Influence and effects from other	Procedure's performance can be affected by other sources					

1

NTNU   **SINTEF**

- **ATTACHMENT B PRØVESERTIFIKAT FOR LOKAL TRYKKTESTING**

Trykktesten skal utføres i følge NS-EN 13445 del 5 (Inspeksjon og prøving).
Se også prosedyre for trykktesting gjeldende for VATL lab

Trykkpåkjent utstyr: ....

Benyttes i rigg: ....

Design trykk for utstyr: ....bara

Maksimum tillatt trykk: ....bara
(i.e. burst pressure om kjent)

Maksimum driftstrykk i denne rigg: ....bara

Prøvetrykket skal fastlegges i følge standarden og med hensyn til maksimum tillatt trykk.

Prøvetrykk: ....bara   (........ x maksimum driftstrykk)
                                    I følge standard

Test medium: ....

Temperatur: ....°C

Start: Tid: ....
          Trykk: ....bara

Slutt: Tid: ....
          Trykk: ....bara

Eventuelle repetisjoner fra atm. trykk til maksimum prøvetrykk:.............

Test trykket, dato for testing og maksimum tillatt driftstrykk skal markers på (skilt eller innslått)

Sted og dato   Signatur

1

Appendix

NTNU · SINTEF

ATTACHMENT G PROCEDURE FOR RUNNING EXPERIMENTS

	Date/ Sign
Experiment, name, number:	
Project Leader:	
Experiment Leader: Sofie Aarnes	
Operator, Duties: Sofie Aarnes	

Conditions for the experiment:	Completed
Experiments should be started up in normal working hours, 08.00–15.00 during summer time. When experiment are running outside working hours tell a friend/colleague when you will be back from lab.	
Experiments outside normal working hours shall be approved.	
One person must *regularly* be present while running experiments, and should be approved as an experimental leader. The experiment may be leaved up to 8 hours in the first 12 hours of running, after 12 hours the experiment shall be looked after every 1 hour. Eventually a remote desktop connection may be set up to monitor the experiment.	
An early warning is given according to the lab rules, and accepted by authorized personnel.	
Be sure that everyone taking part of the experiment is wearing the necessary protecting equipment and is aware of the shut down procedure and escape routes.	

Preparations	Carried out
Post the "Experiment in progress" sign.	
Start up procedure	
1) Turn on cooling system (glycol loop) and open valves (use gloves and goggles) when the temperature is -25C . Follow the picture attached for how to turn on glycol loop. Make sure the water valve is open outside "glycol room". 2) Turn on fan 3) Turn on PID regulator. Make sure the bucket is filled with water 4) Check outlet velocities. Equal? 5) Wait for app 2 hours to let the system stabilize 6) Connect the HX with tape. Make sure it is sealed. 7) Start logging	

During the experiment	
1) Observe the experiment set up every 1 hour the first 2-4 hours and after 12 hours. Check that everything work as intended. 2) Stop logging when pressure drop rises significantly. Take picture of HX. Take out HX and take picture from sides	

1

NTNU · SINTEF

End of experiment			
Shut down procedure			
1) Stop PID and close valves and shut down fan 2) Shut down cooling system 3) Empty drain water buckets if full. Use gloves and goggles.			
Remove all obstructions/barriers/signs around the experiment.			
Tidy up and return all tools and equipment.			
Tidy and cleanup work areas.			
Return equipment and systems back to their normal operation settings (fire alarm)			
To reflect on before the next experiment and experience useful for others			
Was the experiment completed as planned and on scheduled in professional terms?			
Was the competence which was needed for security and completion of the experiment available to you?			
Do you have any information/ knowledge from the experiment that you should document and share with fellow colleagues?			

2

NTNU | SINTEF

13 ATTACHMENT I FORM FOR SAFE JOB ANALYSIS

SJA tittel:

Dato: | Sted:

Kryss av for utfylt sjekkliste:

Deltakere:

SJA-ansvarlig:

Arbeidsbeskrivelse: (Hva og hvordan?)

Risiko forbundet med arbeidet:

Beskyttelse/sikring: (tiltaksplan, se neste side)

Konklusjon/kommentar:

Anbefaling/godkjenning:	Dato/Signatur:	Anbefaling/godkjenning:	Dato/Signatur:
SJA-ansvarlig:		Områdeansvarlig:	
Ansvarlig for utføring:		Annen (stilling):	

4

NTNU | SINTEF

● ATTACHMENT H TRAINING OF OPERATORS

Experiment, name, number:
Membrane based heat exchanger

Project Leader:
Hans Marin Mathisen

Experiment Leader:
Sofie Aarnes

Operator
Sofie Aarnes

	Date/Sign

Knowledge to EPT LAB in general
Lab
- Access
- routines and roules
- working hour
Knowledge about the evacuation procedures.
Activity calendar for the Lab

Knowledge to the experiments
Procedures for the experiments
Emergency shutdown.
Nearest fire and first aid station.
HSE datasheet for GlycoShell

Dato _____

Signert _____   Operatør _____

3

14 ATTACHMENT J APPARATURKORT UNITCARD

NTNU **SINTEF**

Apparatur/unit

Dette kortet SKAL henges godt synlig på apparaturen!*This card MUST be posted on a visible place on the unit!*

Faglig Ansvarlig (Scientific Responsible)	Telefon mobil/privat (Phone no. mobile/private)
Hans Martin Mathisen	73593870
Apparaturansvarlig (Unit Responsible)	Telefon mobil/privat (Phone no. mobile/private)
Håvard Rekstad	91897990

Sikkerhetsrisikoer (Safety hazards)

Lekkasje av etylen glycol (GlycoShell). Moderat irriterende for øye og hud ved kontakt. Giftig ved svelging. Dødelig i store doser.

Overoppheting (tørrkoking) i vannbøtte om termostat/regulator ikke virker og varmeelement står på over veldig lang tid (>28t).

Sikkerhetsregler
Safety rules)

Bruk hansker og vernebriller når ventil for kjølevæske håndteres og når smeltevannsbøtter tømmes. Sjekk at vannbøtte i oppvarmings boks er full før forsøk startes opp. Om forsøk kjøres lengre enn 24 timer må bøtte etterfylles.

Nødstopp prosedyre
Emergency shutdown)

Koble ut strømmen for PID-regulator.
Koble ut glykolanlegg med styrestrømknapp (på vegg i lab mot Hovedbygget)

Her finner du (Here you will find):	
Prosedyrer (Procedures)	
Bruksanvisning (Users manual)	

	Nærmeste (nearest)
Brannslukningsapparat (fire extinguisher)	Near inlet to metal workshop
Førstehjelpsskap (first aid cabinet)	Near inlet to metal workshop

NTNU
Institutt for energi og prosessteknikk

Dato

Signert

6

NTNU **SINTEF**

HMS aspekt	Ja	Nei	Ikke aktuelt	Kommentar / tiltak	Ansv.
Dokumentasjon, erfaring, kompetanse					
Kjent arbeidsoperasjon?					
Kjennskap til erfaringer/uønskede hendelser fra tilsvarende operasjoner?					
Nødvendig personell?					
Kommunikasjon og koordinering					
Mulig konflikt med andre operasjoner?					
Håndtering av en evnt. hendelse (alarm, evakuering)?					
Behov for ekstra vakt?					
Arbeidsstedet					
Uvante arbeidsstillinger?					
Arbeid i tanker, kummer el.lignende?					
Arbeid i grøfter eller sjakter?					
Rent og ryddig?					
Verneutstyr ut over det personlige?					
Vær, vind, sikt, belysning, ventilasjon?					
Bruk av stillaser/lift/seler/stropper?					
Arbeid i høyden?					
Ioniserende stråling?					
Rømningsveier OK?					
Kjemiske farer					
Bruk av helseskadelige/giftige/etsende kjemikalier?					
Bruk av brannfarlige eller eksplosjonsfarlige kjemikalier?					
Må kjemikaliene godkjennes?					
Biologisk materiale?					
Støv/asbest?					
Mekaniske farer					
Stabilitet/styrke/spenning?					
Klem/kutt/slag?					
Støy/trykk/temperatur?					
Behandling av avfall?					
Behov for spesialverktøy?					
Elektriske farer					
Strøm/spenning/over 1000V?					
Støt/krypstrøm?					
Tap av strømtilførsel?					
Området					
Behov for befaring?					
Merking/skilting/avsperring?					
Miljømessige konsekvenser?					
Sentrale fysiske sikkerhetssystemer					
Arbeid på sikkerhetssystemer?					
Frakobling av sikkerhetssystemer?					
Annet					

5

A-51

⊡ NTNU

⊚ SINTEF

15 ATTACHMENT K FORSØK PÅGÅR KORT

Forsøk pågår!

Experiment in progress!

Dette kort skal settes opp før forsøk kan påbegynnes This card has to be posted before an experiment can start

Ansvarlig / Responsible	Telefon jobb/mobil/hjemme
Operatører/Operators Sofie Aarnes	Forsøksperiode/Experiment time(start – slutt) May. 2012
Prosjektleder	Prosjekt Membrane Based Heat Exchanger

Kort beskrivelse av forsøket og relaterte farer
Short description of the experiment and related hazards

The purpose of the experimental set up is to test the ability for a membrane based heat exchanger to avoid frost formation compared to a plastic based heat exchanger. Cold air is to be taken from the lab's existing glycol cooling system (cooling battery). Warm and humid air is made by adding heat to a bucket of water with an electrical water heater regulated by a thermocouple and a PID-regulator. Leakage of glycol and overheating (ignition) in the warm air box is the greatest risks.

NTNU
Institutt for energi og prosessteknikk

Dato

Signert

7

Component list:

Node1(green):

- Fan and transformer (12V el supply)
- Cooling coil
- Ducts
- Damper
- Vaisalma RH and T measurement instrument
- Micromanometer pressure measurement instrument

Node 2(purple):

- Existing loop in lab (compressor, filter etc)
- Valves
- Ducts
- Cooling coil
- Control board. See picture

Node 3(blue):

- (air from cold side)
- Damper
- Duct
- Polystyrene box
- Plastic bucket
- Electrical Coil heater
- Thermo element
- PID-regulator
- Vaisalma RH and T measurement instrument
- Micromanometer pressure measurement instrument

HSE report attachments

Google SketchUp drawing:

PID-diagram:

Places where leakages of glycol is likely to occur.

Control board of glycol loop.

Polystyrene box. Should not be opened during experiments.

Overview of set up:

Water supply to glycol room. Down most valve should be open!

Bucket with heater and thermo element